Observational and Analytical Studies on the Convergence Band Clouds Occurring along the West Coast of Hokkaido, Japan

Fumiaki Kobayashi

(1)

Observational and Analytical Studies on the Convergence Band Clouds Occurring along the West Coast of Hokkaido, Japan

Fumiaki Kobayashi

CONTENTS

Abstract

It is well known that heavy snowfalls in Japan are brought by convective cloud lines. On the west coast of Hokkaido, the more larger band cloud is frequently observed under the winter monsoon synoptic situation. This larger band cloud having 200 to 300 km in length and several tens of kilometer in width is formed along the west coast of Hokkaido and is called as the convergence band clouds (CBCs).

It is important to understand therefore that why the CBC is maintained for a relatively long time along the west coast of Hokkaido. The purpose of this study is to clarify the life cycle, mesoscale features and mechanisms of the long-lasting CBC.

From the analyses of synoptic situations and satellite data, the long lasting CBCs were divided into two types; Type A and Type B. In this study, especially, we focused our attention to the CBCs of type A. The CBCs of type A are originated under the following situations. The main cyclones are located far to the east of Hokkaido and cold air covers over Hokkaido where the cloud streaks are recognized over the Japan Sea and the Okhotsk Sea. The initial stage of CBCs is characterized by the disturbances which generate to the west of the Soya Strait according to the low T_{BB} area under the convergence of the northwesterly monsoon wind and the northeasterly cold wind. The mature stage is characterized by the organized CBC for 200 to 300 km along the west coast of Hokkaido under the convergence of the monsoon wind and the southeasterly land breeze. After that, the CBC decays at the same place (the dissipating stage). Considering the pressure field around the west coast, the low

pressure area is formed over the Japan Sea in the initial stage and the high pressure area is formed inland in the mature stage. Therefore, the relative low pressure field is maintained along the west coast of Hokkaido through the lifetime.

During the special radar observations at Haboro, echo structures of the mesocyclone generated in CBC and the merging process of CBC were observed. The mesocyclones have about 30 km in diameter which is one order of magnitude smaller than CBC. The distinct wind field, the pressure drop and the thermal structure of the warm core of mesocyclones are the remarkable features. The mesocyclones are formed at the south edge of CBC near the west coast and it is considered that the mesocyclones are generated at the surface convergence zone where the cyclonic three different winds are prevailed and the surface temperature gradient is steep between the relative warm airmass of the monsoon wind and the cold airmass of the land breeze.

Considering the merging and separation processes of echo bands, it is recognized that the CBC as seen from the satellite is constructed of several echo bands which merge under the difference of the propagation speed.

The theoretical explanation of the maintenance process of CBC is performed through the two-dimensional dynamical model. In the model, the effects of diabatic heating from the sea surface are calculated. As a result, non-geostrophic wind circulations are formed over the coast line which is characterized by the convergence zone over the sea. The solutions correspond well with the analytical field. We conclude therefore that the CBCs are possible to consider as a coastal front.

Chapter 1. Introduction

It is generally well known that heavy snowfalls in the winter monsoon seasons are brought to the coast of the Japan Sea of Japan Islands. Further, it is recognized that these heavy snowfalls are brought about by convective cloud lines, namely, cloud streaks and cloud bands formed over the Japan Sea under the conditions of northwesterly monsoon wind when the typical west-high and east-low pressure patterns are formed over the Japan Islands. While still larger band clouds, which are 200 to 300 km in length and several tens of kilometer in width are formed over the Japan Sea. The more larger band clouds are called the Convergence Band Clouds (hereafter referred to as CBC). One of such CBC phenomena is formed along the west coast of Hokkaido Island, while another is formed on the west side of the Noto Peninsula, Ishikawa Prefecture. And further it is well known that the landing areas of CBC are subjected to the local heavy snowfalls. A number of analyses regarding CBCs were carried out mainly from the synoptic point of view to raise the accuracy of the weather forecast till the present. Recently, the numerical experiments for CBC have been studied by Nagata (1987) and Sasaki and Deguchi (1988). Moreover, doppler radar observations have been carried out in the Ishikari Plain at Hokkaido University (Fujiyoshi et al., 1988, Tsuboki et al., 1989b). However, many questions regarding such points as formation and disappearance processes, meso-scale features of CBC over the Japan Sea and the

time and space relationship between CBC and " small cyclones over the Ishikari Bay" remain unsolved.

Since the meteorological radar and satellite data were useful, meso-scale disturbances associated with snow clouds along the coast region of the Japan Sea have been reported frequently (Miyazawa, 1967; Magono, 1971; Yamaguchi and Magono, 1976; Asai and Miura, 1981). These meso-scale vortex-like disturbances which have a dimension of several tens of kilometer to several hundred of kilometer in diameter have been referred to by different names, i.e., "meso low", "small low", "small cyclone" and so on. However, the differences of individual scale and the structures of the disturbances have not been clarified to date.

These disturbances such as, vortex-like disturbances and CBCs which are important for forecasting heavy snowfalls have been mainly investigated in the Hokuriku district using a special observation network of heavy snowfalls (Miyazawa, 1967; Matsumoto and Ninomiya, 1969). On the other hand, meso lows developed in the Ishikari Bay, Hokkaido, have been discussed (Kono and Magono, 1967; Harimaya, 1970; Muramatsu et al., 1975; Yagi et al., 1979). Because the area covered by radar is limited, the development and movement of snow clouds, especially, the features of CBC in the initial stage in the northern area of Hokkaido have not been observed till the present. Since the CBC is considered as a particularly intense type of the cloud band generated in cold airmasses in midwinter seasons, the formation process and the disturbances formed in CBC should be investigated in detail.

In this paper, we describe meso-scale features of CBC using

satellite data, radar data, AMeDAS data and so on. Firstly, the general characteristics of CBC, such as synoptic patterns, surface wind patterns and the location of snowfall are noted in the chapter 2. In the chapter 3, using the GMS cloud pictures and the black body temperature of cloud top (T_{BB}) data, the characteristic features of CBC are pointed out from two case studies. The formation processes of meso-scale lows in the CBCs and band formation processes observed by the radar are described in the chapter 4. And the dynamical mechanism of CBC as a coastal front is proposed and discussed in the chapter 5. The chapter 6 is the conclusions.

2. General characteristics and synoptic situations of the convergence band clouds

It is well known that a band cloud elongated from the Mamiya Strait southward is observed frequently from the satellite after the passage of the main cyclone over Hokkaido when a typical west-high and east-low pressure pattern is formed. Okabayashi and Satomi (1971) took note of this band cloud that was differentiated from general cloud streaks and cloud bands parallel to the monsoon wind direction, and they referred to them as " the convergence band cloud" as seen from the satellite cloud pictures. Also Muramatsu (1975) classified the heavy snowfalls around the Ishikari Plain caused by the meso-scale lows over the west coast of Hokkaido, and he indicated that there were two typical types of heavy snowfalls, one was a clear circulation field of a synoptic cyclone over Hokkaido (Etorofu type), and another was the low pressure zone over the west coast of Hokkaido (Kamchatka type). In this paper, however, we call these types of cloud bands parallel to the coast line as the convergence band cloud (CBC) in accordance with Okabayashi(1971), but the definition of CBC is not clear to the present and the term of CBC is not international. We regarded CBC as an organized cloud band from the west coast of Sakhalin or the Soya Strait elongated southward by the satellite cloud pictures.

Figures 2-1 and 2-2 show some examples of CBC from GMS pictures taken by the Meteorological Satellite Center of J.M.A. (Japan Meteorological Agency). Several significant features are

recognized in these pictures. In Fig. 2-1, the main cyclones are located far to the east of Hokkaido and cold air covers over Hokkaido where cloud streaks are recognized over the Japan Sea and the Okhotsk Sea. On the other hand, a CBC in Fig. 2-2 is in the circulation field of the main cyclone near Hokkaido and the cloud bands formed on the west coast of Hokkaido blows into the rear side of the cyclone. And, it is also found that the generation points of the north side of CBC are from around the Soya Strait in the Fig. 2-1 and from the Mamiya Strait in 2-2. Based on these differences, the former is named type A which elongates for 200 to 300 km under the uniform monsoon wind and is accompanied with a disturbance in the initial stage. The latter is named type B which is influenced by a synoptic force of the main cyclone and formed under the cyclone in the initial stage. It is assumed that the classification is essentially corresponded to that of the heavy snowfall types classified by Muramatsu considering the position of a main cyclone.

One of the important features of CBC is that a local heavy snowfall is often observed in the Ishikari Plain. Figure 2-3 shows an example of a band echo accompanied with CBC in the Ishikari Plain on the most typical case of heavy snowfall. The case study on this day will be mentioned in the chapter 4. The developing band echo was almost stationary, and the area of heavy snowfall of more than 50 cm in snow depth was concentrated, whereas only snowfall of several cm was observed at other stations in the Ishikari Plain.

The difference between type A and type B mentioned above means

that of a synoptic field around Hokkaido. For executing, the cross-section analysis of the equivalent potential temperature and temperature, upper air sounding stations were selected as shown in the Fig. 2-4. The east-west cross sections along four latitudes of 50° N (1 - 1'), 47° N (2 - 2'), 45° N (3 - 3') and 43° N (4 - 4') were analyzed. Figures 2-5 and 2-6 show the cases of type A and type B, respectively. In the figure, the equivalent potential temperature and temperature are drawn by solid lines and dotted lines, respectively. As shown in the Fig. 2-5, the type A is characterized by the cold dome up to the 700 mb level over the north part of Hokkaido (47° and 45° N), and the thermal trough between the cold domes of the continent and the east side of the Japan Sea indicated by solid wide bars. On the other hand, high equivalent potential temperature exists over Hokkaido and a center of the cold airmass is to the far west of Hokkaido in the type B as shown in Fig. 2-6. That is to say, whereas there is relative thermal trough over the Japan Sea under the synoptic situation accompanied with a cold advection field of type A, type B is characterized by the pressure trough of under the circulation of a synoptic cyclone. Therefore, it is supposed that the formation process of echoes is quite different between both cases.

Figure 2-7 denotes the relationship between the lifetime and the occurring date of 30 cases of CBC from 1980 to 1984. In the figure, the type C indicates the one which is not clear the shape at the generation time from satellite pictures or can not be classified into type A or type B from synoptic situations. It is recognized that type B and type C exist in all winter seasons,

however type A is limited from late January to late February, that is to say, in the midwinter seasons. And many cases of type A are found to be long-lasting for several tens hours in the lifetime relatively. In the next chapter, we discuss two case studies of the most long-lasting CBCs in the figure.

Usually, an outbreak of cold air follows after the passage of a cyclone. In the midwinter seasons, the cold airmass is characterized by -30 ˚C isotherm at 700 mb or -40 ˚C isotherm at 500 mb level. Further, this cold airmass often remains for several days over Hokkaido. Under this stationary synoptic situation of a long staying cold airmass, it is considered that CBC of type A is long-lasting for two or three days. Some examples of synoptic weather charts which are the typical cases of the generation of CBC will be shown in the next chapter. The surface weather charts are characterized by the west-high and east-low synoptic pressure pattern of the stationary winter monsoon situation.

Under these circumstances, CBCs of type A develop along the west coast of Hokkaido in the cold airmass covered over Hokkaido and have relatively longer lifetime. Therefore, it is the most important in forecasting heavy snowfall areas to understand the maintenance mechanism of a long-lasting CBC which is defined as type A.

Chapter 3. Characteristic features of the convergence band clouds by the satellite data

3-1. Life cycle of the convergence band clouds

In this section, the GMS data obtained every 3 hours were used to understand the time change of CBC during their lifetime. Typical and long-lasting two cases of CBC were analyzed using GMS pictures and T_{BB} (Black Body Temperature) data (the grid scale is about 4 km in the east-west direction and about 8 km in the south-north direction) from the JMA Satellite Center (Kobayashi et al., 1987).

Figure 3-1 shows sequential displays of GMS pictures and T_{BB} distributions in the right hand side for two days in the case of February 5, 1982. In the early stage in the Fig. 3-1(a), a curved cloud band which has high brightness and low T_{BB} temperature was recognized on the west side of the Soya Strait. The shape of CBC is clear from the west side of the Soya Strait to the Shakotan Peninsula in a whole day in the mature stage (d). But the low temperature area of the T_{BB} over Hokkaido in Fig. 3-1(e) is considered as the ground cooled by the radiation cooling. After that, CBC decayed gradually and disappeared as the approach of a synoptic cyclone from the Asian continent. The total lifetime of this case was more than for two days. Figure 3-2 shows the surface and 700 mb synoptic weather charts. It is clear that a cold airmass lower than -30 °C at 700 mb passed over Hokkaido. The surface synoptic pattern of the west-high and east-low had

been held almost through this CBC period.

The east-west cross sections of T_{BB} distributions at four latitudes represented in the Fig. 3-3 indicate that the cloud top of CBC is about 3.5 km characterized by T_{BB} below -30 ˚C while that of cloud streaks is about 2 - 2.5 km in average. It is quite obvious that CBC is quite different from cloud streaks and cloud bands parallel to the wind direction. It is therefore suggested that the cumulus convection is more active in CBC.

Comparing with surface weather situations, significant features were observed. Figure 3-4 shows surface meso-scale charts of the early and mature stage of CBC. The northwesterly wind blew in all area on the west coast of Hokkaido affected by the strong winter monsoon pattern, however, the northeasterly wind was recognized around Wakkanai and the area of the northeasterly wind spread southward. Therefore, the isobars became loose at the northern area of Hokkaido. Looking at the surface temperature fields over the northern area of Hokkaido in three stages, that is, the developing, mature and dissipating stages in the Fig. 3-5, it is recognized that the northeasterly wind is colder than the northwesterly monsoon wind, and a distinct shear line of surface wind exists between the northeasterly and northwesterly winds. In the mature stage, the central part of northern area of Hokkaido was affected by the radiation cooling through the night time when the surface temperature recorded below -30 ˚C. Therefore, it is expected that a mesoscale high pressure zone (shown in Fig. 3-4 (b)) will be formed in the central part of northern area of Hokkaido and the divergent flow from the meso-high is seen clearly around the

coast line of Hokkaido, especially, the southeasterly wind is recognized along the west coast accompanied by the meso-scale high. As a result, three different type of winds, that is the northwesterly monsoon wind, the northeasterly colder wind and the southeasterly coldest wind exist along the west coast area of Hokkaido.

Figure 3-6 shows sequential displays of the GMS pictures of another case of February 26, 1983 which brought the first record of heavy snowfalls around the Ishikari Plain. In the early stage of CBC, the disturbance had an organized cloud system which recorded low T_{BB} area below -40 °C over the Ishikari Plain. In the mature stage, the CBC became clear in the shape as shown in Fig. 3-6(d) and (e). Figure 3-7 is the horizontal distribution of 3 hourly precipitation amounts using AMeDAS data. It is denoted that the moderate snowfall area (2 - 4 mm per 3 hours) corresponds well to the location of the cloud system in time. The snowfall was concentrated in the districts of the Ishikari Plain, the Shakotan Peninsula and the southwestern direction slopes in the Iburi Sub-prefecture that showed a quite different snowfall pattern when the northwesterly monsoon wind prevailed. Time changes of the surface wind, temperature and pressure fields were similar to that of 1982. Especially, the shear line of surface wind was obvious between the northwesterly monsoon wind and the northeasterly wind in the initial stage. In the mature stage, the meso-scale high accompanied by the radiation cooling over the central area of Hokkaido and meso-scale low around the west coast were analyzed.

Figure 3-8 shows the time changes of the areas of T_{BB} through the lifetime of CBC. It is indicated that the areas below -30 ˚C and -40 ˚C are the noticeable in the regions of the CBC disturbances. While each absolute value is quite different in both cases, a common trend was found from the figure. The peak of low T_{BB} area appears in the initial stage and it indicates the generation of the disturbance. After that, the area decreased gradually, however, the second peak of the area, which is relatively small, is confirmed. The second peak is corresponded with the mature stage and it means that CBC is developed and organized for 200 to 300 km under the influence of some surface weather conditions. Moreover, the second peak appears at the time during midnight to early morning. Namely, the condition of synoptic weather situations was quasi-stationary through the mature stage to the dissipating stage, and so it is considered that the surface weather conditions, such as differential heating between the sea and land, and the development of a mesoscale low along the west coast and a mesoscale high over the inland were important for the development and the maintenance of CBC.

3-2. T_{BB} distributions of the convergence band clouds

The movement of the lowest T_{BB} center of CBC in the initial stage is shown in the Fig. 3-9. The lowest T_{BB} centers at each time are indicated in parentheses in the figure. It is remarkable that the lowest T_{BB} centers move southward after the generation. The T_{BB} rises in the case of 1982, however, drops in the case of 1983 which the disturbance develop over the Ishikari Bay. Therefore, it is understood that the cumulus convection is most active in the south edge of CBC in the both cases. Actually, the locations of the south edge of CBC characterized by -40 °C of T_{BB} are corresponded with the locations of the shear line of surface wind as shown in Fig. 3-10. The shear line of surface wind, which is formed between the northwesterly monsoon wind and the northeasterly colder wind, moved southward together with the movement of the south edge of CBC. Figure 3-11 shows an example of changes of meteorological elements recorded at the passage of the south edge of the CBC corresponded with the shear line of surface wind. The atmospheric pressure dropped when the shear line passed the Haboro weather station and after that the pressure rose for 1.0 mb. The wind direction changed abruptly from WNW to NE and a gust wind stronger than 15 m/s was recorded at the same time when the pressure jump was recorded. A temperature drop of about 1 °C/ 10 min was recorded during one hour before and after the pressure jump, and relative humidity reached 100 % after the gust wind was recorded. Therefore, it is supposed that the gust wind from developing cumulus clouds was

accompanied with the falling graupel particles when the shear line of surface wind was formed.

The formation process of CBC is most interesting, and then T_{BB} distributions of CBC were scrutinized in the initial stage of two cases of CBC. Looking at the lowest temperature area characterized by -40 °C which is considered the most active area of the cumulus convection, the area develops rapidly and increases in the west side of the Soya Strait, and the area changed curved shape in both cases as shown in the Fig. 3-12 and Fig. 3-13. It is, therefore, confirmed that we can decide the generation of CBC as a rapid development of low T_{BB} area from GMS pictures in the west side of the Soya Strait.

Figure 3-14 shows the examples of hodographs at Wakkanai before and after CBC is organized. While the westerly wind is distinct at almost layer at 09 JST as seen in the figure, the northeasterly or northerly wind appears below 850 mb level at 15 JST. It is understood that the wind direction is backing and the wind speed weakens up to 700 mb level in the convective layer. This northeasterly wind mentioned in the Fig. 3-5 has the thickness of about 1 km from the surface and makes a wind shear line against the westerly monsoon wind. Further, thinking of the topography around the Soya Strait where is located between Sakhalin and Hokkaido Islands the northeasterly wind blows most likely through this strait. And then, it is surmised that the disturbances are influenced by the horizontal wind shear of the low level which formed the surface convergence. On the other hand, the synoptic situations also must be considered, because the vertical extention of the disturbances in the initial stage

is very high, i.e., the cloud top reachs up to 5 km estimated from T_{BB} data. Figure 3-15 is a time-height cross section of the equivalent potential temperature (θe) at Wakkanai. It is recognized that a cold dome below 700 mb level is formed after the passage of the cyclone under the cold advection from the continent. The cold dome continued for two days which is equal to the lifetime of CBC. Especially, the temperature gradient was sharp up to 500 mb, and convective instability layers shown by shaded areas in the figure developed to 700 mb level after the passage of the cyclone in the initial stage of CBC that suggests the possibility of the generation of disturbances.

3-3. Discussion

From the results of T_{BB} analysis, it is realized that there are two disturbances through the life cycle of CBC considering changes of the low T_{BB} area as shown in the Fig. 3-8. The first disturbance of the T_{BB} represents a cloud system having higher vertical structure generated at the region on the west of the Soya Strait influenced by a synoptic forcing under the condition of cold airmass advection in the rear side of the cyclone. The second disturbance means CBC formed along the west coast of Hokkaido. As shown in the Fig. 3-15, it develops again under the condition of a quasi-stationary synoptic field covered by the cold dome below 800 mb level and influenced by the meso-scale surface conditions, such as the differential heating or the local wind shear.

Considering the life cycle of long-lasting CBC, each stage of CBC well corresponded with the synoptic condition after the passage of the cyclone. The initial stage is the generation of CBC when cold airmass advected from the continent over Hokkaido. The northeasterly wind blows at the northern part of Hokkaido from the cold airmass up to 1 km and makes the wind shear line between the northwesterly monsoon wind. The mature stage is the continuance of CBC under the quasi-stationary synoptic situation. Looking at a wind along the west coast of Hokkaido, the southeasterly wind from a meso-high formed inland is distinct for this stage through the dissipating stage.

Consequently, the disturbance at the initial stage is

considered as a cancellation process of the developing convective instability layer which formed up to 500 mb at the rear side of a main cyclone. On the other hand, the organized CBC at the mature stage is considered as the maintenance process influenced by the surface weather conditions under the stationary synoptic situation.

Therefore, it is thought that a thermal trough is formed as the advection of a cold airmass after the passage of a synoptic cyclone. In fact, the shear line of surface winds moved southward gradually together with the cold advection. The disturbance over the shear line has lowest T_{BB} area and relatively higher in the vertical scale. As shown in the Fig. 3-7, at the south edge of CBC, a heavy snowfall was recorded. In particular, a local heavy snowfall is recorded in the area where CBC lands and stagnates.

And so, the long-lasting and stationary CBC is very important and must be made clear in its maintenance process. It was the problems to make clear the structure of disturbances in CBC as seen from the satellite and echo patterns in the initial stage at the northern part of Hokkaido at that time.

Chapter 4. Echo structure of the convergence band clouds by the radar observations

4-1. Outline of the observations

Based on these meteorological characteristics described in the chapters 2 and 3, special radar observations were carried out from the middle of December 1986 to the middle of January 1987 at Haboro Town (44° 21' N, 141° 42' E) located at the west coast of Rumoi Sub-prefecture of Hokkaido Island about 150 km north from Sapporo. Figure 4-1 shows the observation network around the radar site. The mobile meteorological radar of the Meteorological Laboratory, Faculty of Science, Hokkaido University marked by a star in the figure was set up on the cliff of 30 m in height along the coast line from north to south in Haboro Town. Figure 4-2 shows our radar system set up at Haboro. Long period recording wind vane and anemometers, thermometers and microbarometers were also placed at the two special observation sites, namely, Yagishiri Island and Onishika 25 km apart to the south from Haboro marked by solid circles, respectively. Weather stations of J.M.A. are located in Haboro and Rumoi marked by double circle, and the AMeDAS stations marked by solid triangles covered this area (Kobayashi et al., 1989).

The range scrutinized by the radar was 63.5 km in radius. Fortunately, there were no obstacles to hinder radar detection around the radar site. Radar data were recorded on magnetic tapes

with CAPPI and RHI modes at every 10 minute intervals. For the analysis, radar data were recorded on the average over 1 km x 1 km mesh in horizontal and 0.5 km in vertical. Continuous weather data observed at Yagishiri and Onishika sites, and Haboro (J.M.A.) station were used and satellite pictures of GMS taken by Meteorological Satellite Center of J.M.A. and NOAA data received at the Meteorological Laboratory in Hokkaido University were also taken into account in the analysis.

4-2. Mesoscale vortices

A large number of meso-scale vortices accompanied by CBC have a dimension from 20-30 km to 200-300 km in diameter. However, the relation between CBC and vortices is well unknown till the present. Of course, a relatively large vortex can be recognized easily from GMS pictures, however, relatively small disturbances accompanied with CBC can not be recognized without the weather radar. Figure 4-3 indicates several records of the atmospheric pressure at the Haboro Weather Observatory of J.M.A. during our observation period. The records represent that pressure disturbances accompanied with snow storms appeared in several different patterns, that is, 1.0 - 2.0 mb of the pressure drop per 20 minutes to 2 hours during their lifetime. From the recording charts of atmospheric pressure, it is thought that smaller vortices generate more frequently than larger vortices. Actually, as many as 6 cases of meso-scale vortex-like disturbances were observed only for one half month during our observation period at Haboro as shown in Table 1. Each value of gust winds, pressure drop, temperature change was decided from continuous weather records of the Yagishiri and the Haboro Observatory. The maximum values of divergence and vorticity were calculated from hourly wind data of three AMeDAS stations, Yagishiri (13146), Haboro (13181) and Shosanbetsu (13121). Except for one case (case 2), each disturbance has some similarities in its dimension and lifetime. That is to say, the pressure drop

was 1.0 - 2.0 mb, and gust winds were 15-25 m/s at the Yagishiri Observatory and 10-20 m/s at the Haboro Observatory under the convergence and positive vorticity field. The temperature change appears as both rise and drop which means that the temperature change is placed under the control of the different airmasses. As a result, it is considered that meso-scale vortices having the dimension of 20 - 50 km in diameter generate in CBC more frequently than our expectation.

In this section, three case studies of meso-scale vortices observed by the radar are discussed. The meso-scale vortices accompanied with CBC have several kinds of the structure. Here, three typical case studies are presented, that is, (1) a mesocyclone (30 km in diameter) generated at the south edge of CBC, (2) a wave train pattern in a band echo, and (3) a vortex developed in the disturbance of 100 km scale at the initial stage of CBC.

< A case study of mesocyclone on January 12,1987 >

Figure 4-4 shows a GMS infrared picture just before the development of this mesocyclone. There was a distinct curved band cloud southward from the Soya Strait. According to the time change of GMS pictures, this band cloud (CBC) was formed on 18 JST, January 11, 1987. The southern end point of this band moved northward gradually and a meso-scale vortex disturbance was formed at the south end point of CBC. Because of the lack of the time and space resolution this disturbance could not be found in the GMS picture.

Figure 4-5 indicates the time sequence of PPI radar echo patterns of the mesocyclone. Before this disturbance, a band shaped echo which was located in the southern region of the radar coverage area, began to shift to the northward direction from 21 JST, January 11. When the band shaped echo arrived at the west end of the radar coverage area, the band shaped echo became stationary. As shown in Fig. 4-5 (a), the echo pattern of " the initial stage " was formed from an isolated echo which was located at northward of Yagishiri Island and the main band echo was progressing from the northwest direction. Afterwards, the isolated echo elongated and showed a cyclonic curvature at northeastward of the main band echo as shown in (c). At this time, the cyclonic echo pattern showed the shape of a mesocyclone in " the mature stage " showing a spiral band echo pattern. The dimension was 30 km in diameter including the outer band echoes with an echo free area of 7 km in diameter which is generally

called the cyclone eye. At this stage, the disturbance is called a mesocyclone. Afterwards, the mesocyclone moved eastward and the echo free area surrounded by a spiral echoes increased in its diameter. The southward echo band corresponding to the main band extended to the southeastward slowly as shown in (d). As shown in (e), after the mesocyclone landed near Haboro, it began to stagnate while the echo area and the echo free area spread to about 40 km and 20 km in diameter, respectively as shown in (f). This stage was termed " the dissipating stage " and the echoes were disappeared. The movement course of the center of the mesocyclone indicated by 10 minute intervals is shown in the Fig. 4-6. It revealed that the mesocyclone moved eastward uniformly with an average velocity of 30 km/h. The mesocyclone disappeared at 15 km into the inland after landing. The life time of the mesocyclone was approximately 2 hours.

Figure 4-7 shows a formation process of the mesocyclone at 0330, 0350 and 0410 JST at 1.1, 1.7 and 2.5 km in altitude above the sea level which were made from the CAPPI mode data. Each vector in the figure indicates the relative wind to disturbance. As a result, the cyclonic echo flow pattern became more clear. Whereas the vortex circulation of echoes appeared at low altitude (1.1 km) alone at each observation time. Contrary to this, at 2.5 km level, the main band echo alone from the northwest direction was obvious. Therefore, it is considered that the vortex generated at lower level. In fact, the time change of divergence and vorticity calculated from wind data averaged at 10 minute intervals using Yagishiri, Onishika and Haboro stations corresponded with both the time of development and the position

of the mesocyclone represented in Fig. 4-8. The calculated values showed 4 x 10^{-4} s^{-1} for the maximum convergence and 7 x 10^{-4} s^{-1} for the maximum vorticity at 0400 JST when the mesocyclone moved and developed in the calculated area of the strong convergence field. These values are permitted for its scale compared with that of other case studies such as Miyazawa (1967) and Asai and Miura (1981).

Three vertical cross sections perpendicular to the 315° direction as shown an A-A' line in Fig. 4-5 (b), are shown in Fig. 4-9 as a form of RHI mode displays which made from CAPPI mode data. From the figure, the vertical structure of the mesocyclone in the mature stage at 0350JST in Fig. 4-5 (c) indicated that convective cells with an echo top of 4 km in height were confirmed in the southwest side main band. On the other hand, the northeast side echo was relatively low with an echo top of only 2.5 km and located in the rear side of the mesocyclone center. In particular, an inner cell of the main band inclined to the center of the mesocyclone behind the mesocyclone center. Thus, the mesocyclone was clarified to have an asymmetric echo structure.

Each surface meteorological element changed remarkably at the passage of the mesocyclone. The mesocyclone passed near by the south side of Yagishiri and by the north side of Haboro station. As seen in the Fig. 4-10, the atmospheric pressure decreased from 0430 to 0530 JST at the passage of echo free area and the maximum pressure drop was 0.8 mb. This pressure drop of about 1.0 mb corresponded to the typical pressure change of mesoscale low

pressure systems occurred in the west coast of Hokkaido. The wind direction also changed systematically at Yagishiri, namely, the northwesterly gust wind was recorded in the maximum velocity of 17 m/s at 0400 JST just after the passage of the mesocyclone center. On the other hand, the gust wind was recorded two times at Haboro as shown in the figure. The first gust was recorded at 0420 JST when the eastern edge of the outer spiral echo band arrived at the radar site and the second gust was at 0500 JST when the spiral band entered from the northwest behind the mesocyclone center. The maximum wind velocity was recorded at 10.5 and 11.5 m/s, respectively. The gust wind was in good correspondence with the time of movement of the spiral echo bands. Corresponding to the time of these gust winds, two remarkable temperature rises of 3 ˚C/10 min and 1 ˚C/10 min were recorded, respectively. The first temperature rise suggests that the relatively cold and dry land breeze from the southeast direction was replaced with the relatively warm and moist northwest monsoon wind. However, the second temperature rise corresponded with the time at the passage of the mesocyclone center. Figure 4-11 represents the temperature field at the landing of the mesocyclone which was made from the continuous weather records of Haboro, Onishika and Yagishiri stations using the time-space inversion method. From this figure, it revealed that a relatively warm area warmer than -7 ˚C accompanying the mesocyclone invaded inland. As a result, it is considered that the sharp temperature gradient of about 10 ˚C between both air masses was formed. Furthermore, near the center of the mesocyclone, the most warm area characterized by -6 ˚C isotherm

appeared and it corresponded to the location ahead of the spiral band echoes. Moreover, these features implied the existence of gust winds which were located to the southeast ahead and the northwest behind the mesocyclone center as shown in the schematic figure 4-12. And it is suspected that a gust front was formed at the front of the mesocyclone between northwesterly monsoon wind and southeasterly land breeze which were shown by wide arrows in the figure.

As a result, it is most important that the mesocyclone generated at the end of CBC is one order smaller (30 km in diameter) than the CBC clouds. Figure 4-13 indicates a mesoscale chart at the time of the generation. The mesoscale low pressure zone along the west coast is corresponded with CBC as shown in the Fig. 4-4, not with that of the mesocyclone. It is considered that the mesocyclone formed at the south edge of CBC where the different three winds produce a surface wind shear line with the strong temperature gradient. And so, it is assumed that the thermal structure of a warm core was observed in the mesocyclone center. Some observations of vortices which generate in the Ishikari Plain, such as Motoki (1974) and Yagi et al. (1979), has not reported a clear thermal structure to the present.

< A wave train pattern on January 15, 1987 >

Figure 4-14 shows a GMS infrared picture on 01 JST January 15, 1987, just after the passage of a synoptic scale cyclone over Hokkaido. It can be recognized that there is a cloud mass accompanied by the synoptic scale cyclone over the east side of Hokkaido. And a curved cloud pattern was observed in the quite spread area over the Japan Sea. It is recognized that differential winds were there over the Japan Sea on the west side of Hokkaido. This disturbance is thought to be generated at the rear side of a synoptic scale cyclone where wind shear in horizontal or vertical directions formed between westerly monsoon wind and northerly wind caused by the synoptic scale forcing was large and the temperature gradient was the strongest. After that, this curved-shape clouds elongated to southward and CBC was formed along the west coast of Hokkaido.

We observed smaller scale vortices in one cloud band of this disturbance from our radar observation. As the cloud band was moving southward, the band began to meander and two vortices were linked together as indicated in the Fig. 4-15. The first vortex was formed about 40 km offshore from the radar site and a half hour later, the second vortex developed just above our radar site. The echo free area, i.e., "the cyclone eye" observed in each vortex spread its diameter as a time. The movement of vortices corresponded with that of the band. Each lifetime of vortices was about one hour, and the diameter was 20 - 30 km. Figure 4-16 shows continuous weather records at Haboro, and as

the passage of the second vortex just over the site, the wind direction changed systematically. In particular, the southwesterly gust wind up to 13 m/s was accompanied by the southern band and northerly or northeasterly gust wind up to 16 m/s was accompanied by the northern band. Besides the wind once weakened in the echo free area of the vortex center. This tendency was so resemble of the mesocyclone mentioned above in the case of January 12. The temperature drop was for 2 ˚C/ 20 min as the passage of the band, however, the thermal structure of vortex, such as the warm core was not clear. This temperature change means the existence of different two kinds of airmass, that is to say, the northeasterly cold wind and westerly wind airmass. Considering the second vortex formed over the land, it is supposed that no thermal structure inside reveals a result of no supply of heating from the sea surface.

And so, it is considered that this vortices were generated at the area of frontal zone which was represented by the shear line of surface winds having opposite directions and by the strong temperature gradient zone. The echo structure and the features of surface weather conditions are also well corresponded to the mesocyclone mentioned above.

< A vortex developed at the initial stage of CBC on
February 1, 1987 >

A mesoscale cyclone having 100 km from the satellite pictures in diameter generated under an uniform cold airmass on January 31, 1987. Figure 4-17 shows a time sequence of GMS infrared pictures of the mesoscale cyclone which was formed about 100 km offshore from the radar site. This cyclone generated at 18 JST as shown in the picture of left hand site. When the mesoscale cyclone developed most actively, the cyclone had a clear spiral pattern of clouds at 01 JST. After the dissipation of the cyclone, a CBC had been distinct and invaded into the Ishikari Bay. Figure 4-18 shows the time-height cross section of equivalent potential temperature at Sapporo. At the passage of a synoptic cyclone on January 30, 1987, the temperature gradient was large and after, a cold air advected from the Asian Continent and a cold dome was formed at low troposphere. The cold dome characterized by 270 K isotherm developed from January 31, and it is recognized that this meso-scale cyclone generated not the rear of a synoptic cyclone but in the uniform cold airmass.

From the radar observations at the Sapporo District Meteorological Observatory as shown in the Fig. 4-19, relatively weak echoes were scattered and organized in the initial stage at the location of about 100 km from the offshore of Rumoi. Whereas this radar echo is corresponded to the time of one hour after the Fig. 4-17 (b), no echo circulation and no developing echoes observed in the clouds. After that, unfortunately, no

observations were carried out at the observatory. Figure 4-20 (a) indicates echo pattern of the southern part of the vortex in the developing stage. From the figure, it is obvious that a circular band pattern echo accompanied with the cyclone center as shown in the figure. The double band pattern was observed to change places between outer old band and inner new band (not shown). It means that vortex had a spiral band structure. However, a diameter of the cyclone is not clear, but it is assumed about 50 km. After the landing, these echo pattern disappeared near the coast line that is obvious from pressure fields (Fig. 4-24) and temperature fields (Fig. 4-23).

After the dissipation of the vortex, the echo changed into the straight band which was stationary in the Ishikari Plain. As shown in the Fig. 4-20 (b), the location of the band corresponded with the frontal region characterized by the wind shear line between westerly monsoon wind and the land breeze. As a result, a heavy snowfall was recorded on the local area where the band stagnated. For example, at the Nishinopporo AMeDAS station, the precipitation of 22 mm in water was recorded for a half day whereas there were only 1 - 3 mm precipitations around the area except for Ishikari AMeDAS station of 13 mm as shown in the Fig. 4-21. The snowfall intensity more than 4 mm /h in water continued for 5 hours (21 mm for 5 hours) at Nishinopporo. This is the most typical snowfall pattern of CBC.

Regarding the formation process of this cyclone, the surface weather conditions must be considered under a uniform synoptic situation. Figure 4-22 indicates the temperature change at

Yagishiri as a small island in the Japan Sea (upper figure), and the temperature deviations from Yagishiri at Haboro as the coast line (middle figure) and Nayoro as the inland (lower figure) at the same latitude. The temperature at Yagishiri station was almost constant of -8 ˚C from 06 JST Jan.31 under the coverage of cold airmass. On the other hand, a distinct diurnal temperature variation was recognized at both coast line (more than 5 ˚C) and inland (more than 10 ˚C) caused by the radiation cooling during the night time. As a result, a meso-high was formed inland, and the cold land breeze that is, the southeasterly wind around Haboro blew from night to early morning. The mesoscale cyclone was generated when the temperature difference between sea and land became large and the land breeze began to blow to seaward. Figure 4-23 shows the wind and temperature fields at 02 JST (time of the development of meso-scale cyclone) and 06 JST (time when CBC invaded into the Ishikari Bay). Over the sea to the west coast of the northern part of Hokkaido, the northeasterly wind was recognized remarkably. Contrary to this, the westerly wind was recognized along the Shakotan Peninsula. Moreover, the southeasterly cold land breeze began to blow from 18 JST, and high vorticity field was formed over the sea where the meso-scale cyclone was generated. Compared with the figures at 02 JST and 06 JST, it was recognized that there was a relative warm area of the mesoscale cyclone in the Ishikari Plain at 02 JST, but it changed to a relative cold area at 06 JST characterized by -10 ˚C isotherm which was understood as the border line between the sea and land origin airmasses. It was not clear the thermal

structure because of the lacking of data, but temperature rose about 0.5 ˚C from the AMeDAS stations passed by the mesoscale cyclone.

Figure 4-24 shows three hourly pressure fields and pressure deviations around Hokkaido. It is obvious that the mesoscale low pressure zone was analyzed at the same time of mesoscale cyclone and after that, the mesoscale high pressure zone was analyzed inland when CBC was organized.

4-3. The merging process of the band clouds

Considering the formation process of band clouds which have several tens of km in width and several hundreds of km in length, the merging or separation processes of cloud bands in winter seasons are very important to understand the structure of CBC and forecast heavy snowfalls. However, a few case studies have been reported until the present, for example, Muramatsu (1978) suggested that the stationary band cloud was caused by the upwind orographic effect. He found that a single large cloud band about 40 km in width and 400 km in length was sometimes recognized in the satellite pictures over the northern part of the Japan Sea in winter monsoon seasons, and the cloud band was enhanced by the lee of a chain of mountains located 45.5° N, 137.1° E in the Sikhote Align in the Maritime Territory of the USSR. This is a case of a large scale cloud band caused by the upwind mountains, but from the radar observation, it is often confirmed that the merging or separation phenomena of the band echoes are observed in cloud streaks during short intervals. In this section, we attend the formation processes of the band clouds in mesoscale feature based on the radar observation, such as the cases of a band parallel to the monsoon wind direction and a band parallel to the coast line from north to south direction.

< Case 1: A band cloud parallel to the wind direction >

Figure 4-25 shows the time changes of CAPPI displays at 1.5 km above sea level on December 26, 1986, under the strong winter monsoon weather situation. Stationary cloud streaks were formed parallel to SWS direction of the monsoon wind as shown in Fig. 4-25 (a). As shown in the figure, each line echo had 10 km in width and the space between band and band was 20 km. In the line echoes, each cell moved parallel to each line echo at the speed of 60 - 70 km/h which was equal to that of monsoon wind. After 1500 JST in the Fig. 4-25 (a), these two line echoes began to merge sporadically, and a strong band echo developed in (b) and (c). After that, the width of the band spread gradually and separated into two lines in (d) and (e). It was recognized that the merging and separation occurred at about 2 hours intervals in this case. Using the data in the rectangular area drawn by stripes in Fig. 4-25 (a), the time section of the echo from north to south was shown in Fig. 4-26. From 1400 JST, new echo cells generated between line echoes. After that it seems two line echoes were merged at 1530 JST and a band echo developed. Figure 4-27 indicates the time change of echo areas larger than each reflectivity value so as to investigate the development of the band echo. The total area (> 16 dBZ) increased before the merging and at the time of the separation again, and decreased at the time of the merging. While the strong reflectivity area (> 19 dBZ) increased gradually after the merging.

Figure 4-28 represents the time change of radar echoes from

north to south vertical cross section of the band clouds at 20 km offshore. In the figure, the developing stage of the echo in the life cycle of the band was indicated. It was recognized that when each echo began to dissipate, new echo generated between line echoes, for instance, on 1420 JST. That is to say, at the developing stage of the line echoes, the updraft existed in the echo areas. On the other hand, at the dissipating stage, the updraft areas were changed into the downdraft areas. It is well known that the lifetime of each cell in a band cloud is several tens minutes and that of a band cloud is several tens hours. However, a band cloud also changed in the inside by itself during its life cycle. It is thought therefore that the band cloud changed or shifted in its shape and position repeating the merging and the separation of the echoes. And so, the process which the old echoes changed places with new echoes was seen as the merging or the separation of band echoes at the time intervals of about one hour in this case.

< Case 2: A band cloud parallel to the coast line >

This case corresponds to the merging process of the band echo in CBC on January 14, 1987. Figure 4-29 shows the GMS infrared picture on 03 JST, and CBC is recognized along the west coast of Hokkaido. From the GMS pictures, however, CBC looked like a cloud band alone and moved towards the coast line slowly. From the radar observations of this CBC, it was recognized that two or three band echoes were existed in CBC.

As shown in the Fig. 4-30, three band echoes moved to southeastward at the average speed of 30 km/h. However, approaching to the coast line, the most eastward band began to be stationary. Consequently, the band A and the band B were merged at 0630 JST, after that, the band B and the band C were merged. Figure 4-31 shows the west to east time section of the band echoes of the rectangular area with stripes in the Fig. 4-30. As seen clearly in the figure, the band A and the band B merged at 30 km far from the coast line at 0620 JST and the band B and the band C merged at 20 km at 0710 JST. The time interval of the merging in this case was about 1 hour. From the time change of echo area as shown in the Fig. 4-32, it is obvious that each area increased at the merging and the band echoes developed after the merging. From the figure, the band A moved more slowly approaching the coast line and merged with the band B. Because the cold breeze of south - southeasterly from the inland was dominant around the coast line as shown in the Fig. 4-30. On the contrary, near the coast line where was 20 - 30 km offshore,

there was the convergent zone between two opposite winds that is, the cold breeze from the inland and the relatively warm wind of monsoon wind. Figure 4-33 shows the vertical cross section of the band echoes at the merging of the band B and the band C. After the merging of the band A and the band B, the band B propagated to the eastward as shown in the Fig. 4-33 (a). At 20 km offshore, the band B became to be stationary and dissipated gradually in (b). But, the band B was merged with the band C and they developed once more in (c). As a result, it is thought that the merging of this case occurred under the condition of the difference of the propagation speed of each band.

As a result, considering to the merging process, the following different factors will be presented in these cases. In the case 1 of cloud streaks, the echo bands merge and separate under a factor of the generation of new echoes. On the other hand, a factor of the difference of the propagation speed of each band echoes was dominant in the case 2 of CBC. Of course, it is assumed that a direction of the band propagation was influenced by the motion of a synoptic cyclone or a upwind topography mainly, not the surface weather conditions in the case 1. But, regarding as band echoes parallel to the coast line in the case 2, it is recognized that the surface condition of Hokkaido arranges the propagation.

4-4. Discussion

As described previously, it is understood that mesoscale vortices accompanied by CBC have several orders of size in diameter and some differences in its structure. That is to say, it is considered that the formation mechanism of mesoscale vortices consists of numerous factors. With regard to the structure, there are some mesoscale vortices, that is, the type of a clear vortex circulation of the wind field which accompanies the strong gust winds on the surface which are "mesocyclone" having an echo free area at the cyclone center and a clear thermal structure which appears at the warm core. On the other hand, mesoscale vortices which have no clear wind circulation and thermal structure were often observed on our radar. However, these mesoscale vortices which have several tens of km in diameter, develop along the west coast of Hokkaido over the Japan Sea that are mainly influenced by horizontal wind shears of differential surface winds. First of all, we noted the mesoscale vortices less than 100 km in diameter which are generated in the uniform cold airmass under the synoptic field. In particular, the mesoscale vortices accompanied with CBC were found to generate at the surface wind shear zone where the horizontal temperature gradient is steep and is influenced by the differential heating between the land and the sea.

Considering the mesoscale vortices generating around the northern part of the Japan Sea, relatively larger vortices often are generated by themselves, without CBC. These vortices have a

scale of 200 to 300 km in diameter and generate in cold airmass. Ninomiya (1989) reported comma clouds associated with "Polar lows" in the Japan Sea. Polar lows which are characterized by their shape of comma clouds and less than 500 km in diameter with cloud-free inner eyes of 20-100 km in diameter and have a surface wind velocity stronger than 30 m/s on occasion (Shapiro et al., 1987) generate over the North Atlantic and North Pacific Oceans and embedded in cold polar air masses. Recently, Tsuboki (1990) explained that mesoscale lows of several hundred kms generating on the west side of Hokkaido are a result of disturbances of baroclinic instability. According to his linear theory the low level vertical wind shear is given as an initial condition, it was suggested that two types of disturbances having 200 km and 500 km in horizontal scale are formed. The low T_{BB} disturbances which were formed in the early stage of CBC mentioned above were generated immediately after the passage of the cyclone where the vertical gradients of air temperature and wind are quite steep up to 500 mb level that indicates the presence of a strong baroclinic field of the synoptic scale. Therefore, the disturbance in the early stage is thought to be influenced to some degree by the synoptic baroclinic forces.

Consequently, it is considered that there are different types of meso-scale vortices on the west coast of Hokkaido. And, the vortices on a scale of several tens km in diameter differ from the larger scale vortices in its formation mechanism. In particular, the vortices accompanied with CBC are influenced by surface weather conditions, that is to say, the convergence of the surface winds, the differential heating between the land and

sea and so on. As mentioned previously, the northeasterly wind is likely to blow from around Wakkanai or the Soya Strait and the southeasterly wind from a meso-high formed inland is likely to blow towards the west coast of Hokkaido. And so, it is considered that a number of disturbances of the initial stage of CBC generate to the west at the Soya Strait and many mesoscale vortices are observed at the south edge of CBC near the coast line where the convergence zone of these different surface winds locates. It is assumed that these winds are the main factors leading to the formation of these vortices and the formation process of CBC. Further, considering of the warm sea current along the west coast of Hokkaido, it is suggested that the sensible heat and water vapor that supplies the atmosphere and cumulus convection are active in the region of the higher sea surface temperature. Under these circumstances, we must clarify the formation mechanism of the vortices of several tens km in diameter accompanied by CBC, which show an intermediate characteristic between a barotropic and baroclinic fields.

Recently, many observations of CBC and precipitating snow clouds were carried out in the Ishikari Plain, for instance, we have the reports by Fujiyoshi et al. (1989) and Tsuboki et al. (1989b) and so on. In the Ishikari Plain, however, the band echoes of snow clouds invade from only the northwest direction which coincides with the direction of monsoon wind. As shown in the report by Harimaya and Kato (1989), a case of the confluence between CBC band echoes and cell-like echoes of the cloud streaks is reported in the Ishikari Bay. Moreover, the difference

between the northeasterly wind and the southeasterly land breeze mentioned above is not clear in the Ishikari Plain because the direction of the land breeze is parallel to the northeasterly winds in the plain. Based on the observations of Ohmoto et al. (1989) using a doppler sodar and Tsuboki et al. (1989a) who used a doppler radar, the height of the northeasterly land breeze over the Ishikari Plain is about 300 to 800 m. And so, we must clarify the difference of the structure between the northeasterly wind and the southeasterly wind in the north part region of Hokkaido.

Considering the relation between the surface winds and the band formation, three different cases of the echo motion of cloud bands accompanied by CBC through this observation period are shown in the Fig. 4-34. Considering the directions of surface wind at Haboro (H), Rumoi (R) and Yagishiri (Y) and 850 mb wind at Wakkanai Local Meteorological Observatory as shown in the figure, distinct differences are clear in each case. Whereas in the case on January 15 (left hand in the figure), the band echo was formed by the convergence between northwest and weaker northeast surface winds and the band moved southward. In the case of January 11 (center), the echoes were not a band but cell like echoes which moved parallel to the downstream under the uniform strong northeast wind over the sea. And so, this case corresponds with Type B mentioned in the chapter 2 which is parallel to the wind direction. On the other hand, in the case of January 14 (right hand) in which the merging of echo bands were observed, the northwest monsoon wind blew over the sea and the southeast cold land breeze blew from offshore and the echo bands moved eastward maintaining its shape. Generally speaking,

the direction of the echo bands is parallel to the shear vector at the lower wind and the direction of echo motion depends on the 850 mb wind. In these cases, the lower winds were not uniform but different around the coast line which suggest non-geostrophic winds. The locations of echo bands corresponded with the convergence zone of different directions of the winds. Accordingly, it was recognized that these band echoes were phenomena occurring in the relatively shallow layer above the ground surface along the west coast of Hokkaido that were affected by the cold land breeze from inland or the land effects, for instance, the differential of the friction or topography. However, after the echo bands were formed and developed up to 2 or 3 km, the motion of echo bands (namely the direction of the propagation) depended on the typical winds of the lower atmosphere, for instance, 850 mb. In particular, in a case where the monsoon wind and cold land breeze are exactly in the opposite direction, such as the case on January 14, an echo band was developed parallel to the coast line as the balance of winds having two different directions and moreover the location was almost stationary near the coast line as the merging was reported.

As a result, the characteristic features of the CBC echoes which is the maintenance process of CBC along the west coast of Hokkaido are follows: (1) The CBC maintained in the uniform cold airmass and the stationary field of the synoptic situation. (2) The band echoes propagate to the southward under the conditions of surface winds between the northeasterly wind and the

northwesterly monsoon wind in the initial stage. (3) The band echoes stagnate along the west coast of Hokkaido under the opposite winds of the southeasterly land breeze and the northwesterly monsoon wind in the mature stage and the dissipating stage. (4) The CBC consists of not one band echo but two or three band echoes which took place in time and the merging of the band echoes was observed. (5) The stationary CBC can be regarded as the maintenance process of a mesoscale convergence zone formed along the west coast region of Hokkaido.

5. Dynamical mechanism of the convergence band clouds as a coastal front

5-1. Outline of the model

Based on the mesoscale structures of the wind, by the pressure and temperature fields mentioned in the previous chapter, a two dimensional model was proposed in this chapter. A synoptic situation over Hokkaido is considered to be quasi-stationary, and the CBCs are influenced by the mesoscale surface conditions, such as a differential heating, a differential wind field and friction between sea and land. Thinking that CBCs formed along the coast line and the isotherms on the sea surface are almost parallel to the coast line, a stationary model of two dimensions is permitted to be studied in this case. Moreover, considering that the general monsoon wind blows perpendicular to the coast line, we investigated the effects of diabatic heating from the sea surface mainly.

The model idealized in this case is presented schematically in Fig. 5-1. In the model, a horizontal homogeneous cold air mass passed over the homogeneous sea, and the air above the sea surface were heated below and a convective layer which is capped by an inversion layer is formed. A height of the convective layer is decided as H. Actually, the thickness and temperature of the convective layer increases as it progresses downstream, but a constant H and a constant θ are assumed here. We assume that a basic condition of the geostrophic wind, V^*, and the potential

temperature, θ^* is formed. An X-axis is placed along the coast line and a Y-axis is placed on the sea, and so the monsoon wind is decided as $V<0$ in these coordinates. Upon this basic conditions which represented the barotropic state, a perturbation caused by the mesoscale conditions was added. Considering the homogeneous condition along X-axis, the perturbation is varied with Y and Z coordinates. As a result, the perturbation equations of two (y-z) dimensions were developed as follows (Williams, 1972; Økland, 1990).

The perturbation equations mentioned above, under the Boussinesq approximation and the hydrostatic assumption, are as follows.

$$\partial v / \partial y + \partial w / \partial z = 0 \qquad (1)$$

$$-V^* \partial u / \partial y + v \partial u / \partial y + w \partial u / \partial z - fv = 0 \qquad (2)$$

$$-V^* \partial v / \partial y + v \partial v / \partial y + w \partial v / \partial z + f u = \partial E / \partial y \qquad (3)$$

$$V^* \partial \theta / \partial y + v \partial \theta / \partial y + w \partial \theta / \partial z = Q / c_p \qquad (4)$$

$$\partial E / \partial z = g\theta / \theta^* \qquad (5)$$

Here, u, v and w are the perturbation velocity and θ is the perturbation temperature. The equation (1) is a continuous equation. Equations (2) and (3) denote the movement for v and w, respectively. A force caused by a balance of the thermal wind is also considered in the equation (3). Equation (4) is the first law of the thermodynamics. We assume that θ is only a function of y and is uniform through the vertical direction. In (4), a right hand term denotes the diabatic heating and Q is the heating rate per unit mass per second. Equation (5) is the pressure function,

$E=c_p\theta^*(\theta/\theta^*)^{R/cp} + gz.$

After which, we change the equations to a non-dimensional form and expand each variable in a power series. In this theory, the appropriate scales of horizontal, vertical, the geostrophic wind velocity and the difference of the temperature are follows:

L = 200 km

H = 2000 m

V = 5 m/s

θ = 10 K

Equations (1) - (5) were written in the non-dimensional form:

$$\partial v/\partial y + \partial w/\partial z = 0 \qquad (6)$$

$$-\partial u/\partial y + R(v\,\partial u/\partial y + w\,\partial u/\partial z) - v = 0 \qquad (7)$$

$$-R^2\,\partial^2 v/\partial y\partial z + RR'(v\,\partial^2 v/\partial y\partial z + w\,\partial^2 v/\partial^2 z) + \partial u/\partial z = \partial\theta/\partial y \qquad (8)$$

$$\partial\theta/\partial y - R(v\,\partial\theta/\partial y + w\,\partial\theta/\partial z) = q \qquad (9)$$

where R and R' are the Rossby numbers (R = U /fL, R' = V /fL) and q is the heating rate in a non-dimensional form. Further, each variable is expanded in a power series with the Rossby number. Considering the scale mentioned above, the Rossby number is calculated to be smaller than unity.

$u = u_o + R\,u_1 + \cdots$

$v = v_o + R'\,v_1 + \cdots$

here, each variable inserts equations (6) - (9) and zero order terms are chosen. Finally, the zero order equations are given as follows:

$$\partial v_o / \partial y + \partial w_o / \partial z = 0 \qquad (10)$$

$$-\partial u_o / \partial y - v_o = 0 \qquad (11)$$

$$\partial u_o / \partial z = \partial \theta_o / \partial y \qquad (12)$$

$$\partial \theta_o / \partial y = q \qquad (13)$$

We will calculate the perturbation solutions of zero order of u, v, w and θ. As the surface weather condition, the differential heating q which is a function of y inserted in the equation (13). In fact, once the diabatic heating of q is given, θ, u,v and w are calculated in turn numerically using the boundary conditions. The boundary conditions are thought to be w=0 at z=0 and z=H, respectively. And all variables of the perturbation are zero at minus infinity. As a result, we can calculate each variable from minus (the land) to plus (the sea) direction numerically.

5-2. Results

The behavior of the zero order solutions is investigated in this section. As a surface weather condition, the surface heating was given as a function of y. Figure 5-2 shows one case of a differential heating over the land and the sea (Case 1). In this case, the surface heat flux is given as the hyperbolic tangent distribution which means no heating over the land and a uniform heating over the sea. Therefore, each stationary solution of u,v,w and θ is calculated. Figure 5-3 indicates the wind patterns of v+w perturbation component(top), the u component (center) and the perturbation of θ (bottom), respectively. It is recognized in the figure that there are an upward motions over the sea and downward motions over the land. It is important that the seaward flow is formed at a low level and a maximum of speed appears at the coast line. The circulation is formed at the coast line where the gradient of heating is maximal and is developed all over the convective layer. The field of u component is shown perpendicular to the y-z plane. The -u (the northerly wind) maximum appears at the surface. It is thought that the u component which is the non-geostrophic wind generated in the solution would satisfy the relation of the thermal winds. The gradient of u to the z direction is plus and the wind direction is opposite at the height of H/2. The potential temperature increases linearly over the sea. The reason for θ is thought to be the influence of the uniform heating over the sea that is equal to a continuous heating.

In the second case, the surface heating is given as a probability function as shown in the Fig. 5-4 (Case 2). The peak of the heating is placed at y=0. That is the idealized case of non-uniform sea surface temperature with the concentrated heat source over the sea. In fact, the Tsushima warm current is present along the west coast of Hokkaido. Therefore, the sea surface temperature has its peak along the coast of Hokkaido where the surface temperature difference reaches about 10 K, and decreases toward the west of the Japan Sea where the difference is about 5 K in winter. Figure 5-5 shows the wind patterns of v+w, u and the perturbation of θ. It is clear that the upward motions are formed at the location where the temperature gradient is maximal. Moreover, the convergence zone of the v component is formed near the surface. This means that the the upward motion caused by the differential heating between the land and the sea is strengthened by the difference of sea surface temperature. The u component indicates the concentrated flow such as a jet stream forms near the surface. The potential temperature changes remarkably at the peak of the heating where it corresponds with the surface convergence zone and the strong updraft zone.

As a result, whereas, the geostrophic wind of V and isobars are parallel to the y axis at the initial condition, the deformation of isobars is caused by the non-geostrophic wind components. Figure 5-6 shows u and v pattern of x-y plane near the surface. The u and v perturbation components are multiplied by the geostrophic wind of 5 m/s in order to understand the actual wind field. The curvature of the wind which is equal to the isobars is the steepest at the coast which means that a low pressure area

has formed over the coast line. In fact, the calculated value of the vorticity is in an order of 10^{-5} at $y=0$ and the pressure drop is calculated to one order of 10^{-1}. It corresponds well with the pressure trough and the cyclonic wind field which is observed along the west coast of Hokkaido.

The first order solutions are also investigated in each case as shown in the Fig. 5-7. It is recognized that the second circulations in y-z plane are formed. In case 1, the surface convergence zone is formed over the sea and contributes to the strength of the upward motion. Whereas this result is a stationary solution, considering the actual phenomenon, it is assumed that the second circulation expresses a local motion which is generated from the main circulation field. In case 2, the second circulation stems from the support of the main circulation the same as case 1.

5-3. Discussion

In this section, the maintenance process of CBC is analyzed and discussed mainly. The CBC corresponds with the convergence zone along the west coast of Hokkaido. Therefore, we must consider the dynamical explanation of the CBC formation. Considering the CBC is a phenomenon formed in the mesoscale lower convective layer, it is conjectured that the effects of the heating and friction are important to generate the convergence field along the coast. Roeloffzen et al. (1986) investigated the coastal flows under the influence of the friction. They calculated the secondary flow patterns of existing any geostrophic wind. However, the wind speed used in their calculation was fixed as 20 m/s in their model which value is as strong as an actual monsoon wind. In fact, the moderate wind speed is needed to form the convergence wind field. Hjelmfelt (1990) carried out a numerical study of the lake-effect snowstorms over Lake Michigan in the United States of America. He investigated the environmental conditions, that is, the wind speed, wind direction, differential temperature, stability and so on. His results suggested that the marginal value of the wind speed to generate the lake breeze was 3 - 5 m/s when the temperature difference between the lake surface and the land was 10 ˚C. On the other hand, Nagata (1987) indicated that the thermal effect was more important than the effect of friction to form the convergence zone in the Japan Sea using a very-fine-mesh model of J.M.A.. Therefore, the differential heating was considered as the

main thermal effect.

From the analysis of the life cycle of CBC, it was understood that the CBC was maintained for long time under an almost uniform synoptic weather situation after the mature stage of CBC which was elongated for 200 to 300 km. It is considered therefore that the maintenance process of CBC was characterized by following conditions for simplicity: 1) the presence of relative low pressure area along the coast line, 2) three different wind directions which make a cyclonic flow pattern, especially, a balance of wind between the northwesterly monsoon wind and the southeasterly low level land breeze, 3) the development of the wind shear line which has a front like structure and 4) the stagnation of the band echoes near the coast line which bring about the merging of band echoes. The conditions of 1) and 2) are characterized by the long-lasting field near the sea surface for the CBC and the conditions of 3) and 4) are characterized by the features of band echoes.

The purpose of this linear and dry model is to confirm the presence of the convergence zone near the west coast of Hokkaido. For the four conditions mentioned above, the results obtained could be checked as follows. (1) The low pressure zone on the coast line is formed by the u component that originates when the thermal wind relation is satisfied. And the low pressure zone corresponds to the convergence and cyclonic vorticity fields. (2) Non-geostrophic circulation is generated, that is, the downward motion over the land and the upward motion over the sea are predominant. Moreover, the seaward low level flow (corresponding to the easterly wind) is formed at the coast line.

(3) The horizontal gradient of the potential temperature is concentrated in the area where the upward motion is strongest and the value of heating has its maximal value. In particular, the peak of the temperature gradient appears in the case of the differential heating over the sea considering the conditions of the actual Japan Sea. From these results, it may be realized that the horizontal deformation field is formed at the low level under the non-geostrophic circulation which strengthens the front. In fact, the surface convergence of v component appears in the second circulation (Case 1) and in the main circulation (Case 2). And so, this result expresses the dynamical effects and well explains the analyzed field. (4) However, in this linear and dry model, the heating accompanying the latent heat, the down draft in a cold dome and the cold land breeze could not be treated. For example, according to the satellite pictures of the organized CBC, the eastern edge of CBC is more distinct. Moreover, the merging process of band echoes in CBC also could not be explained from this result. It is suggested therefore that the effects of the thermodynamics in clouds would be important, after the developing of CBC clouds.

Generally, a term of the wind which makes the thermal wind component and the diabatic heating term contribute to frontogenesis (Williams, 1972). In our case, only the diabatic heating is given as an initial condition. As a result, the dynamical effects to the coastal frontogenesis caused by the diabatic heating were made more clear in this model. Still, the direction of the uniform geostrophic wind is also important to

deform the field. Bosart (1975) analyzed the coastal frontogenesis at New England in the United States. He emphasized both importance of the direction of a coast line and the differential friction between the sea and the land. That is to say, it means that the frontogenesis is advanced when a favorable angle between the direction of a pressure gradient and that of the surface temperature gradient is formed. Moreover, the northerly wind caused by the land friction plays a role of non-geostrophic circulation. The direction of the geostrophic wind is decided by the favorable synoptic weather situation. Actually, in many cases of the New England, the coastal front is observed in December.

There is a difference between the coastal fronts in the eastern coast of the United State and that in the western coast of Hokkaido Island, but both cases has s similar relationship between the direction of surface temperature gradient and the geostrophic wind direction. Figure 5-8 indicates the schematic picture of non-geostrophic winds. It is obvious that a pair of upward motions over the sea and downward motions over the land, seaward motions at the surface and landward motions at the top along the coast line, and southerly u component at the surface and northerly u component at the top along the temperature gradient zone. However, no u component appears over the land from this calculations. It is expected that u component (southerly) over the land shown in the figure would supports and strengthen these circulations. Actually, the southeasterly surface cold breeze is observed along the west coast of Hokkaido in the mature stage of CBC. It is considered to play a role for the horizontal

non-geostrophic coast-parallel wind which supports the horizontal circulation at the coast line. Therefore, considering the surface weather conditions over Hokkaido, it is recognized that the cold land breeze acts as a non-geostrophic wind over the land instead of the frictional driven surface wind.

6. Conclusions

In this paper, firstly the time change of long-lasting CBC occurring along the west coast of Hokkaido draws the most attention, and was also analyzed from the satellite data and the radar data. We can summarize our findings as follows. The long-lasting CBC (Type A) occurs in midwinter seasons under the conditions of winter monsoon synoptic situations and the low level cold dome covering Hokkaido. The lifetime of CBC is several hours to two or three days.

The life cycle of CBC is divided into three parts. The initial stage of CBC is characterized by the disturbances which are generated to the west of the Soya Strait and the disturbances are characterized by the low T_{BB} area under the convergence of the monsoon wind and the northeasterly relative cold wind having a thickness of more than 1 km. In the mature stage, the CBC is characterized by the organized CBC for 200 to 300 km in length under the convergence of the monsoon wind and the southeasterly cold land breeze. And the dissipating stage is characterized by the meandering CBC and the CBC disappears from the north end.

The most developed area in CBC corresponded well with the surface wind shear line. The wind shear line which is formed between the monsoon wind and the northeasterly wind moves southward and the CBC elongates gradually. A mesoscale low pressure zone along the coast line is dominant in the initial stage. And in the mature stage, a mesoscale high pressure zone

over Hokkaido Island caused by the radiation cooling inland is dominant. On any event, a low pressure field is continuing relatively for a long time along the west coast of Hokkaido.

Several cases of the disturbances associated with CBC were observed during the special radar observation period carried out at Haboro, Rumoi Sub-prefecture, Hokkaido. The mesocyclones are generated in the center of spiral echoes at the south end of CBC under the mesoscale low pressure zone (200 km). These mesocyclones are about 30 km in diameter and the echo free area is 5 to 10 km in diameter at least from this observation. Furthermore, they have wind fields that bring gust winds to the surface. Accompanying the gust front, a pressure drop of 1 mb is observed. After that the thermal structure of a warm core in the mesocyclone generated over the sea is seen at the echo free region. It is important that these mesocyclones are one order smaller than CBC (the low pressure zone) but have a distinct thermal structure inside.

For the generation of the mesocyclones, it was recognized that the low pressure field and the surface winds with three different directions are necessary. As the horizontal wind shear is most intense at the coast line, the mesocyclones generate around the coast line as expected.

On the other hand, the formation process of line echoes mainly depends on the different wind directions and wind speeds. Regarding as band echoes, the merging and the separation processes are clarified by our radar observations. In particular, the CBCs are constructed from the merging by several band echoes having a difference of propagation speeds near the coast line. As

a result, the CBC appears to stagnate for long time at almost the same place near the coast line.

Considering the mechanism of long-lasting effect of the CBC along the coast line, we investigated the dynamical effects by means of the diabatic heating. The two dimensional model is constructed and calculations are accomplished under a uniform synoptic situation and geostrophic wind field. The effect of diabatic heating constitute a non-geostrophic wind circulation on a y-z plane, that is to say, the downward motion over the land and the upward motion over the sea. Especially, a differential heating between the regions at land-sea and over the sea is very important to produce the surface wind convergence and the surface temperature gradient. The calculation results coincide well with those of the analyses. And so, the CBC is explained dynamically as a boundary layer phenomenon under a balance of the horizontal pressure gradient and the pronounced horizontal thermal gradient. This dynamical feature is similar to that of coastal front.

Finally, we must realize a scenario through the life cycle of CBC. Therefore, further studies are required for the thermal dynamics in CBC to form the surface front and the structure of disturbances in the initial stage which have not been observed to the present.

Acknowledgments

The author wishes to his thanks to Professor Katsuhiro Kikuchi, Meteorological Laboratory, Faculty of Science, Hokkaido University, to give the advice and encouragement through this study. He would like to acknowledge Dr. T. Harimaya and Dr. H. Uyeda of the same laboratory, and Prof. H. Økland of Oslo University. He wishes to express officially his thanks to Sapporo District Meteorological Observatory, Haboro and Rumoi Meteorological Stations and Meteorological Satellite Center of J.M.A. for using meteorological data and permission to utilize GMS data. This study was carried out as a link in the chain of the program of the JSPS Fellowships for Japanese Junior Scientists . And a part of this study was supported by Grant-in-Aid for the encouragement of Young Scientists NO.610380202068 of the Ministry of Education, Science and Culture of Japan.

References

Asai, T. and Y.Miura, 1981. An analytical study of meso-scale vortex-like disturbances observed around Wakasa Bay area. J. Meteor. Soc. Japan, **59**, 832-843.

Bosart, L.F., 1975. New England coastal frontogenesis. Quart. J. R. Met. Soc., **86**, 51-66.

Fujiyoshi, Y., K.Tsuboki, G.Wakahama and H.Konishi, 1988. Doppler radar observation of convergence band cloud formed on the west coast of Hokkaido Island (I) -warm front type-. Tenki, **35**, 427-439. (In Japanese).

Harimaya, T., 1970. On the small scale cyclone formed on the Japan Sea to the west of Hokkaido Island. Geophys. Bull. Hokkaido Univ., **23**, 73-81 (In Japanese with English abstract).

Harimaya, T. and S.Kato, 1988. Confluent phenomena of band-shaped radar echoes in winter. Geophys. Bull. Hokkaido Univ., **51**, 35-45 (In Japanese with English abstract).

Hjelmfelt, M.R., 1990. Numerical study of the influence of environmental conditions on lake-effect snowstorms over Lake Michigan. Mon. Wea. Rev., **118**, 138-150.

Kobayashi, F., K.Kikuchi and T.Motoki, 1987. Studies on the convergence band clouds formed in the mid-winter seasons on the west coast of Hokkaido Island, Japan. Geophys. Bull. Hokkaido Univ., **49**, 341-357 (In Japanese with English abstract).

Kobayashi, F., K.Kikuchi and H.Uyeda, 1989, A mesocyclone generated in snow clouds observed by radar on the west coast of Hokkaido Island, Japan. J. Fac. Sci., Hokkaido Univ., VII, **8**, 381-396.

Kono, Y. and C.Magono, 1967. A study on the small scale cyclone on the Ishikari Bay. Geophys. Bull. Hokkaido Univ., **18**, 71-81 (In Japanese with English abstract).

Matsumoto, S. and K.Ninomiya, 1969. Study on the meso-scale disturbances accompanied with snowfall. Tenki, **16**, 291-302 (In Japanese).

Magono, C., 1971. On the localization phenomena of snowfall. J. Meteor. Soc. Japan, **49**, 824-835.

Miyazawa, S., 1967. On vortical meso scale disturbances observed during the period of heavy snow or rain in the Hokuriku district. J. Meteor. Soc. Japan, **45**, 166-176.

Motoki, T., 1974. A small cyclonic echo pattern formed in the Ishikari Plain. Tenki, **21**, 245-250 (In Japanese).

Muramatsu, T., 1979. The cloud line enhanced by upwind orographic features in winter monsoon situations. Geophys. Magazine, **38**, 1-15.

Muramatsu, T., S.Ogura and N.Kobayashi, 1975. The heavy snowfall arisen from small scale cyclone on the west coast of Hokkaido Island. Tenki, **22**, 369-379 (In Japanese).

Nagata, M., 1987. On the structure of a convergent cloud band over the Japan Sea in winter; a prediction experiment. J. Meteor. Soc. Japan, **65**, 871-883.

Ninomiya, K., 1989. Polar/comma-cloud lows over the Japan Sea and the North Pacific in winter. J. Meteor. Soc. Japan, **67**, 83-97.

Ohmoto, R., H.Uyeda and K.Kikuchi, 1989, Structures of planetary boundary layers observed by a doppler sodar in a cold season at Sapporo, Japan. Environ. Sci., Hokkaido University, **12**, 155-167.

Okabayashi, T. and M.Satomi, 1971. A study on the snowfall and its original clouds by the meteorological radar and satellite (I). Tenki, **18**, 573-581 (In Japanese).

Økland, H., 1990. The dynamics of the coastal troughs and coastal fronts. Tellus, **42A**, 444-462.

Roeloffzen, J.C., W.D.Vandenverg and J.Oerlemans, 1986. Frictional convergence at coastlines. Tellus, **38A**, 397-411.

Sasaki, H. and S.Deguchi, 1988. Numerical experiments of the convergent band formed off the western coast of Hokkaido in winter. Tenki, **35**, 723-729.

Shapiro, M.A., L.S.Fedor and Tamara Hampel, 1987. Research aircraft measurements of a polar low over the Norwegian Sea. Tellus, **39A**, 272-306.

Tsuboki, K., Y.Fujiyoshi and G.Wakahama, 1989a. Structure of a land breeze and snowfall enhancement at the leading edge. J. Meteor. Soc. Japan, **67**, 757-770.

Tsuboki, K., Y.Fujiyoshi and G.Wakahama, 1989b. Doppler radar observation of convergence band cloud formed on the west coast of Hokkaido Island. II: cold front type. J. Meteor. Soc. Japan, **67**, 985-999.

Williams, R. T., 1972. Quasi-geostrophic versus non geostrophic frontogenesis. J. Atmos. Sci., **29**, 3-10.

Yagi, S., T.Yoshida, N.Maeda, A.Kamoshida, Y.Tanaka, H.Kikuchi and T.Nakajima, 1979. Analysis of small scale low in the west coast of Hokkaido. Tenki, **26**, 87-97 (In Japanese).

Yamaguchi, K. and C.Magono, 1974. On the vortical disturbances in small scale accompanied with the meso scale front in Japan Sea in winter season. Tenki, **21**, 83-88 (In Japanese).

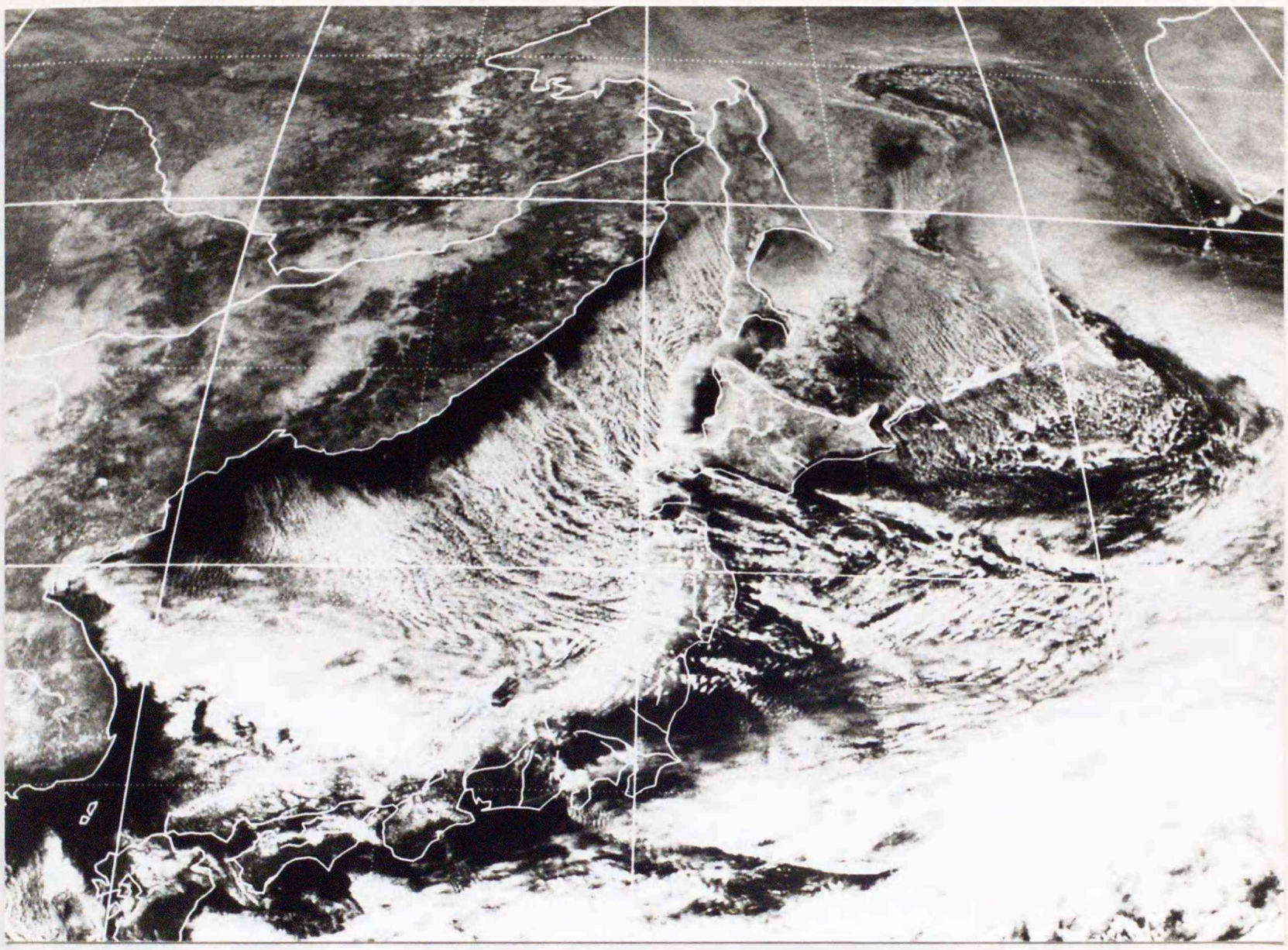

Fig. 2-1 GMS visible picture of the convergence band clouds (CBC : Type A) at 12 JST Jan. 25, 1981.

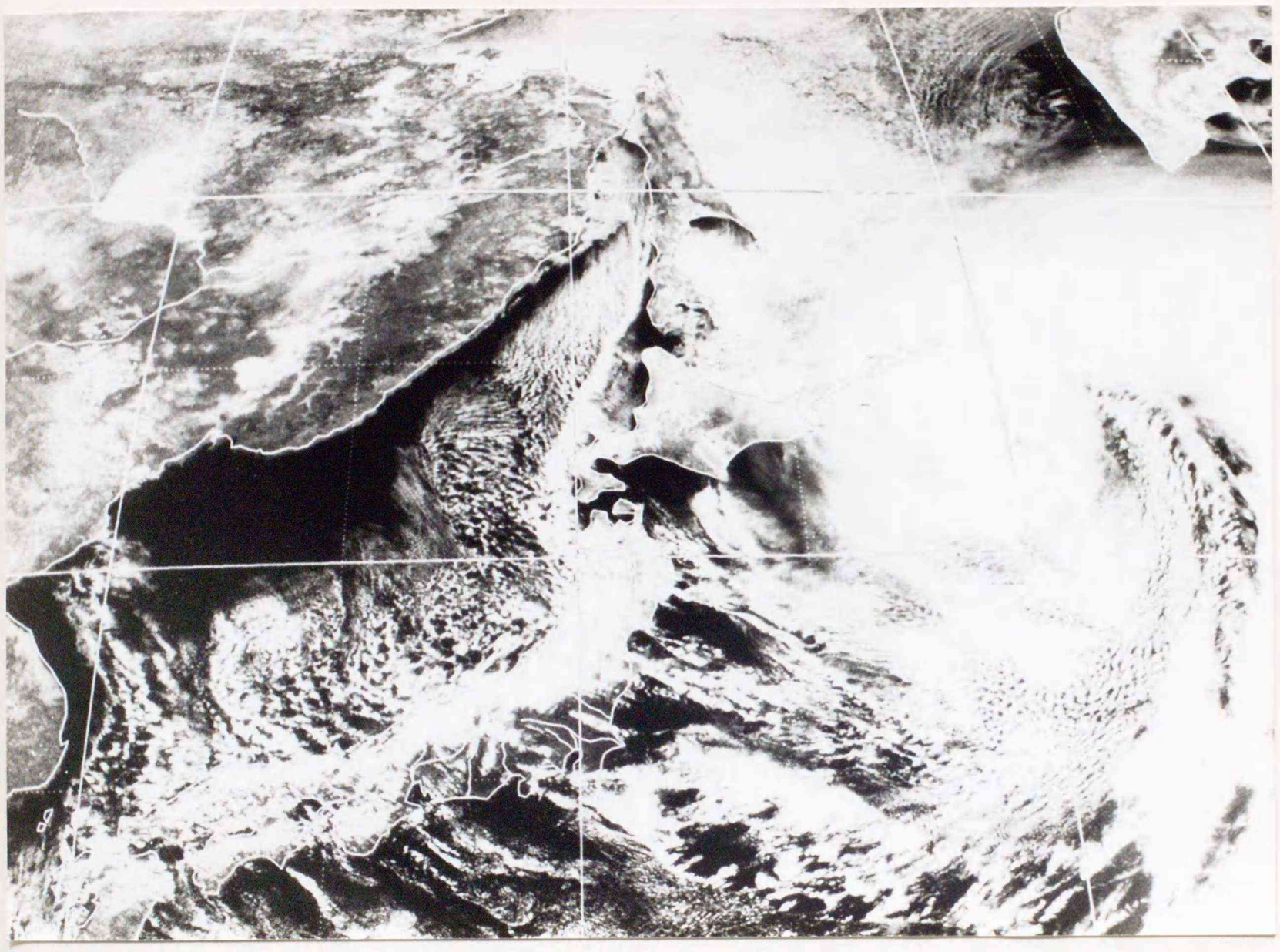

Fig. 2-2 GMS visible picture of CBC (Type B) at 12 JST Mar. 14, 1983.

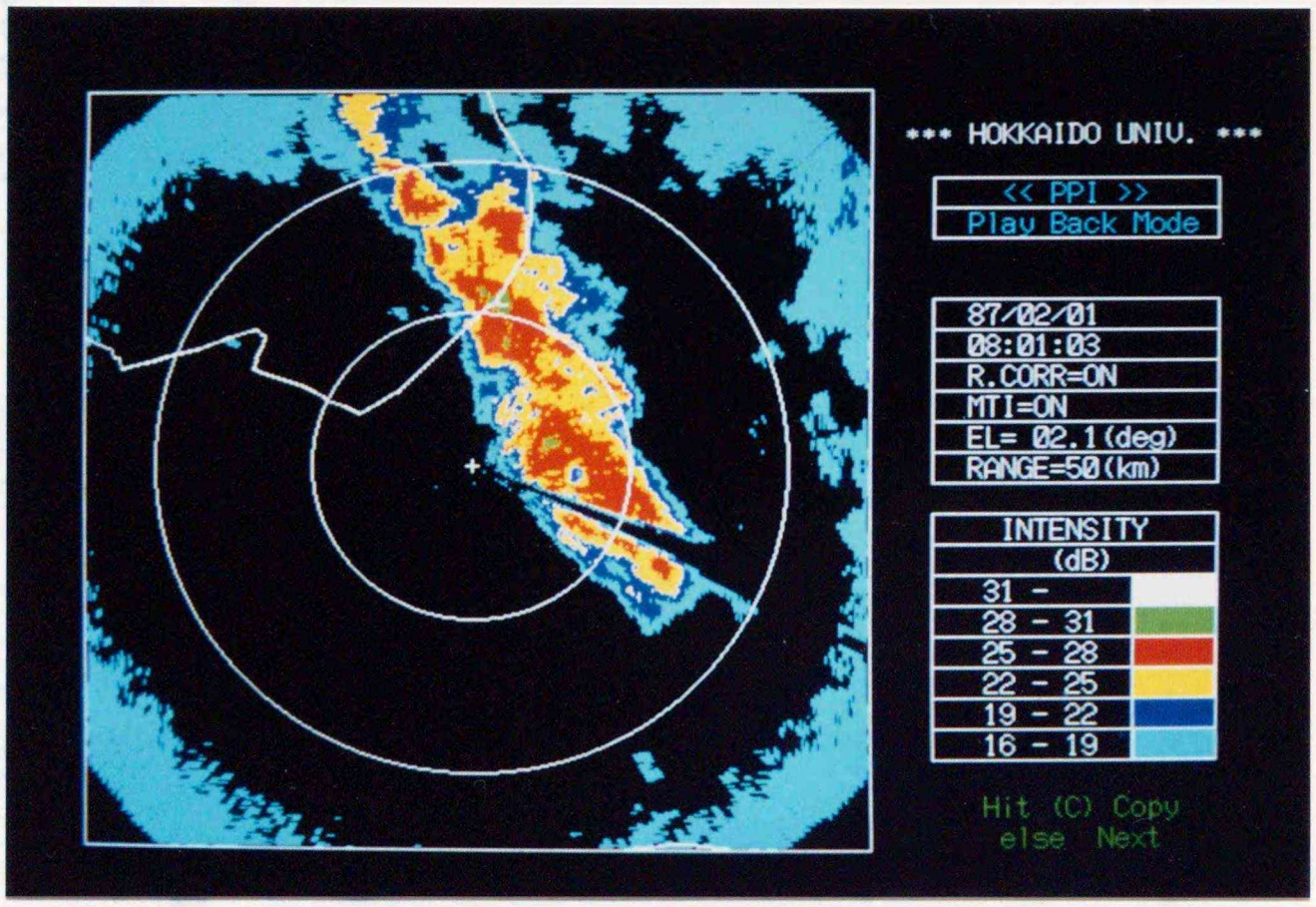

Fig. 2-3 Radar echo display at Hokkaido University on the case of February 1, 1987. The radar range circles are 20 km, 40 km, respectively.

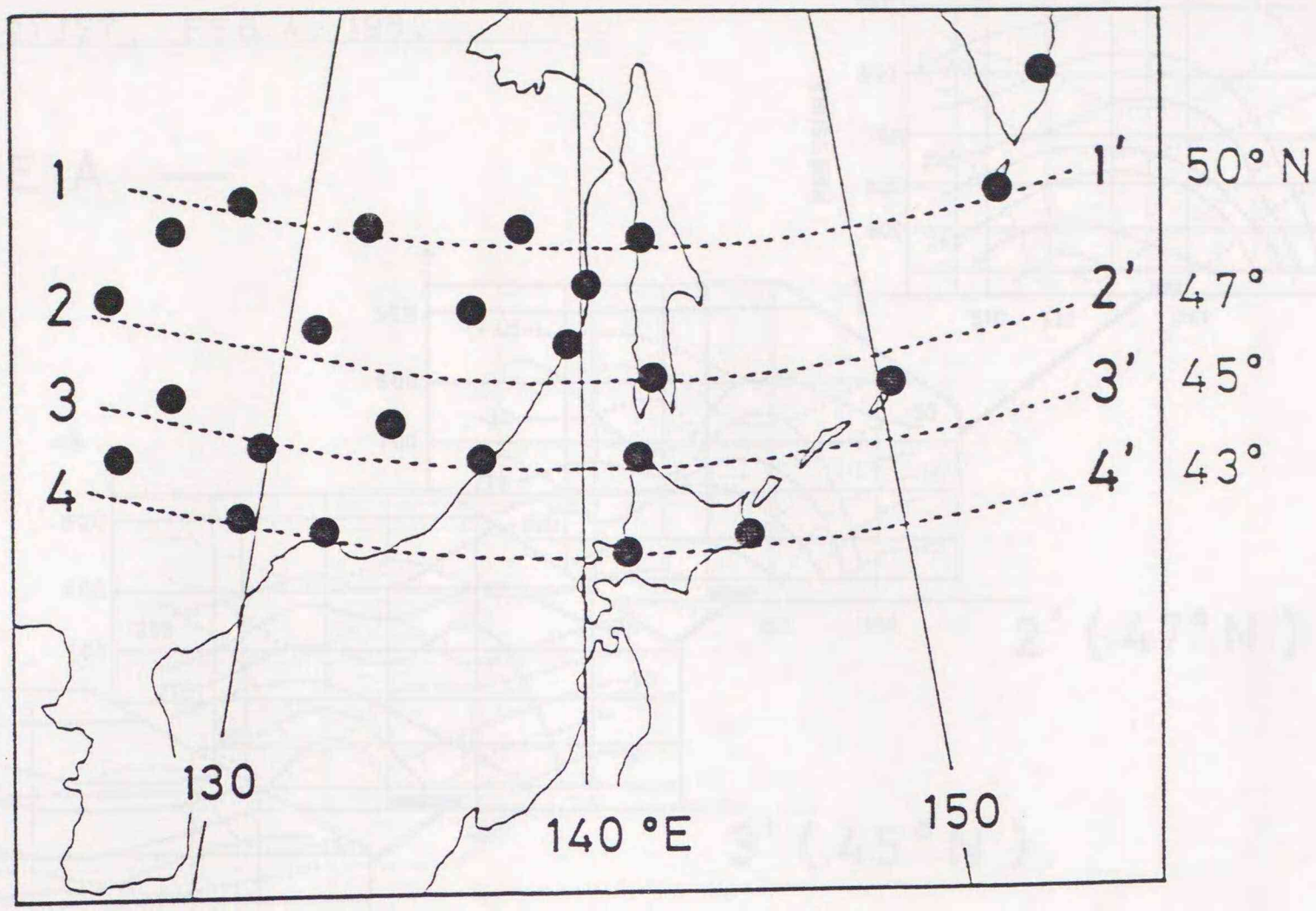

Fig. 2-4 The positions of the upper air sounding stations around Hokkaido.

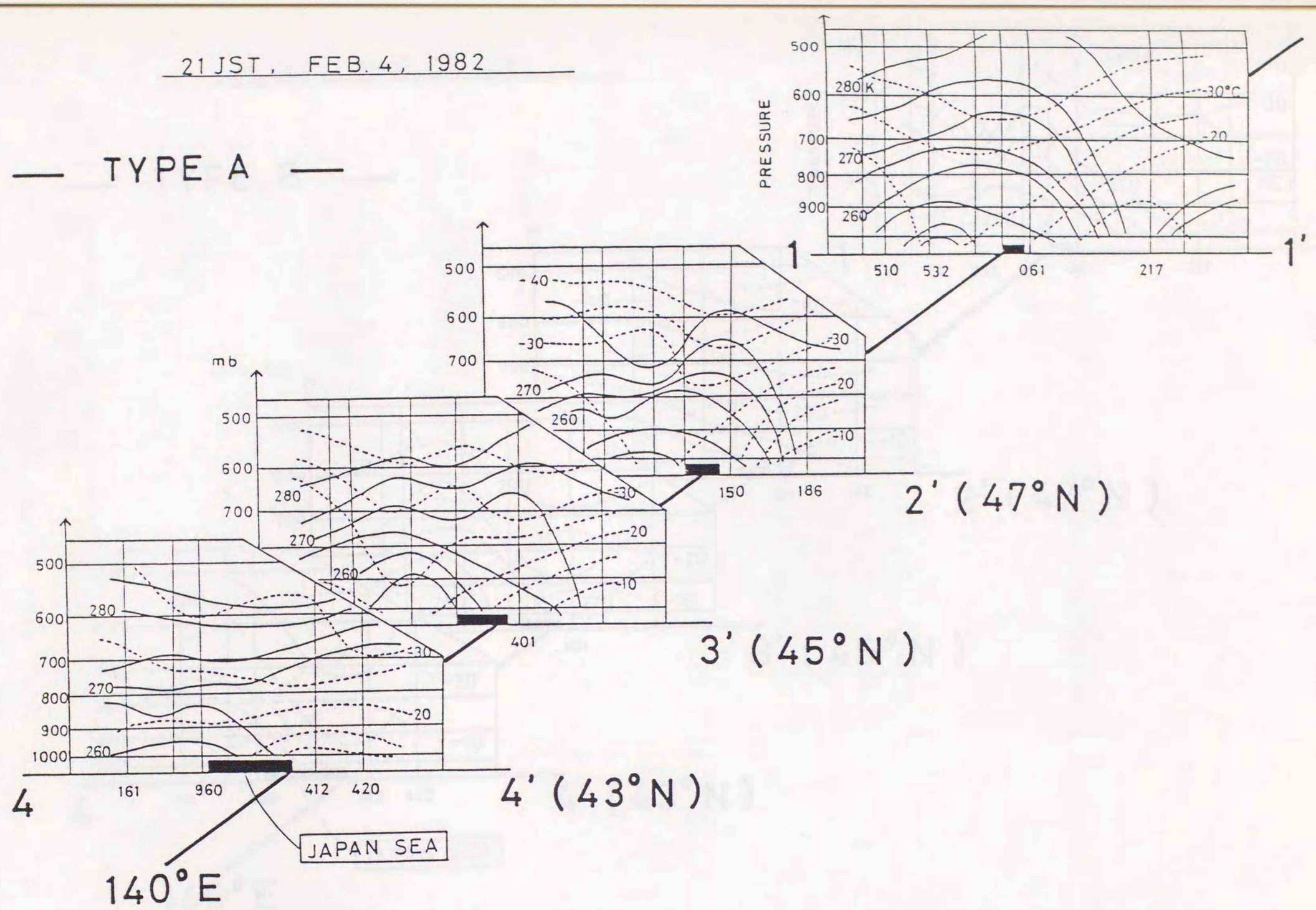

Fig. 2-5 The east-west cross sections of the equivalent potential temperature and temperature along four latitudes at 21 JST Feb. 4, 1982 (Type A).

21 JST, MAR. 7, 1981

— TYPE B —

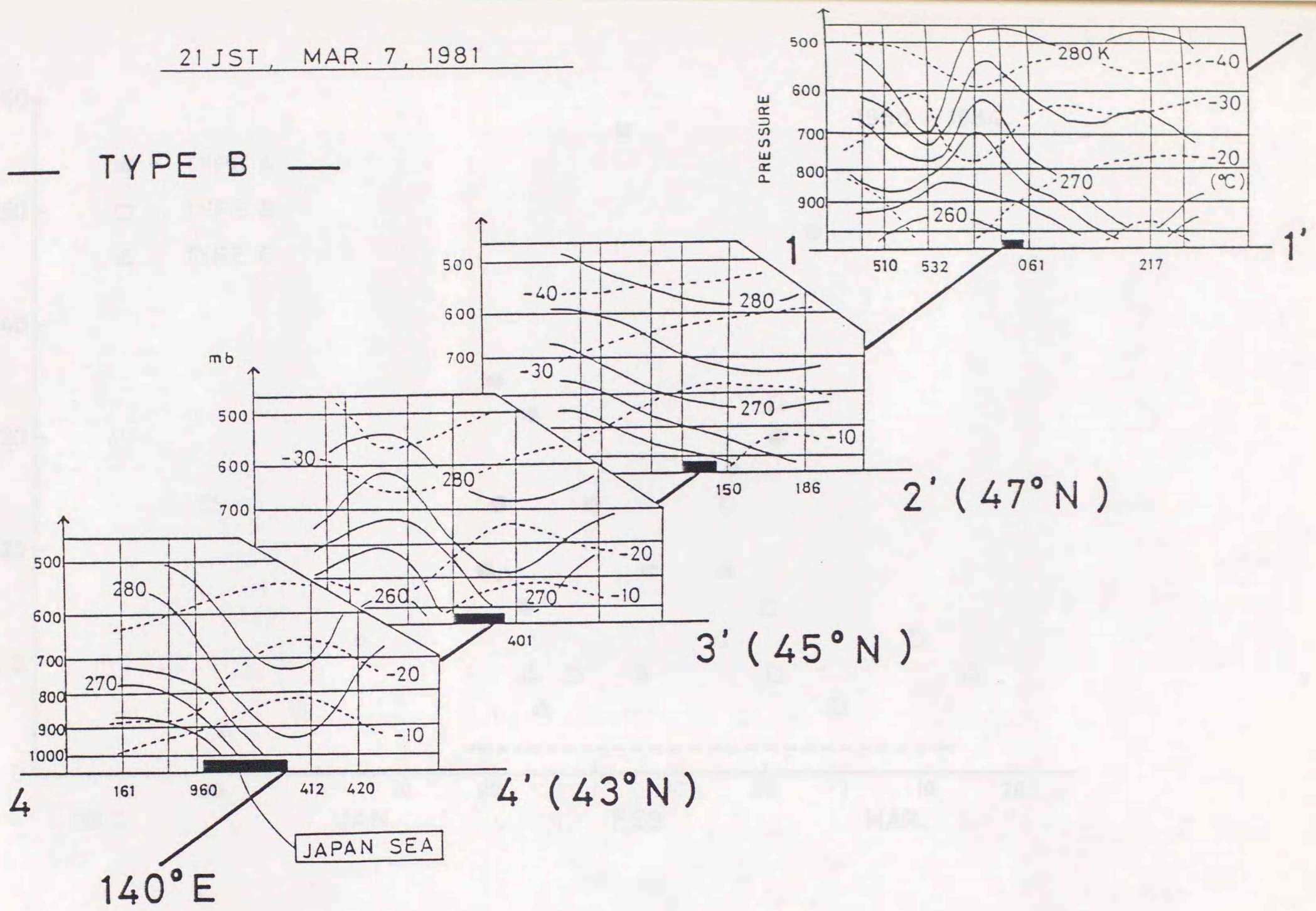

Fig. 2-6 Same as Fig. 2-5 except for at 21JST Mar.7, 1981 (Type B).

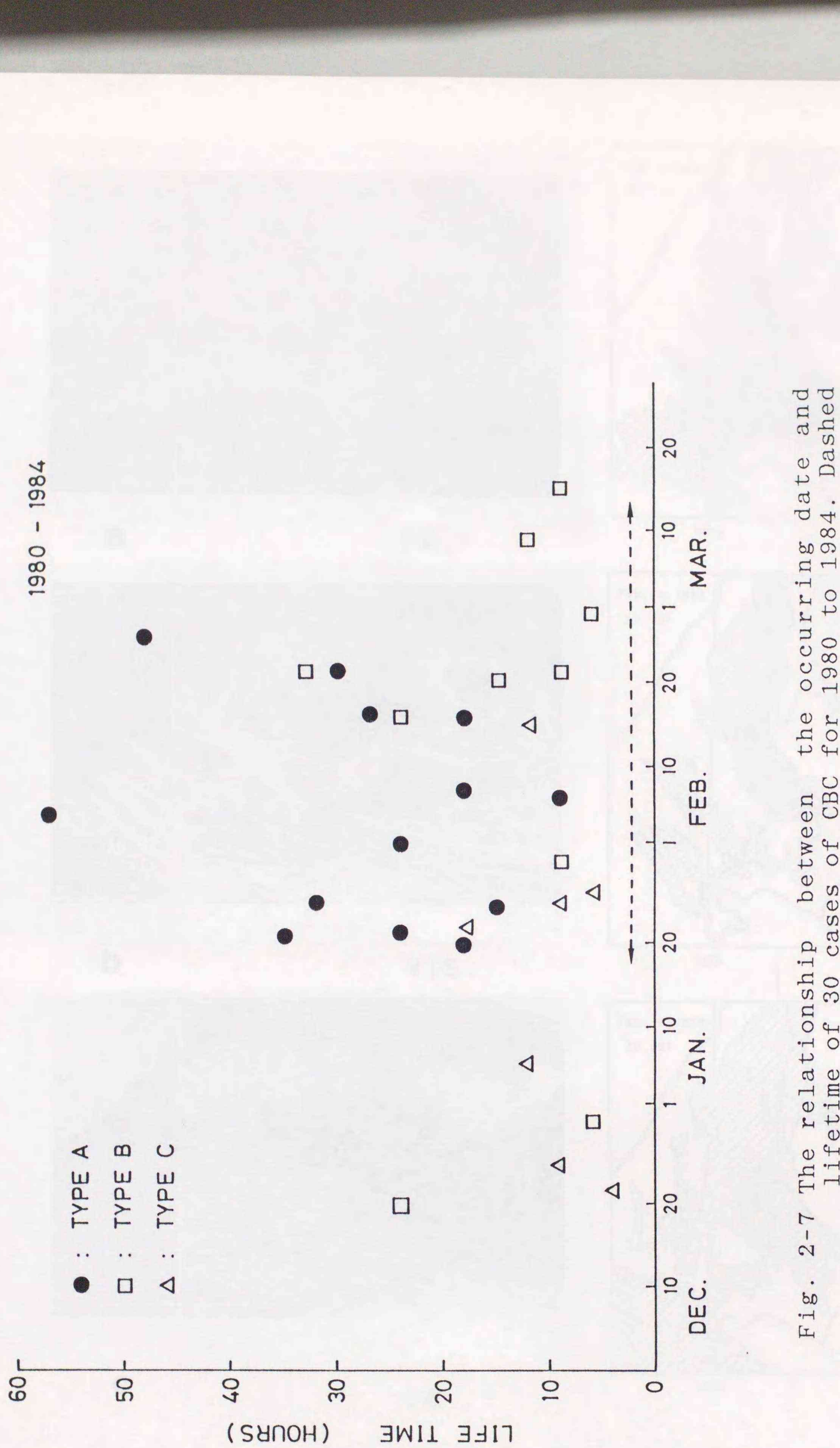

Fig. 2-7 The relationship between the occurring date and lifetime of 30 cases of CBC for 1980 to 1984. Dashed line indicates the average period of the sea ice over the Okhotsk Sea.

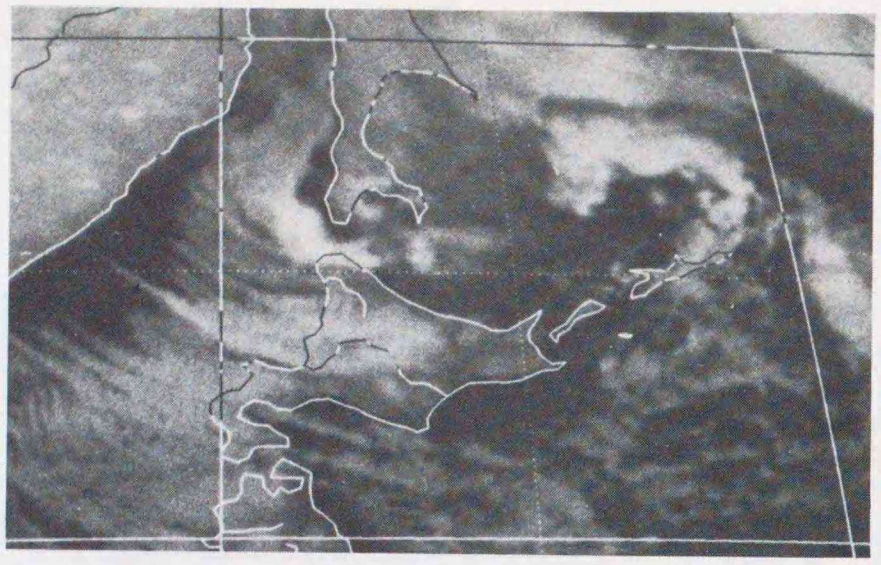

a IR.

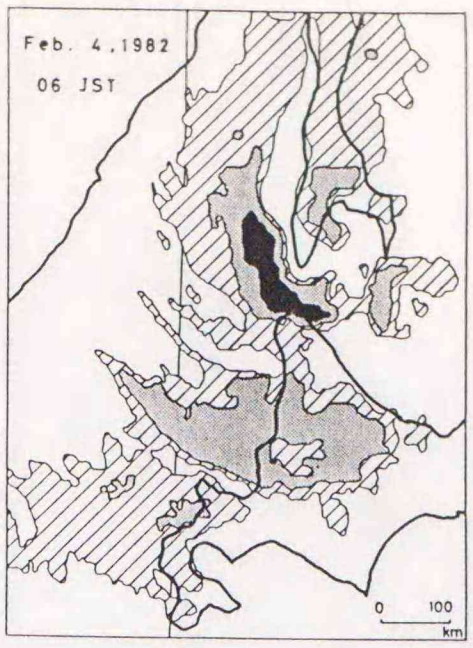

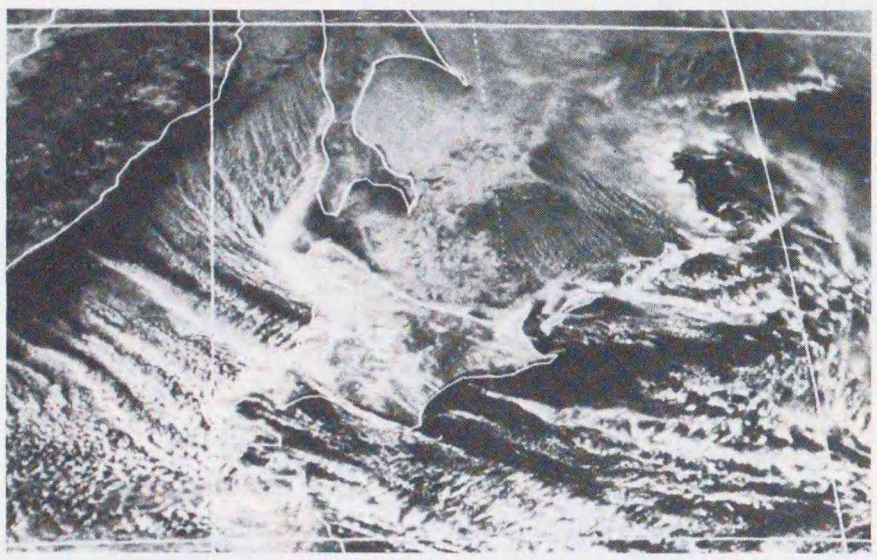

b VIS.

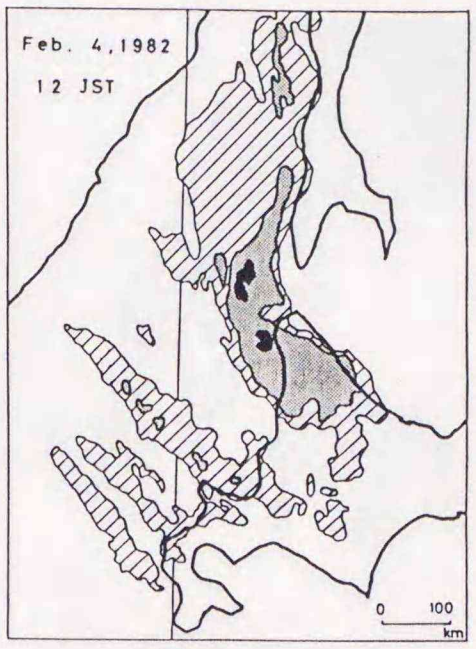

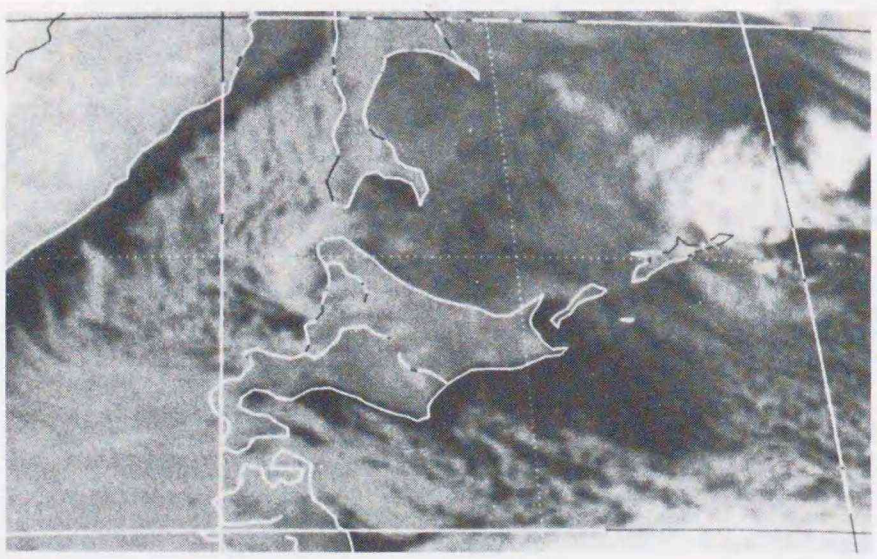

c IR.

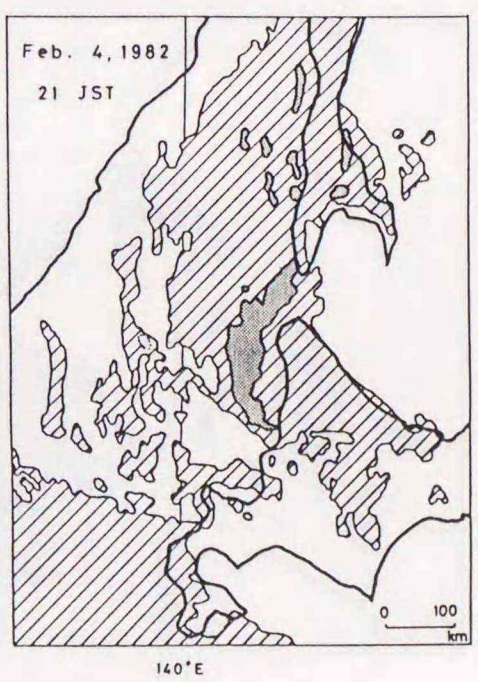

Fig. 3-1 Sequential displays of GMS images and T_{BB} distributions from 06 JST Feb. 4 through 09 JST Feb. 6, 1982, showing the formation process of CBC to the west coast of Hokkaido. Areas of T_{BB} < -22, -30 and -40 °C are indicated by hatched, stippled and solid, respectively.

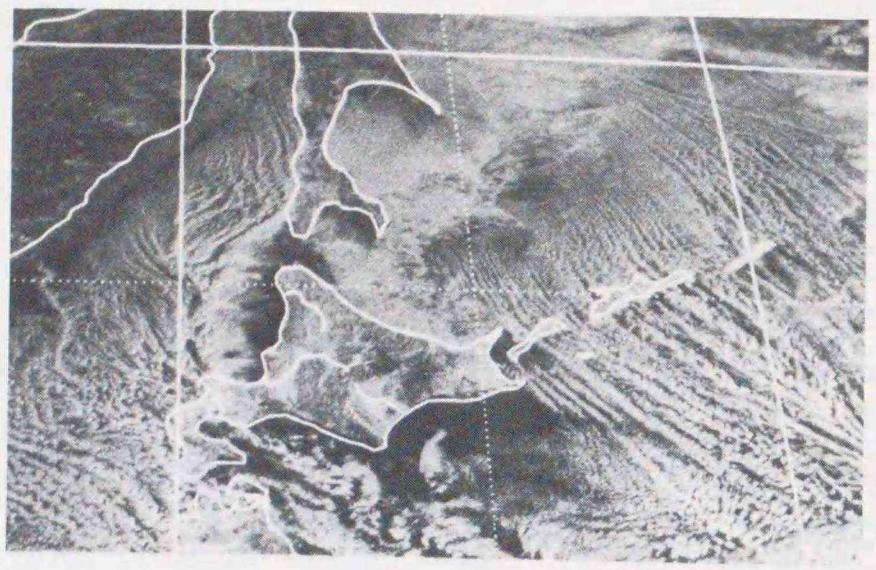

d VIS.

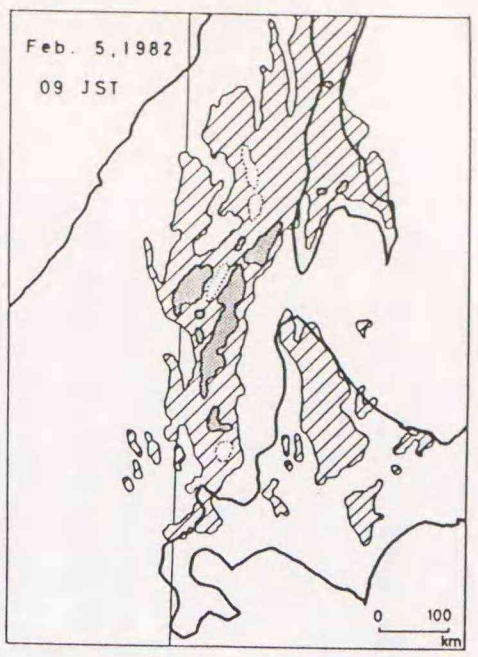

140°E

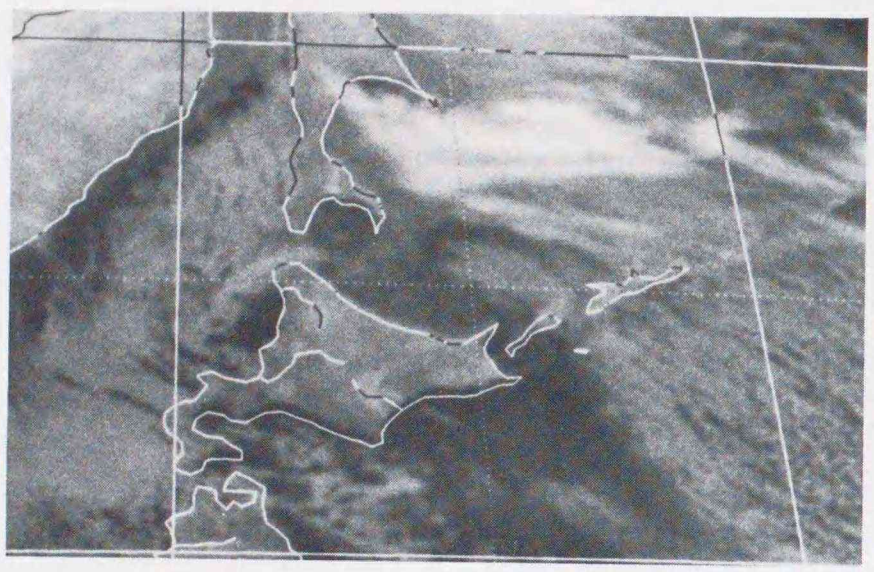

e IR.

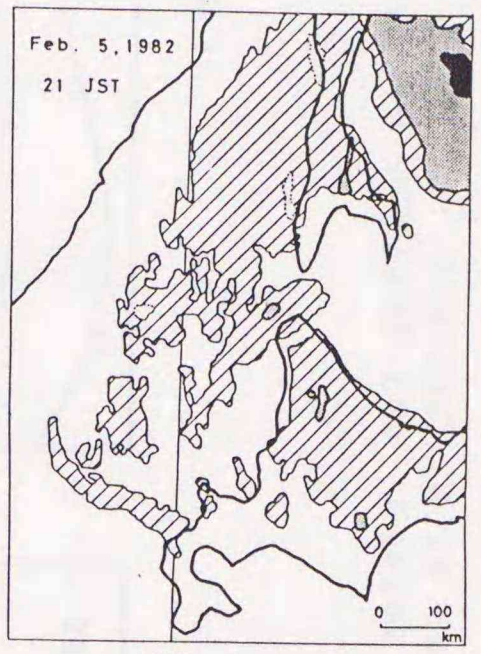

140°E

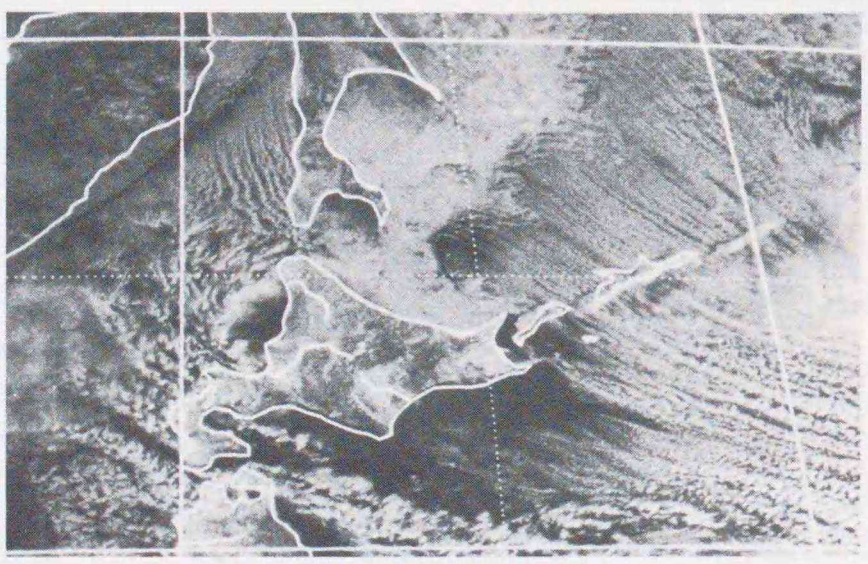

f VIS.

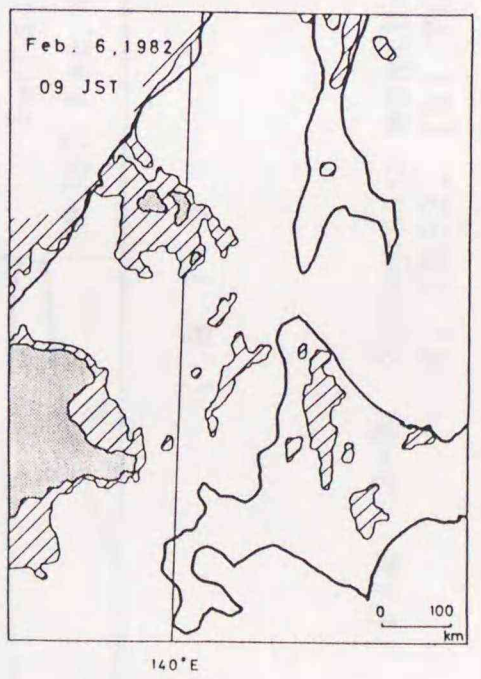

140°E

Fig. 3-1 (Continued)

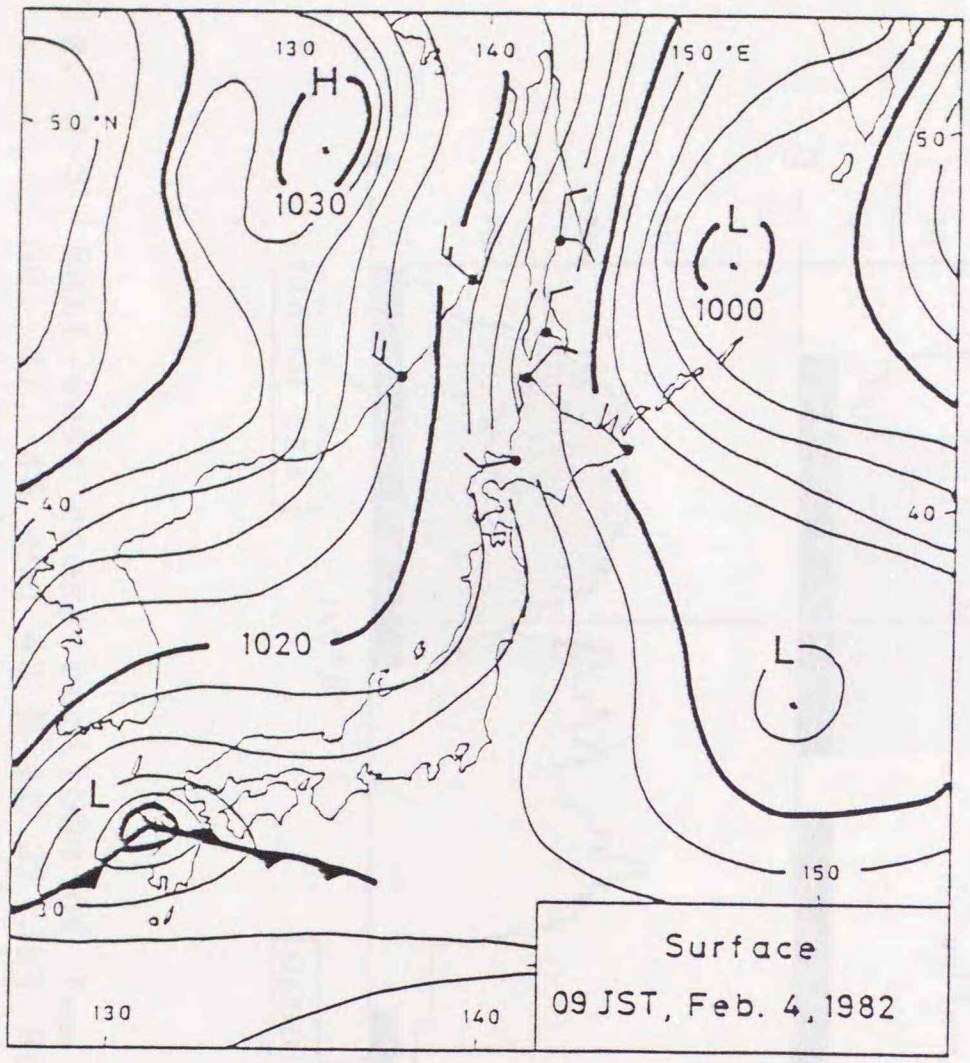

(a)

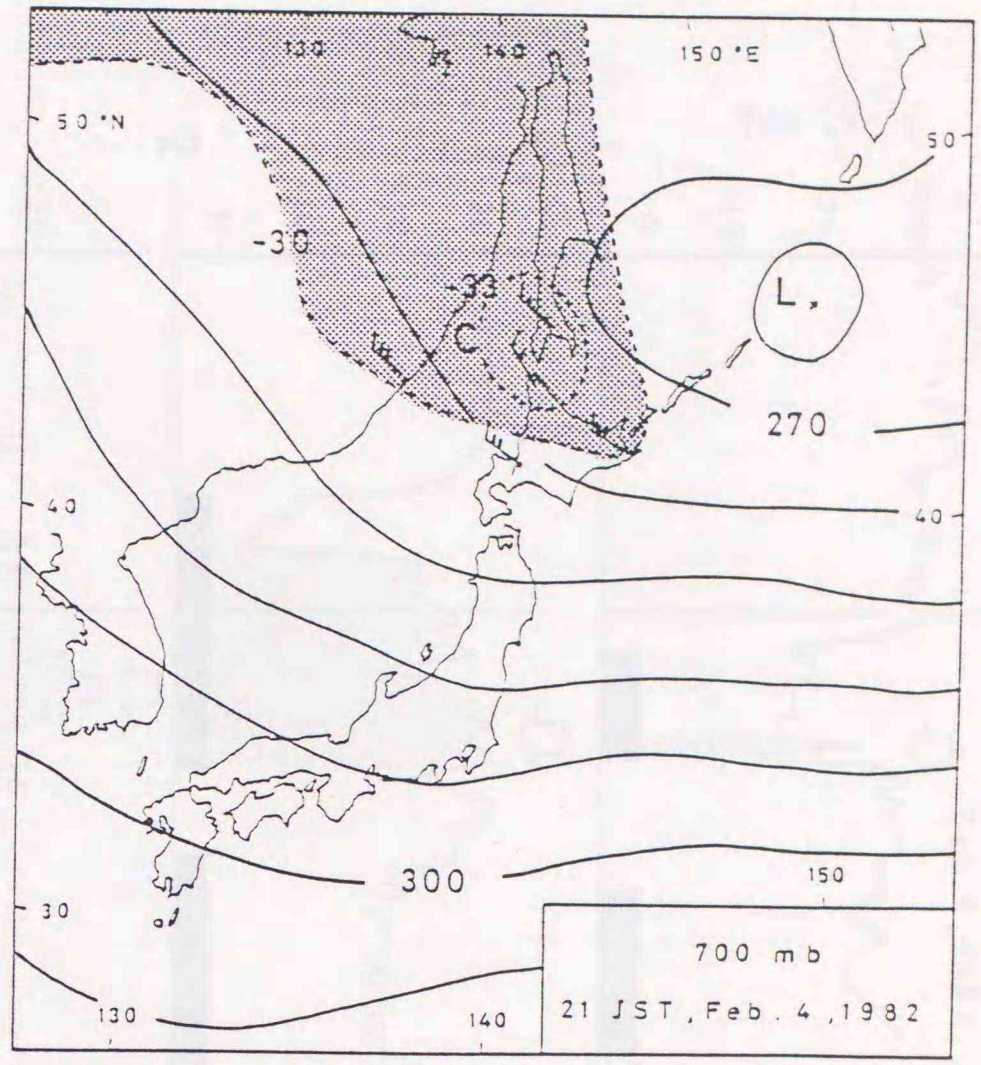

(b)

Fig. 3-2 Synoptic weather charts. (a) Surface at 21 JST Feb. 4, 1982. (b) 700 mb at 21 JST Feb. 4, 1982.

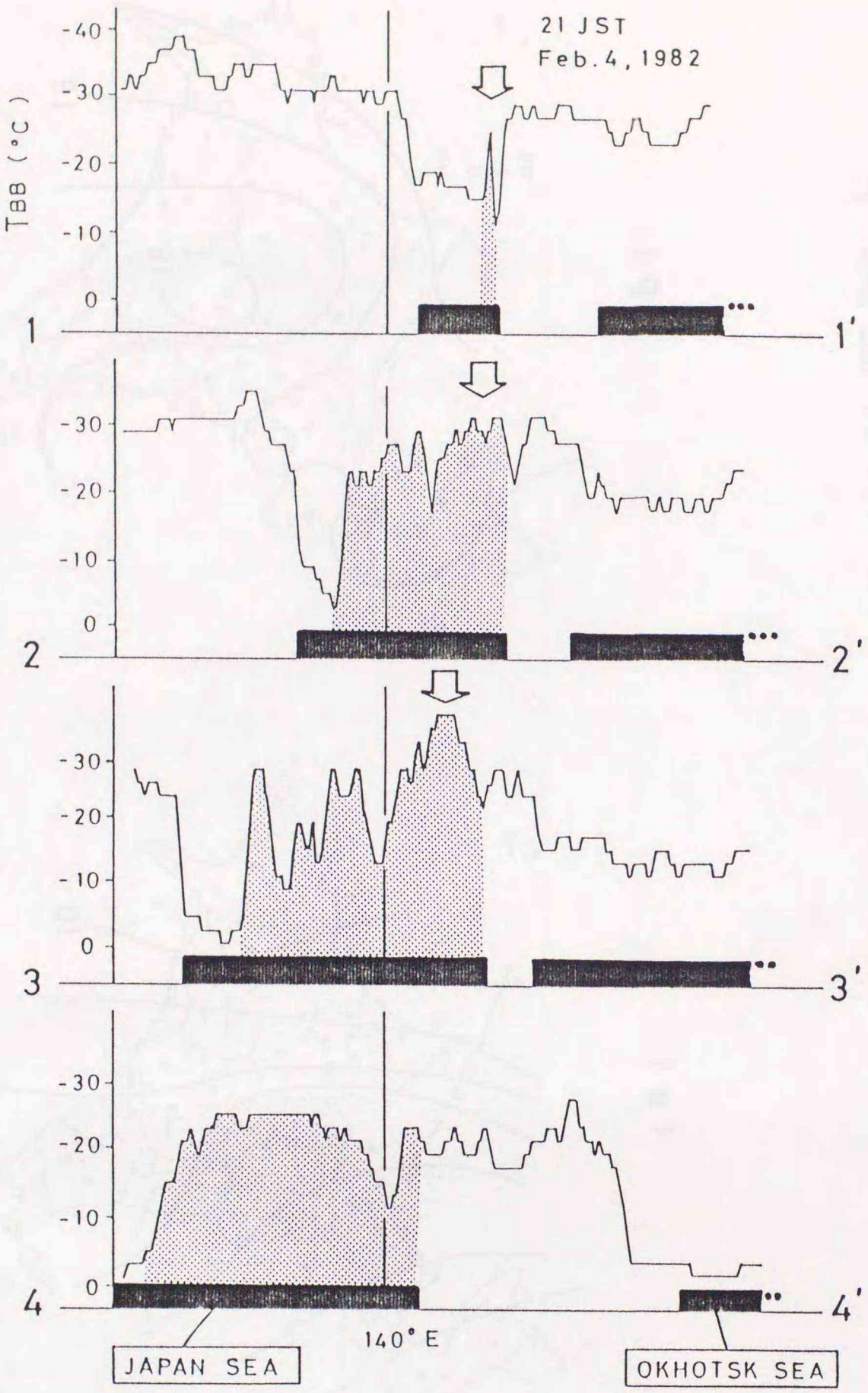

Fig. 3-3 East-west cross sections of T_{BB} in each latitude of 50, 47, 45 and 43° N at 21 JST Feb. 4, 1982. Stippled areas and double arrows denote cloud regions and the position of CBC, respectively.

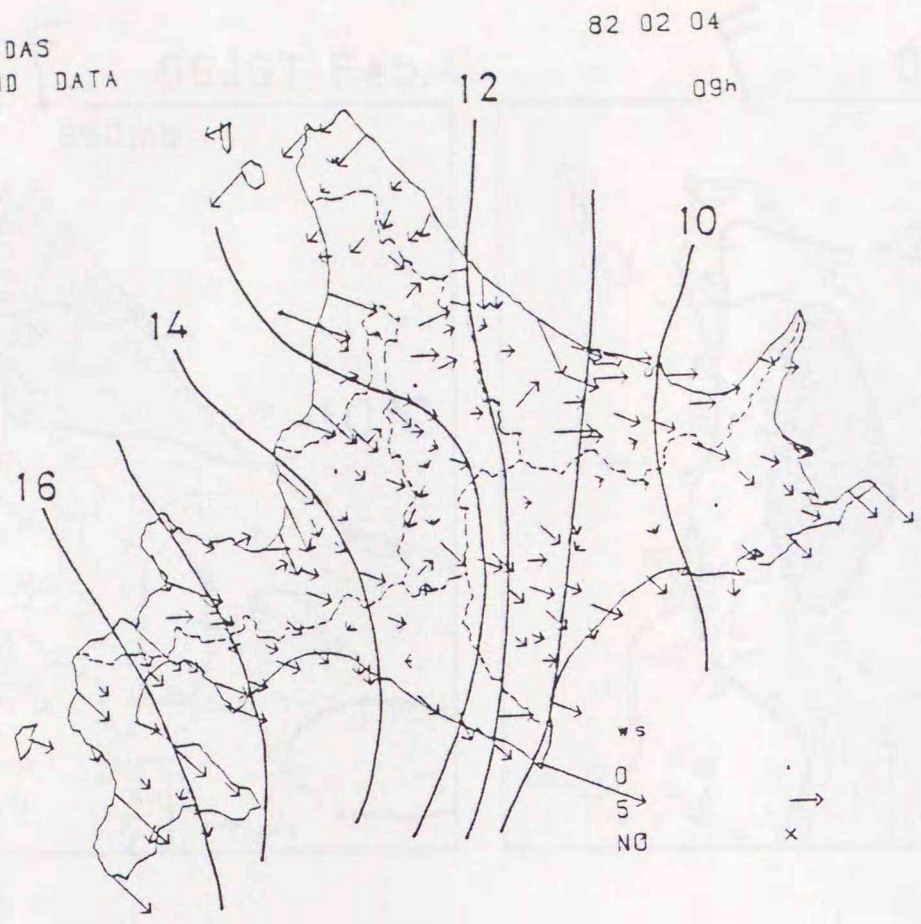

(a)

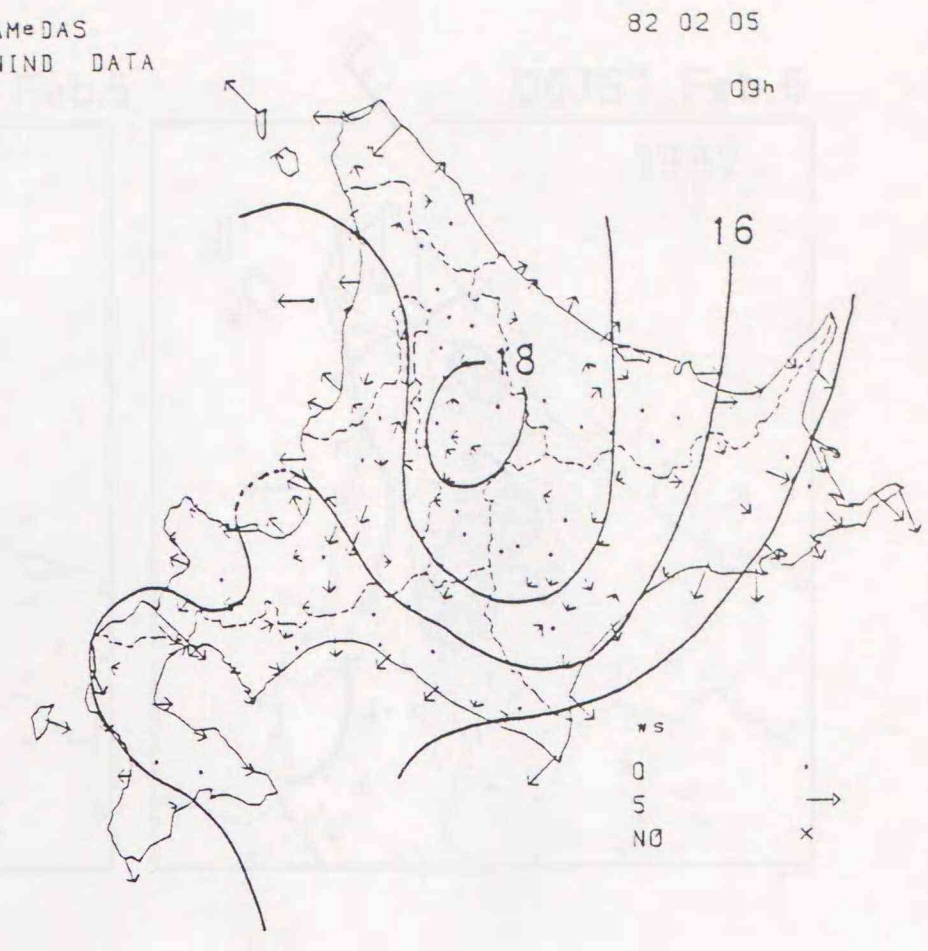

(b)

Fig. 3-4 Mesoscale surface weather charts. (a) 09 JST Feb. 4, 1982. (b) 09 JST Feb. 5, 1982.

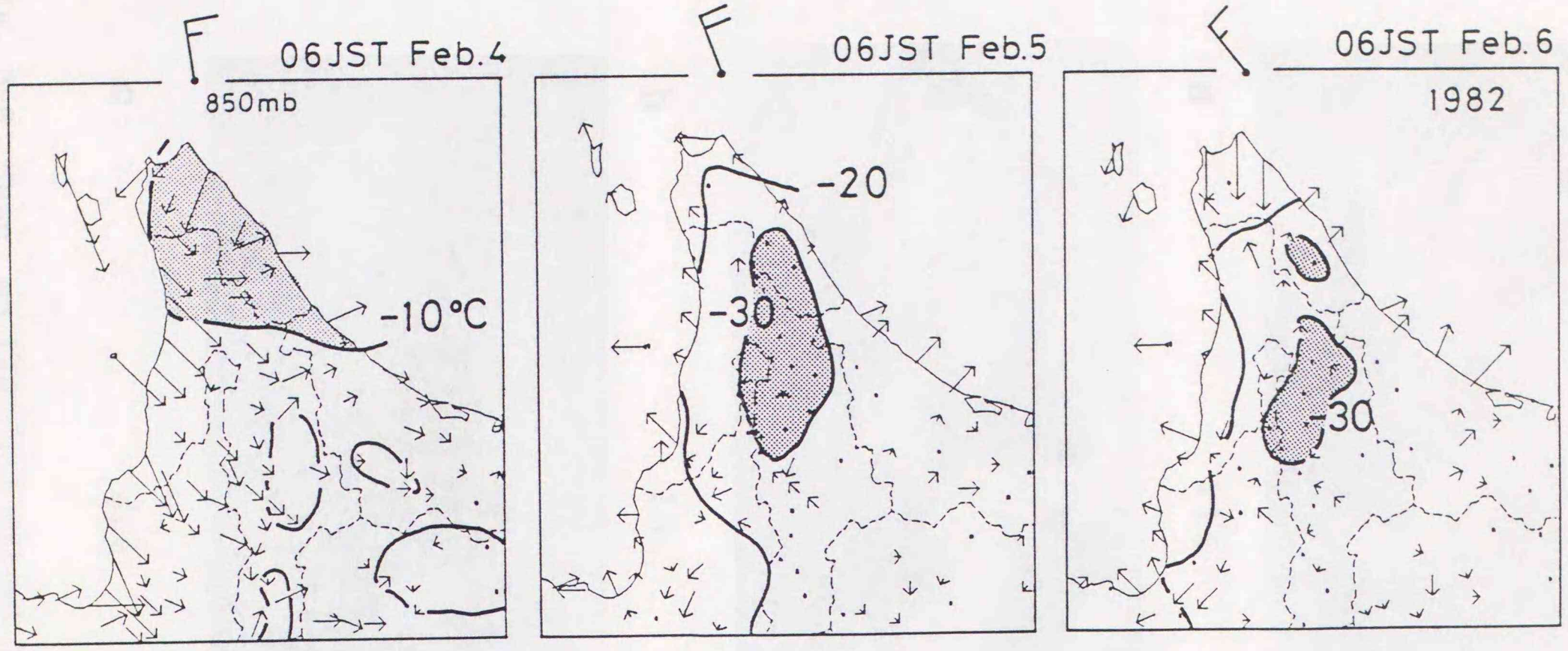

STAGE -

I : DEVELOPING　　II : MATURE　　III : DISSIPATING

Fig. 3-5 The wind and temperature fields in the northern part of Hokkaido at three stages.

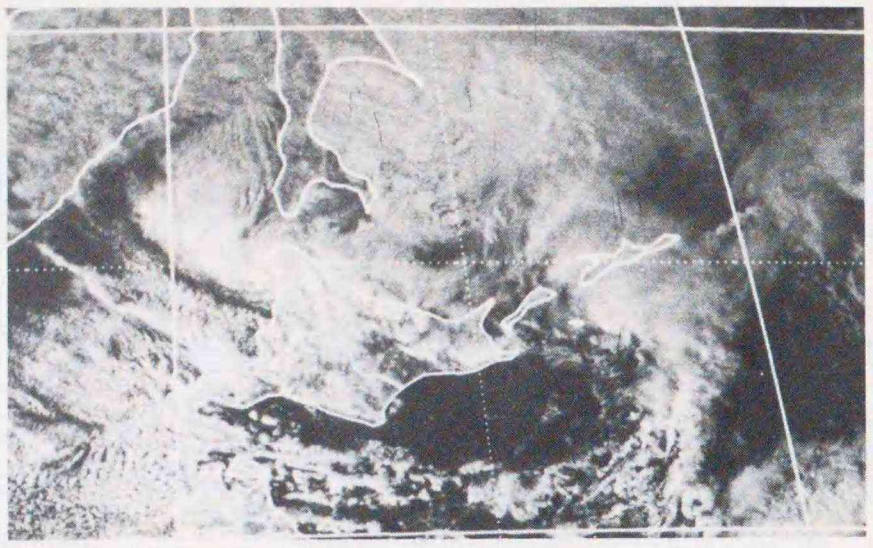

a VIS.

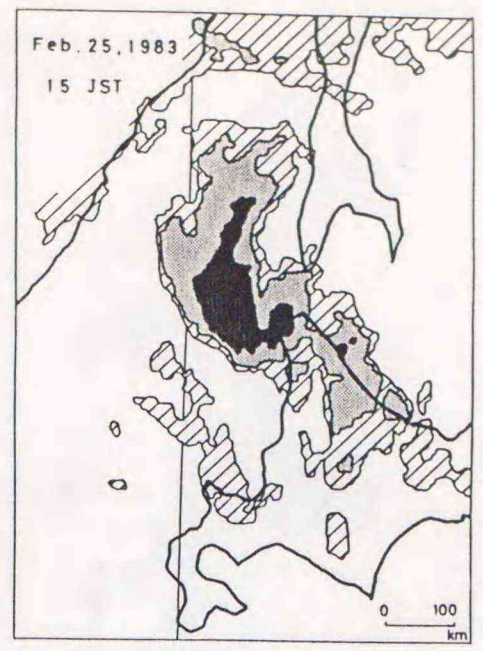

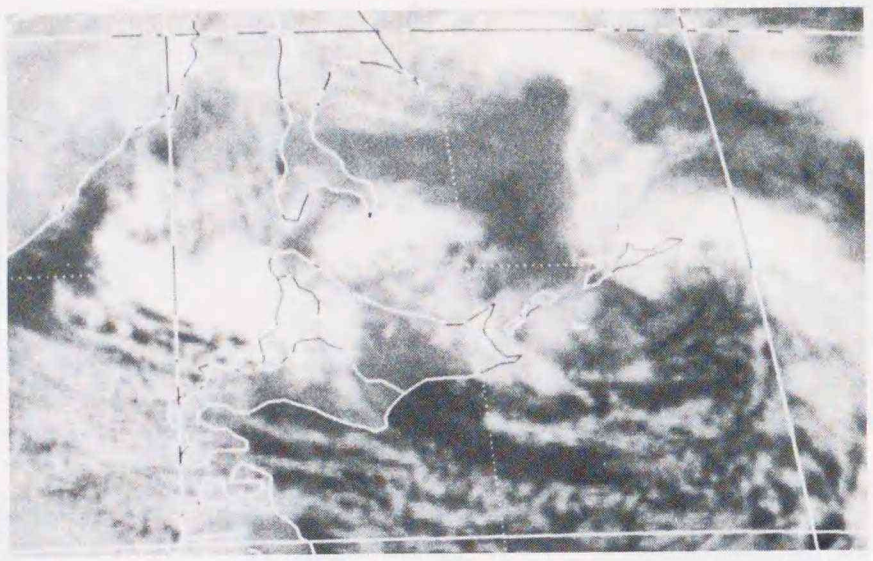

b IR.

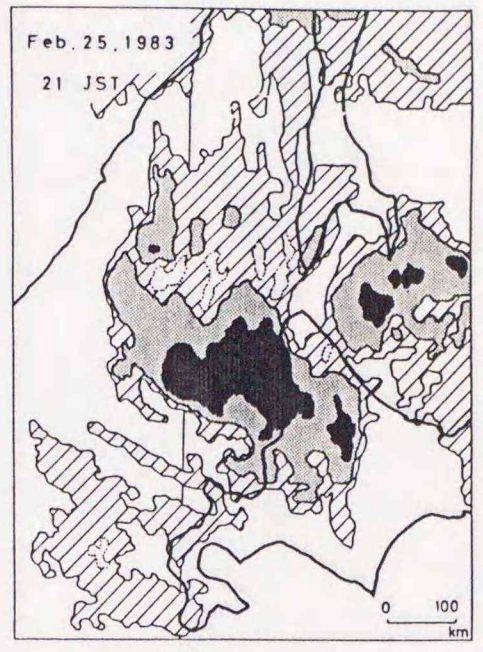

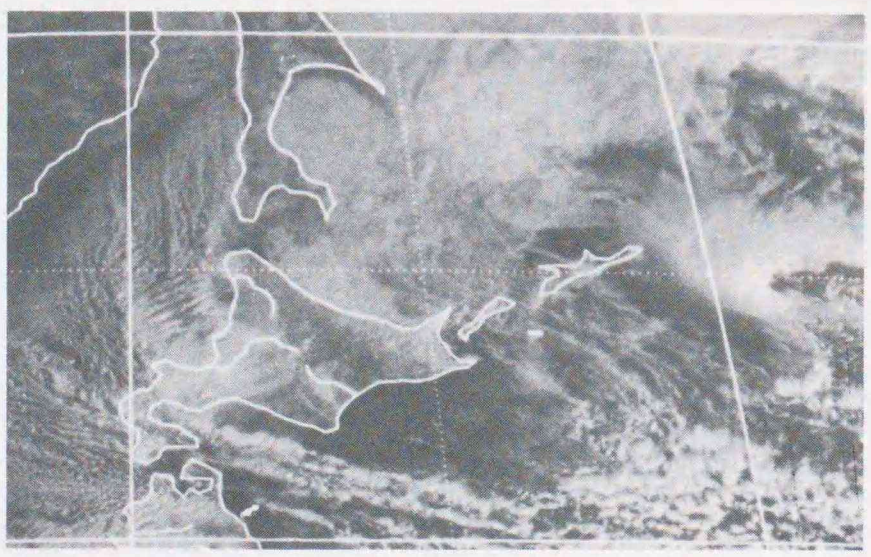

c VIS.

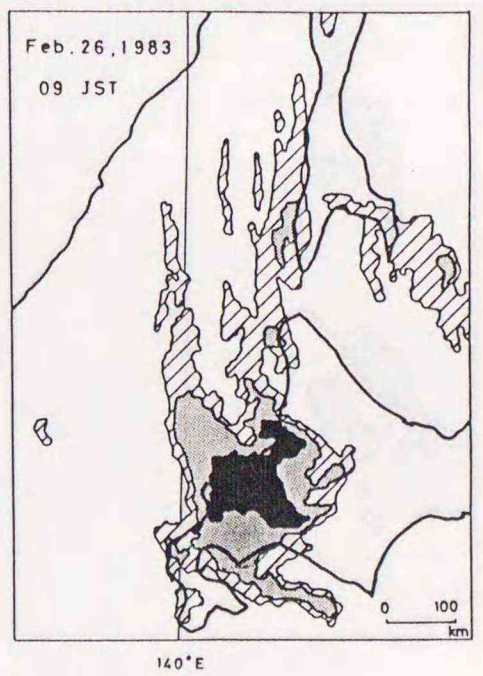

Fig. 3-6 Same as Fig. 3-1 except for from 15 JST Feb. 25 through 21 JST Feb. 27, 1983.

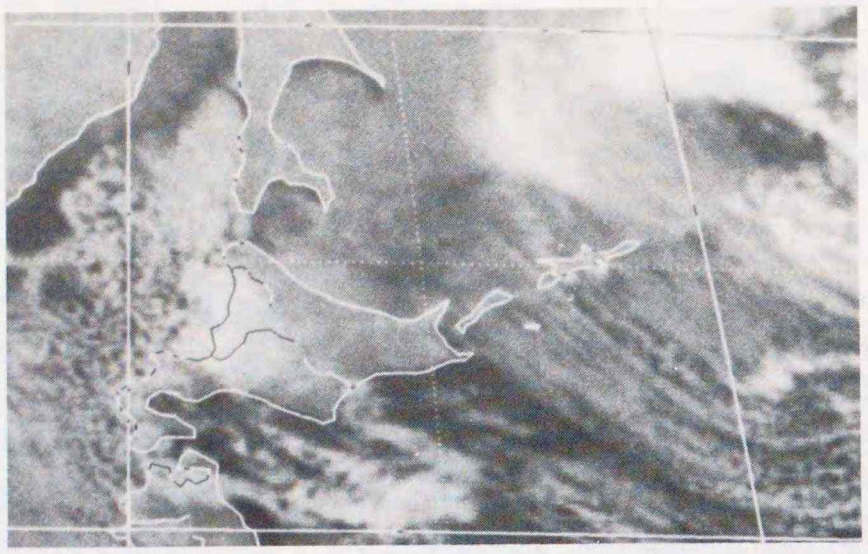

d IR.

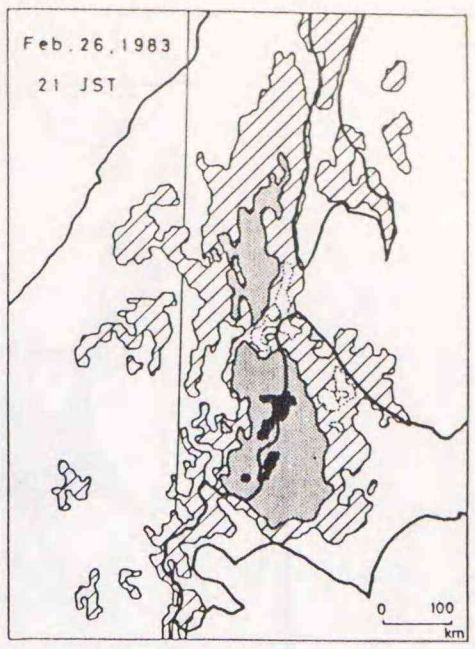

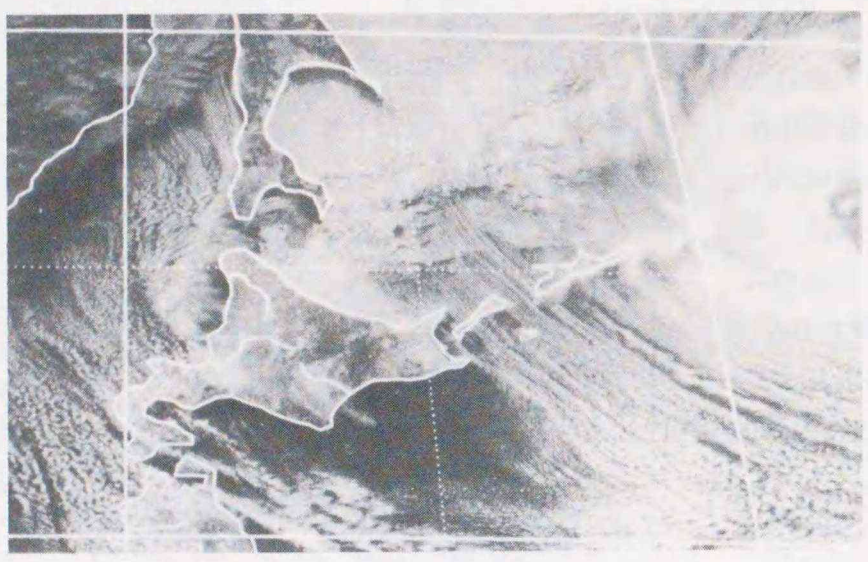

e VIS.

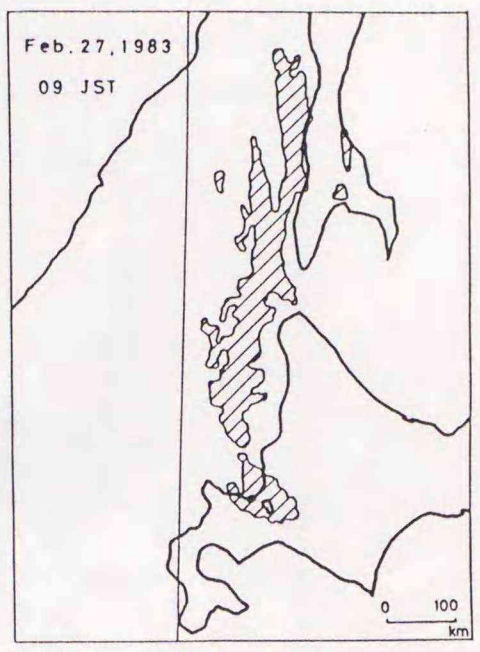

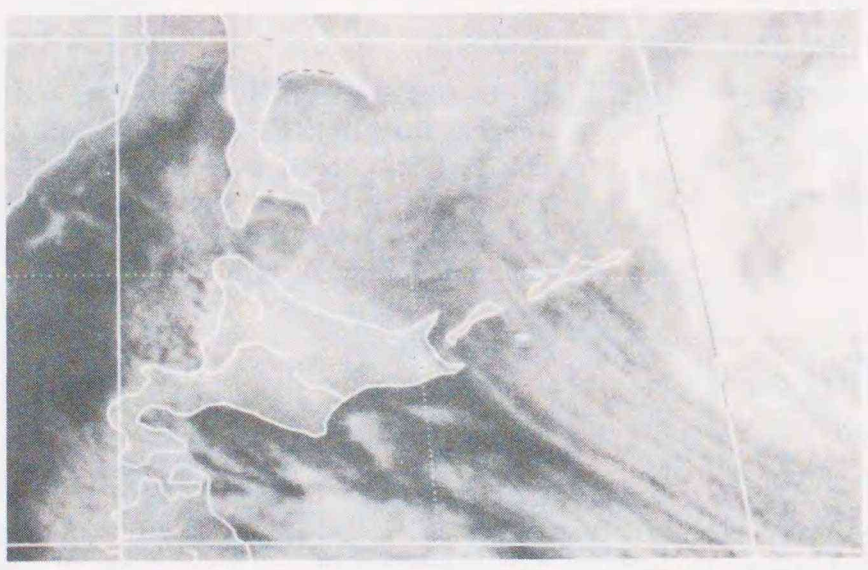

f IR.

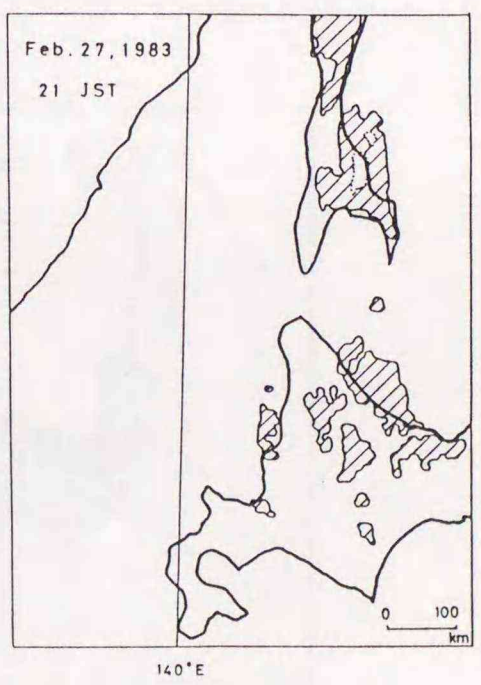

Fig. 3-6 (Continued)

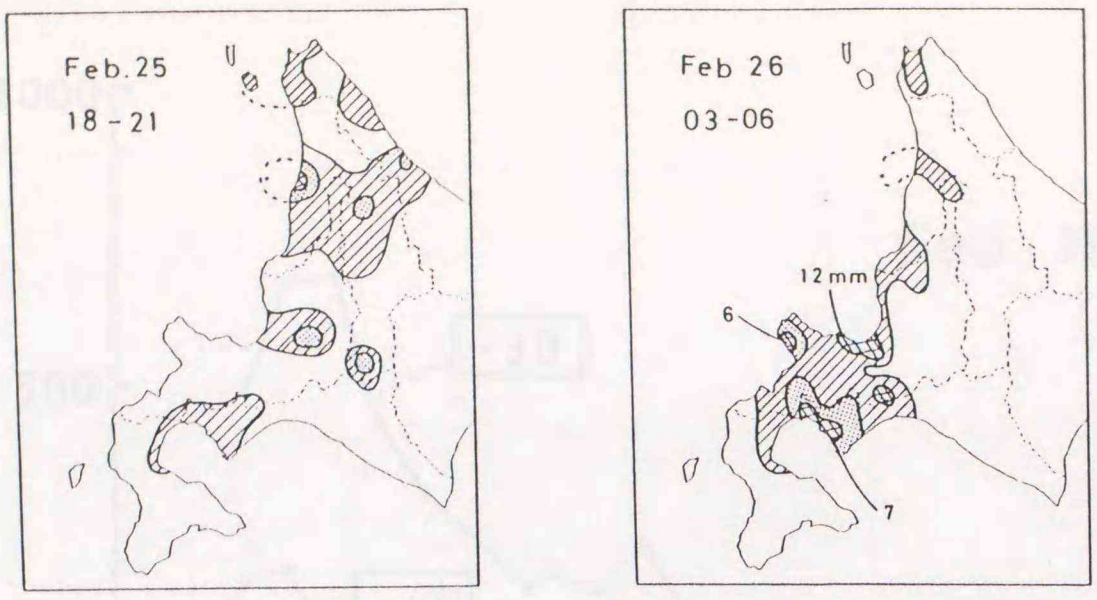

Fig. 3-7 Horizontal distributions of 3hr precipitation amounts from 18 JST Feb. 25 through 12 JST Feb. 26, 1983. Areas of precipitation of < 2 , 4 and > 5 mm are hatched, stippled and meshed, respectively. Heavy precipitation areas are indicated by each value.

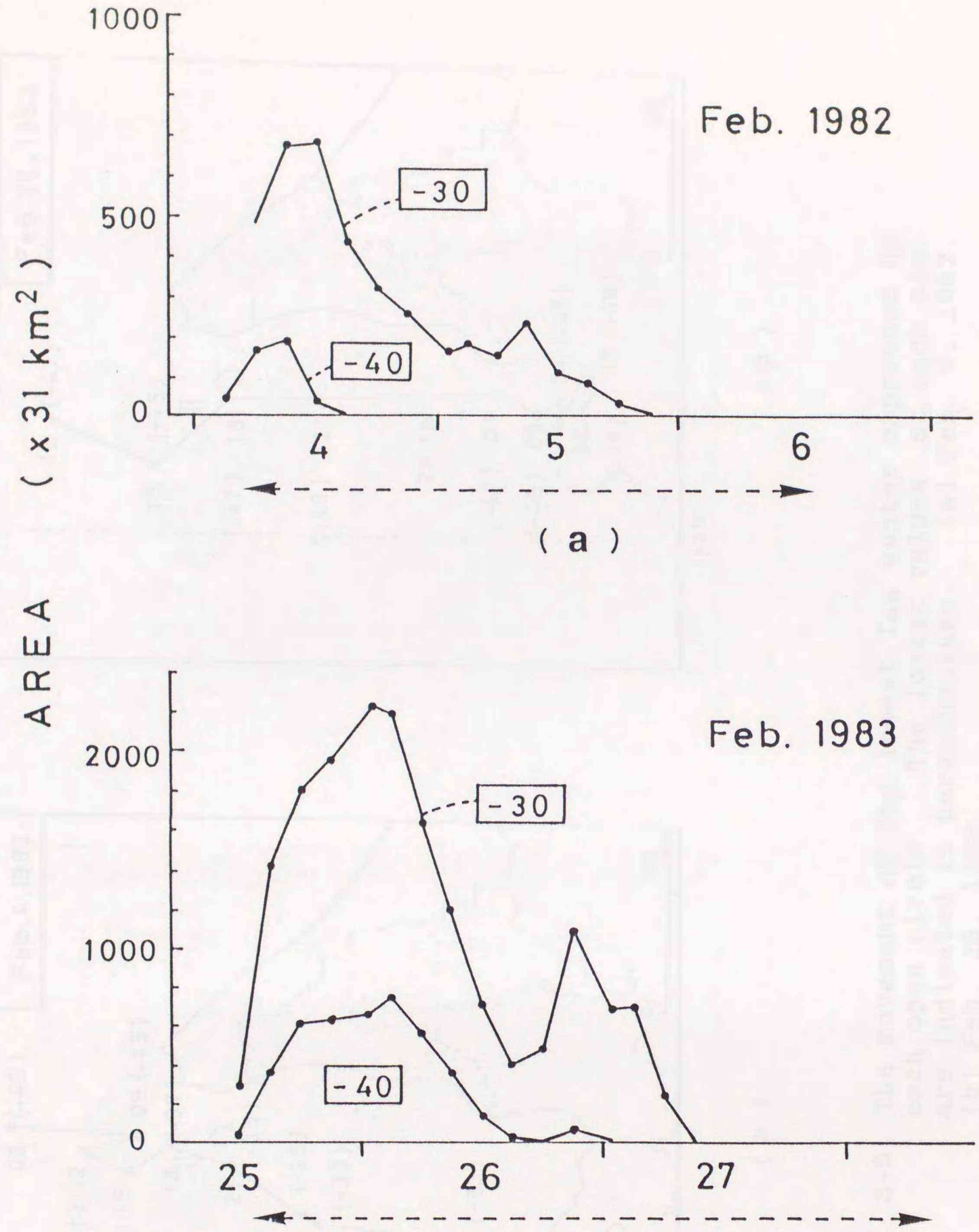

Fig. 3-8 Time changes of the T_{BB} areas. (a) Feb. 4-6, 1982. (b) Feb. 25 - 28, 1983. Dashed lines show the lifetime of CBC.

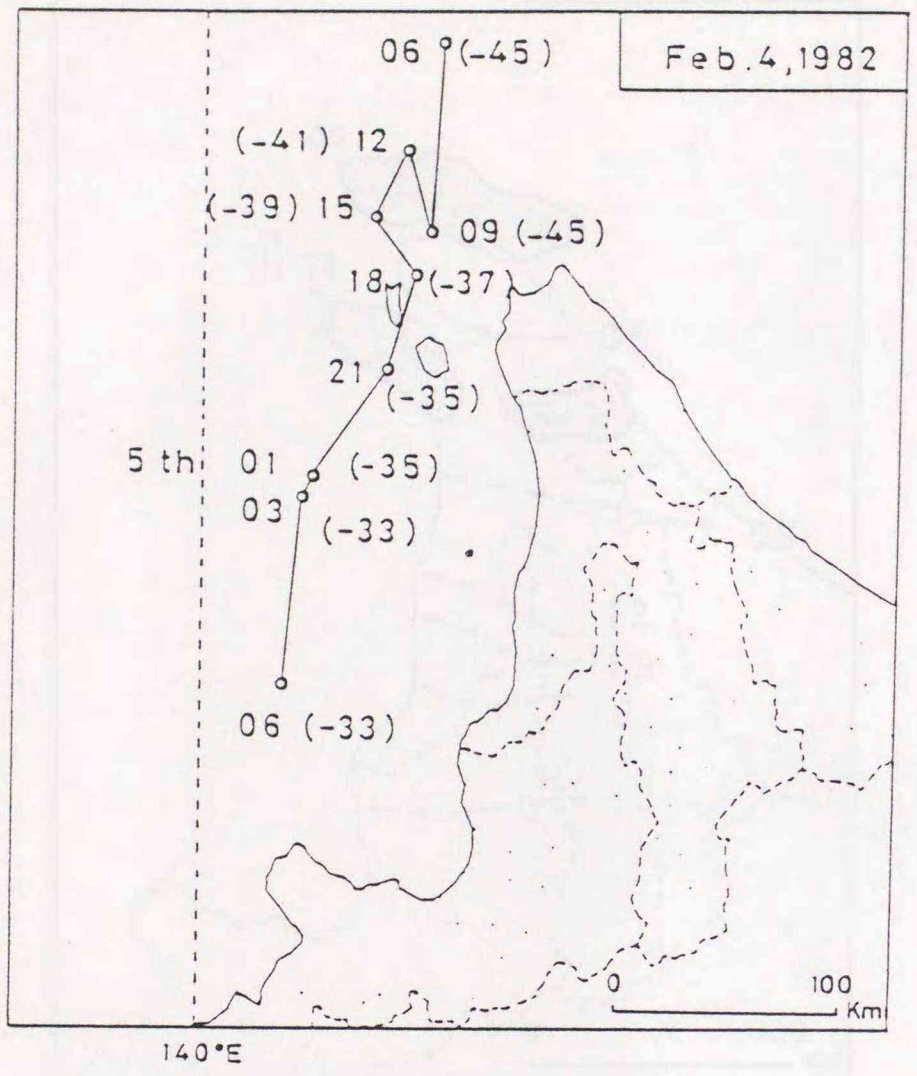

(a)

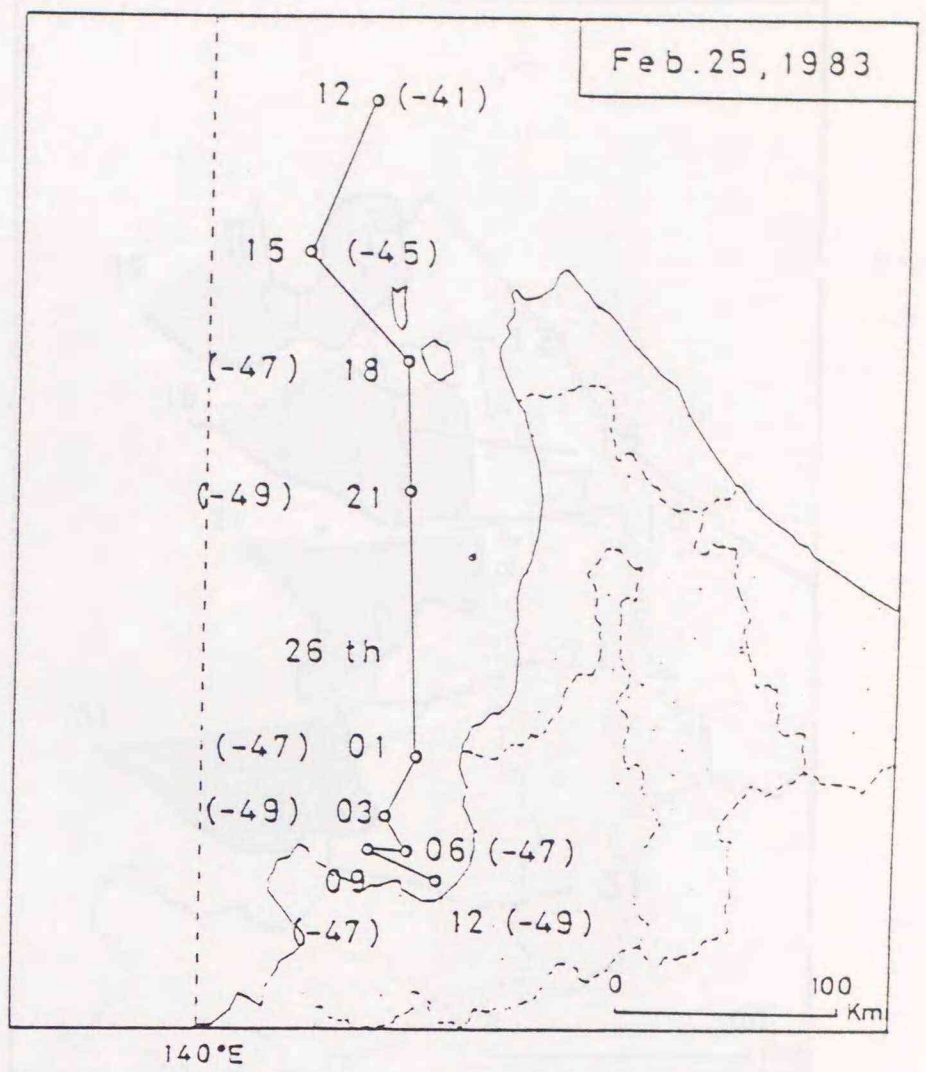

(b)

Fig. 3-9 The movement of the lowest T_{BB} center expressed by each open circle. The lowest values at each time are indicated in parenthesises. (a) Feb. 4, 1982. (b) Feb. 25, 1983.

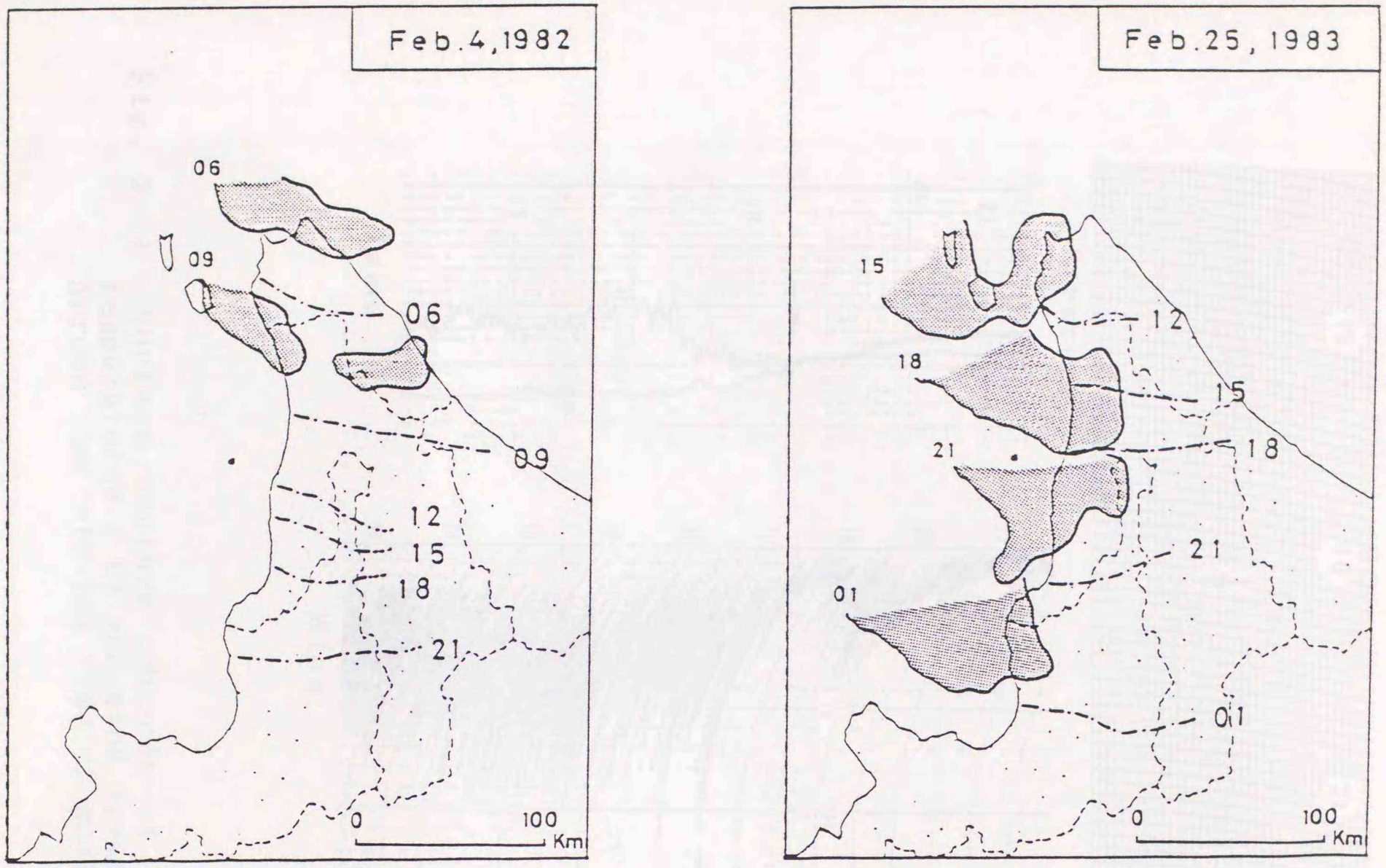

(a) (b)

Fig. 3-10 Time changes of the locations of wind shear line at every 3hr and the locations of south edges of CBC characterized by -40 ˚C of T_{BB}. (a) Feb. 4, 1982. (b) Feb. 25, 1983.

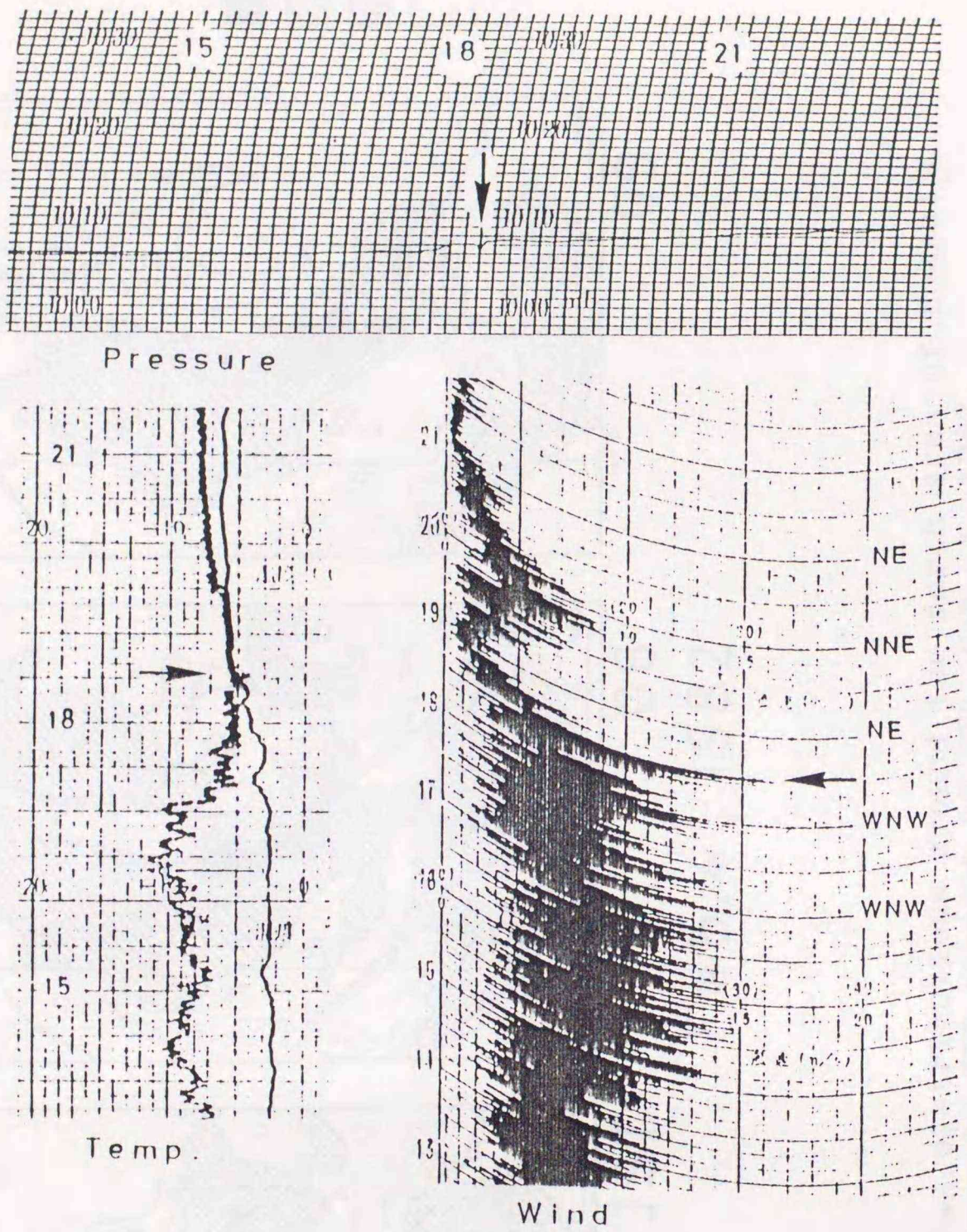

Fig. 3-11 Surface weather records of pressure (mb), temperatures (°C) and wind speed (m/s) at Haboro. Arrows indicate the time of gust wind.

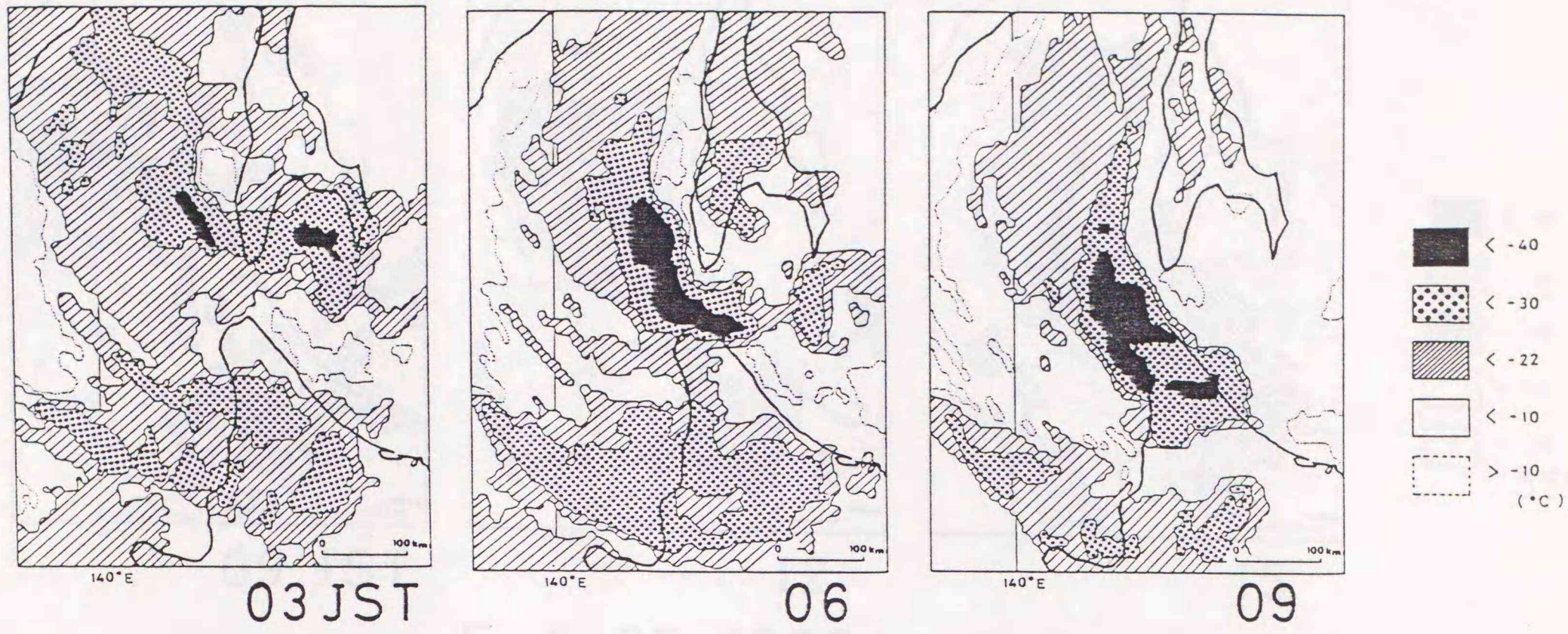

Fig. 3-12 T_{BB} distributions around the north area of Hokkaido from 03 JST through 09 JST Feb. 4, 1982.

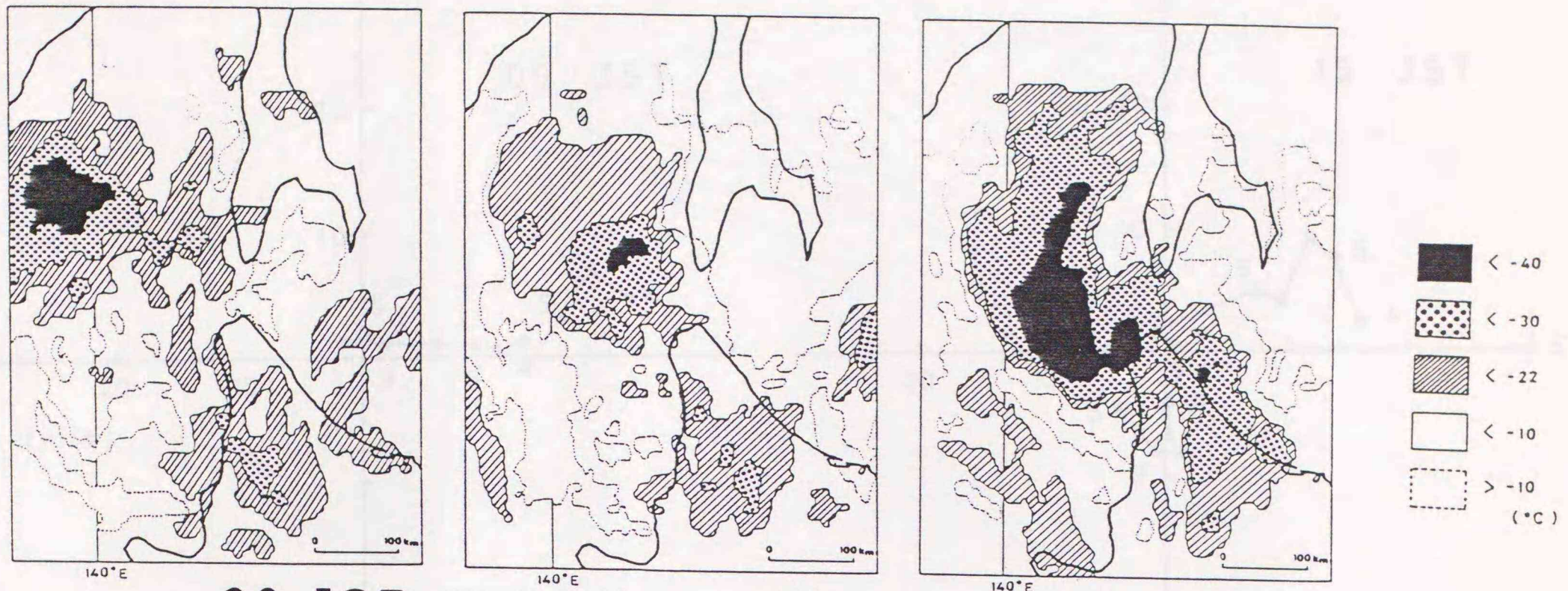

Fig. 3-13 Same as Fig. 3-12 except for from 09 JST through 15 JST Feb. 25, 1983.

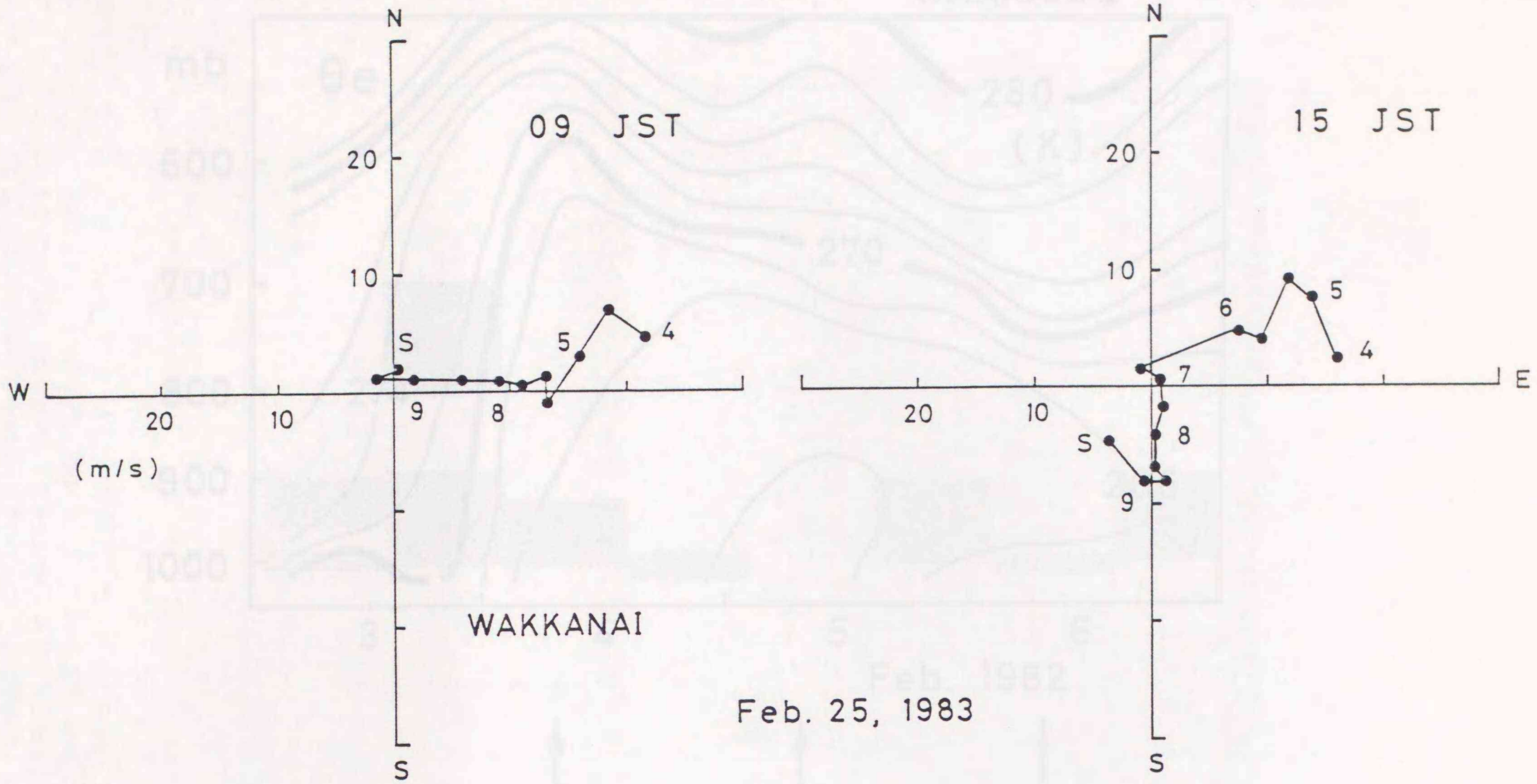

Fig. 3-14 Hodgraphs at Wakkanai before (09 JST) and after (15 JST Feb. 25, 1983) CBC outbreak.

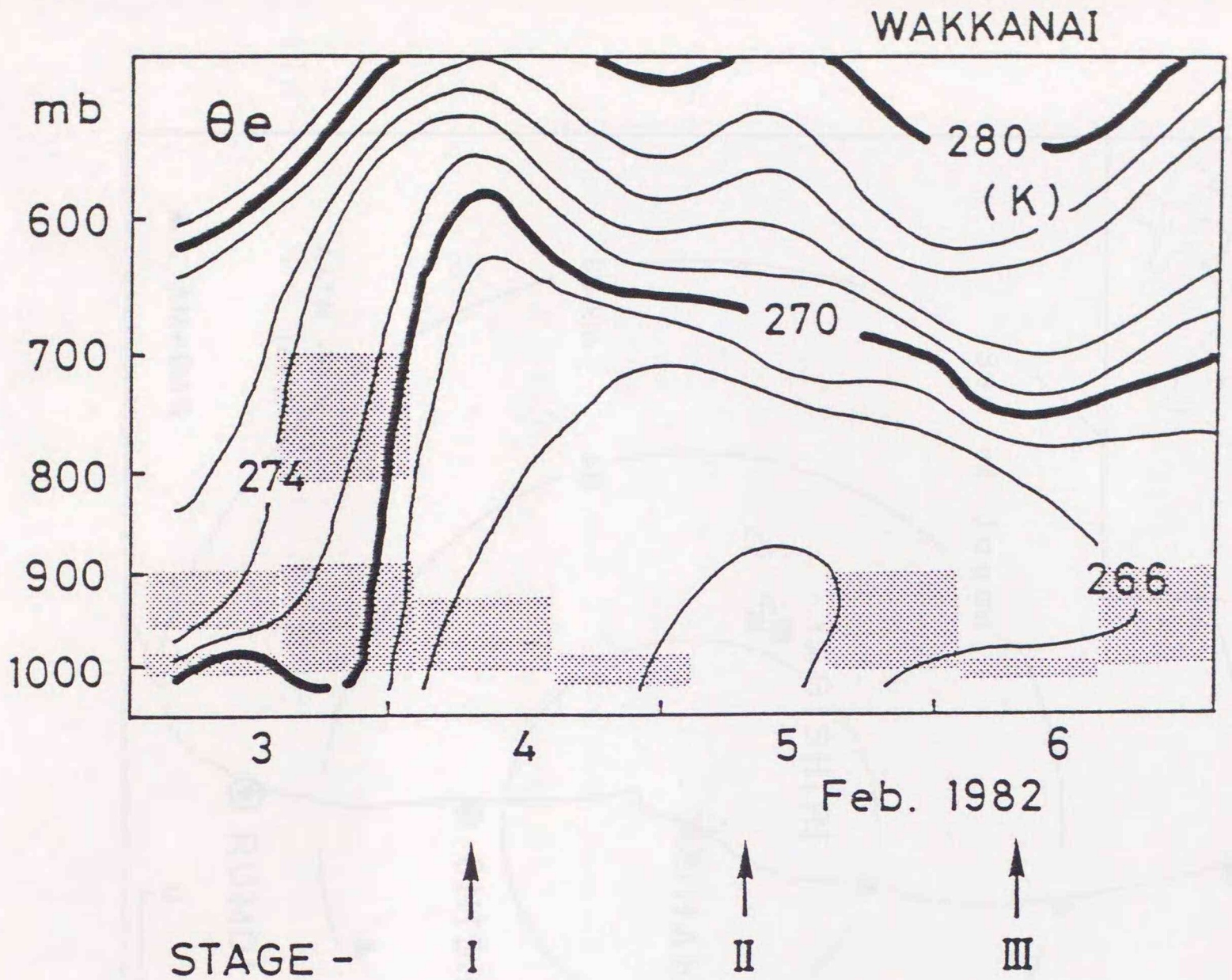

Fig. 3-15 Time-height cross section of equivalent potential temperature at Wakkanai. Shaded areas indicate the convective instability layers.

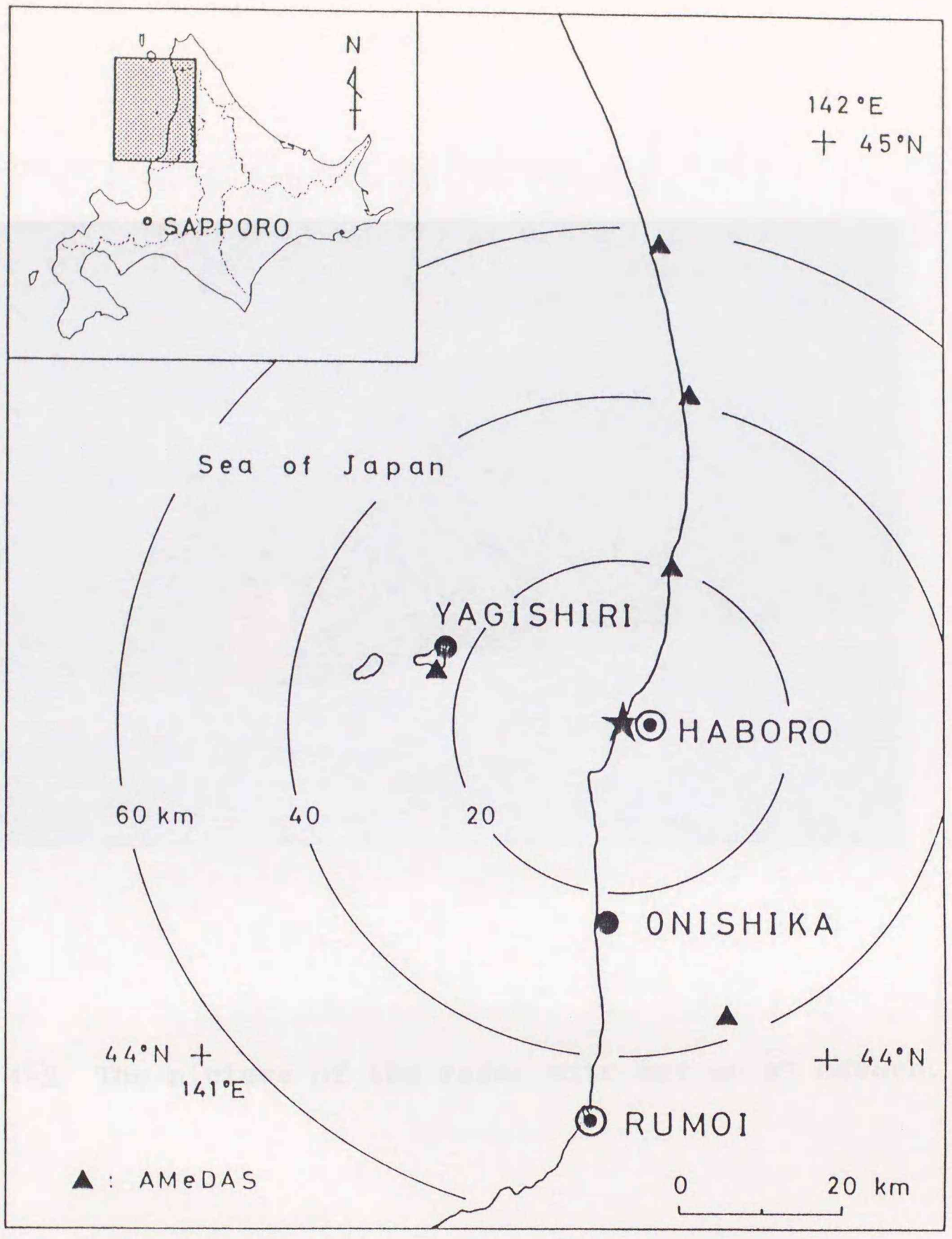

Fig. 4-1 The observation network around the radar site at Haboro (star mark). Solid and open circles denote special observation stations and JMA weather stations, respectively. AMeDAS stations are denoted by solid triangles.

Fig. 4-2 The picture of the radar site set up at Haboro.

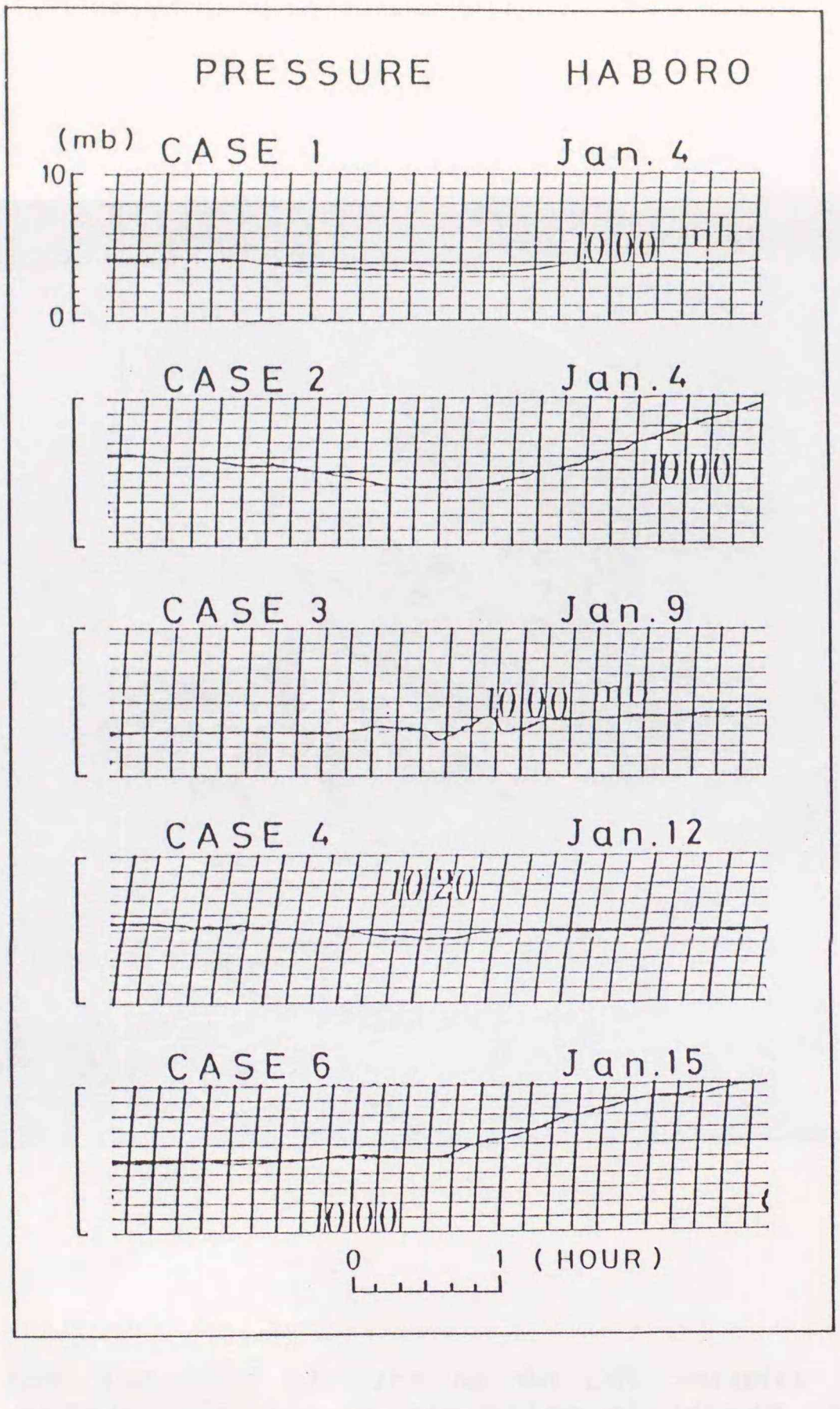

Fig. 4-3 Continuous records of pressure at Haboro. Each case corresponds with Table 1.

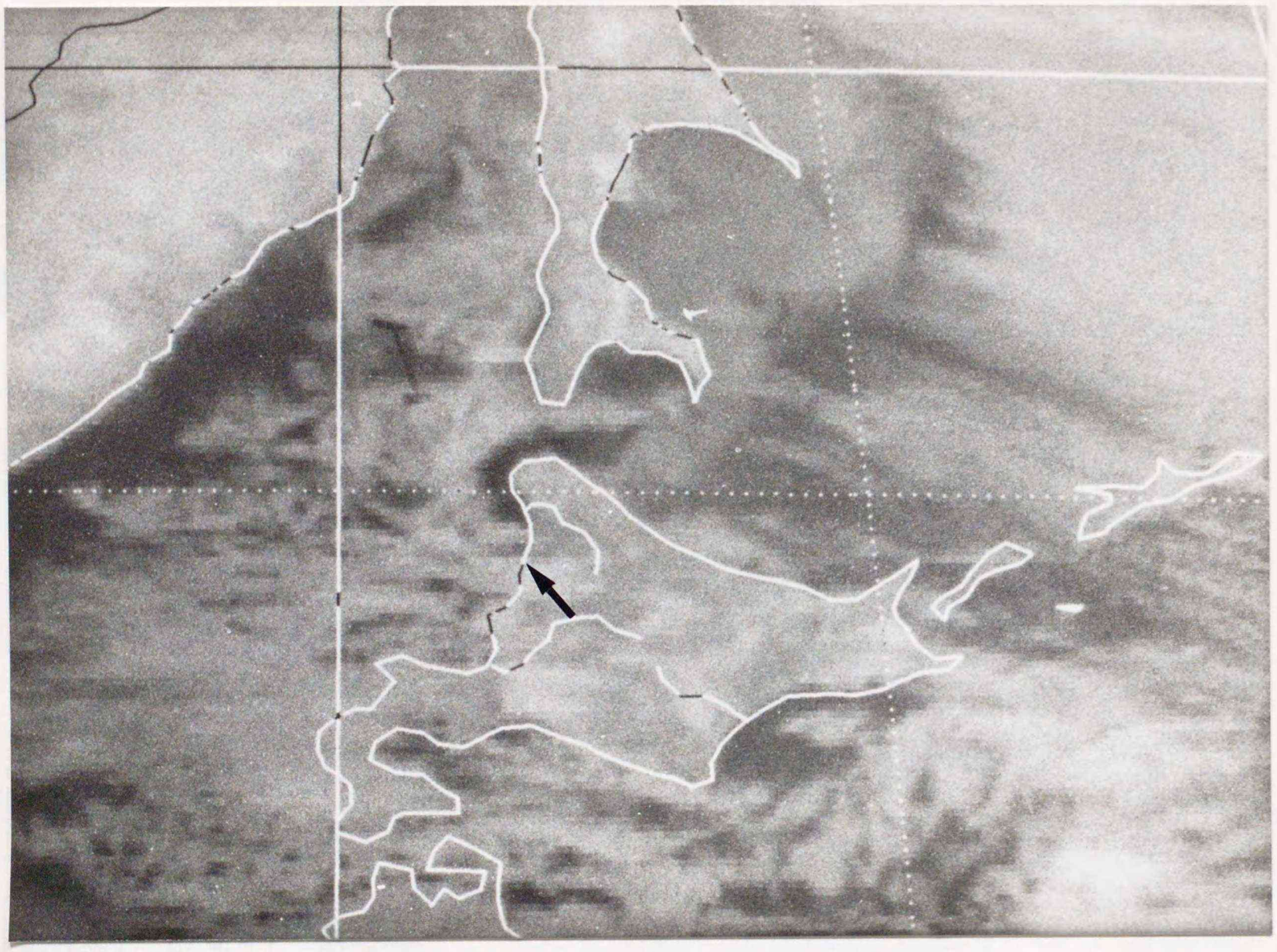

Fig. 4-4 GMS infrared picture at 03 JST January 12,1987. An arrow indicates the location of Haboro radar site.

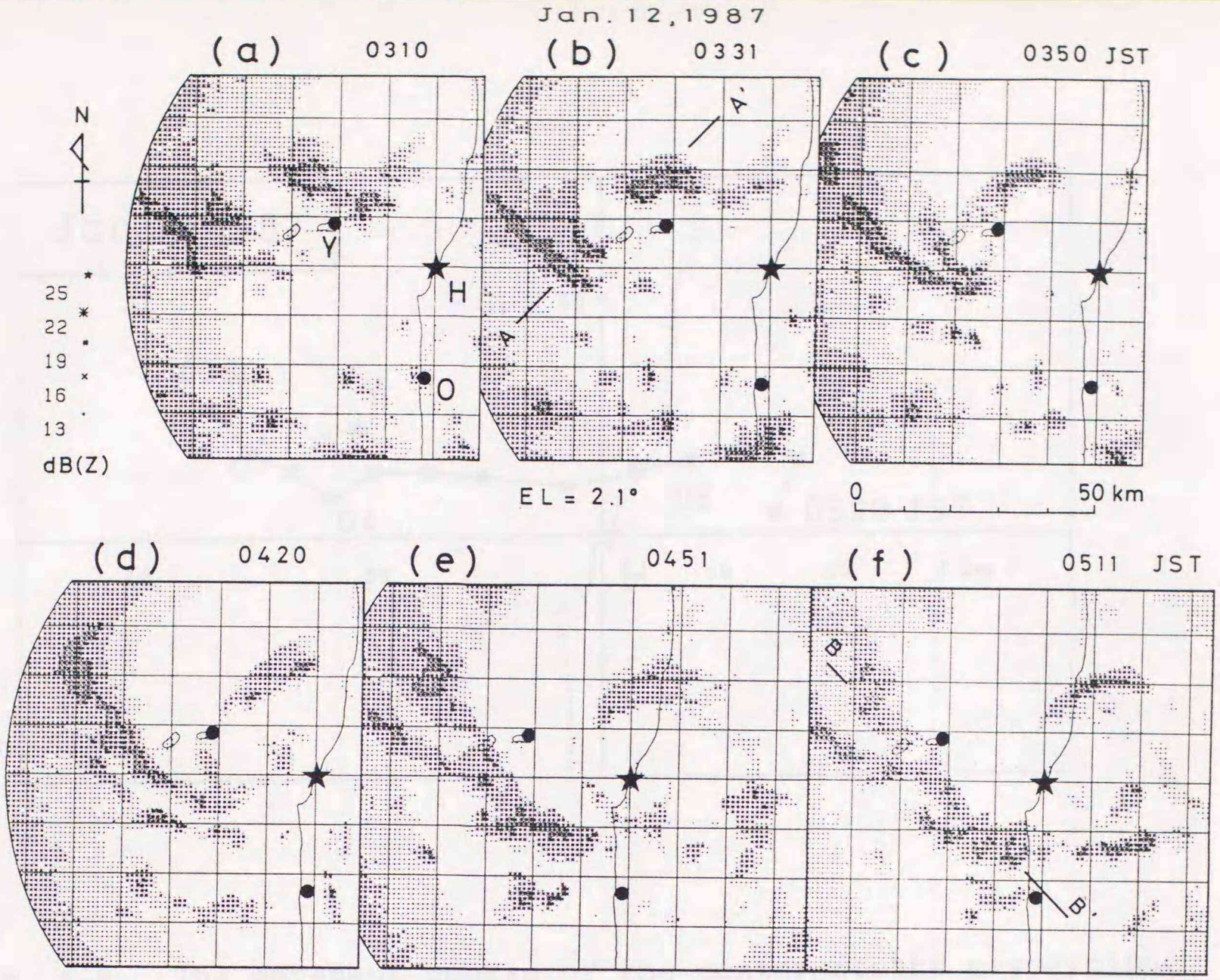

Fig. 4-5 Time sequence of PPI radar echo patterns through a life cycle of the mesocyclone. Star marks show the radar site and solid circles denote the locations of Yagishiri and Onishika stations, respectively.

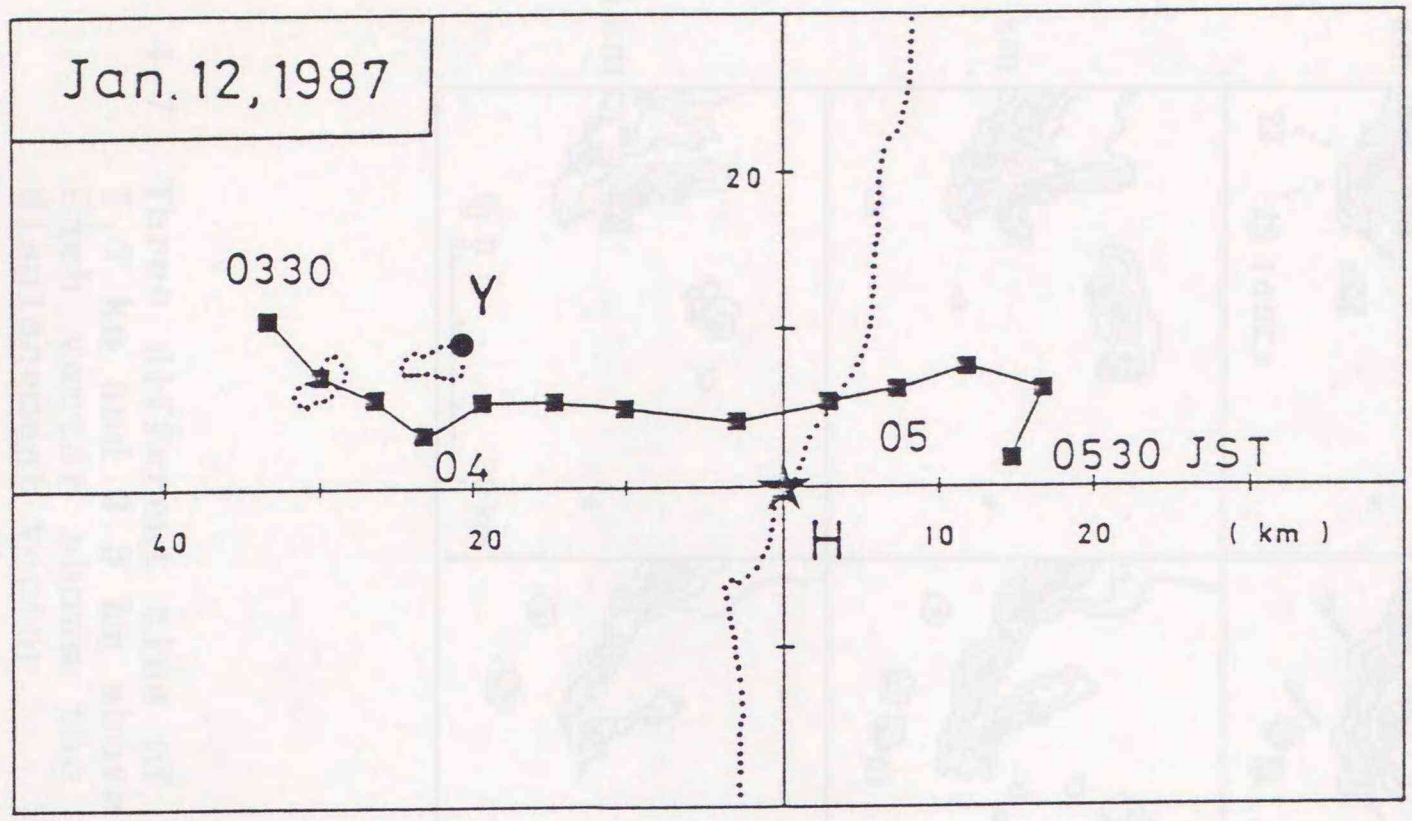

Fig. 4-6 The movement course of the center of the mesocyclone indicated by 10 minute intervals.

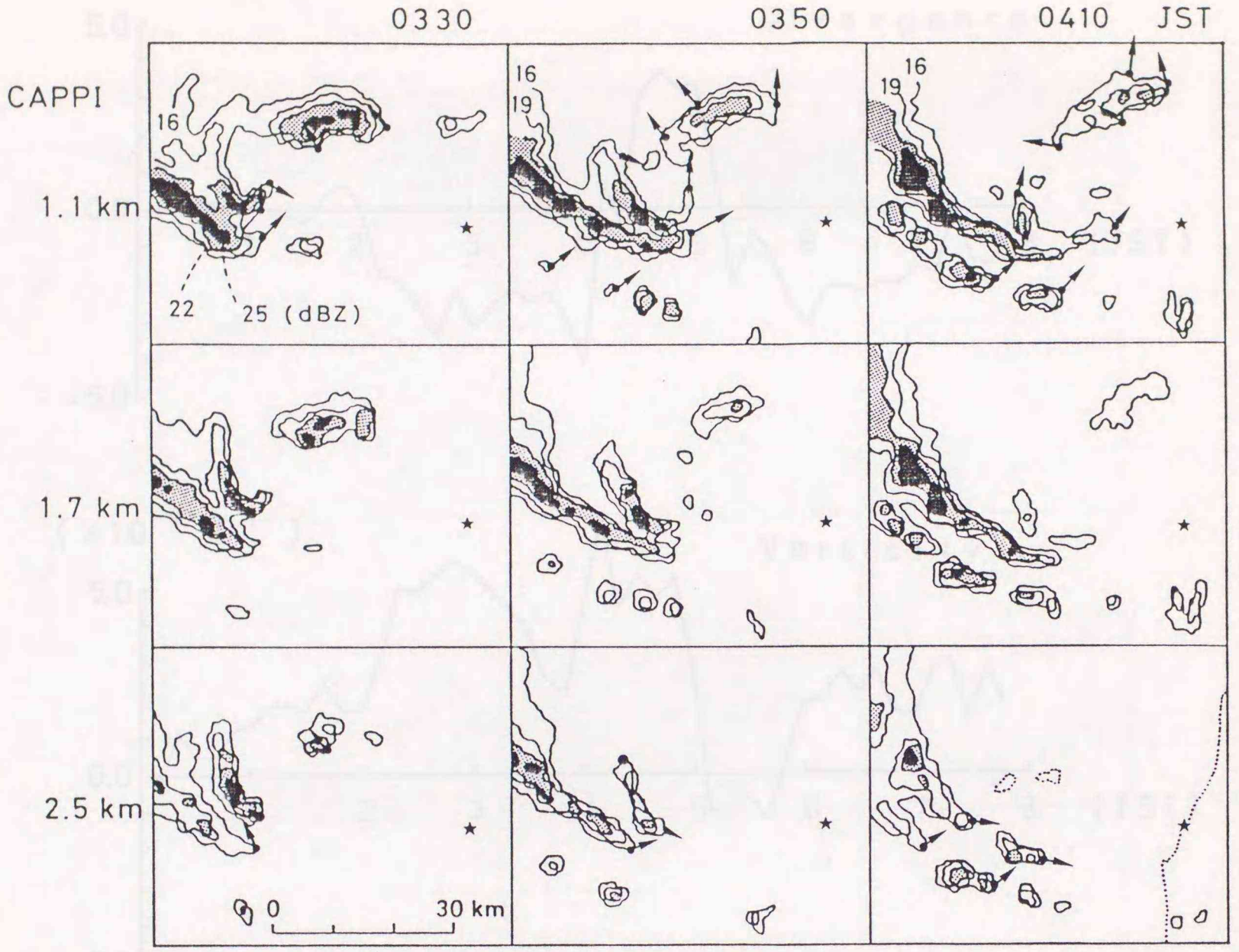

Fig. 4-7 Three different time of CAPPI displays of 1.1 km, 1.7 km and 2.5 km above sea level, respectively. Each vector shows the storm relative 10 minute displacement vector.

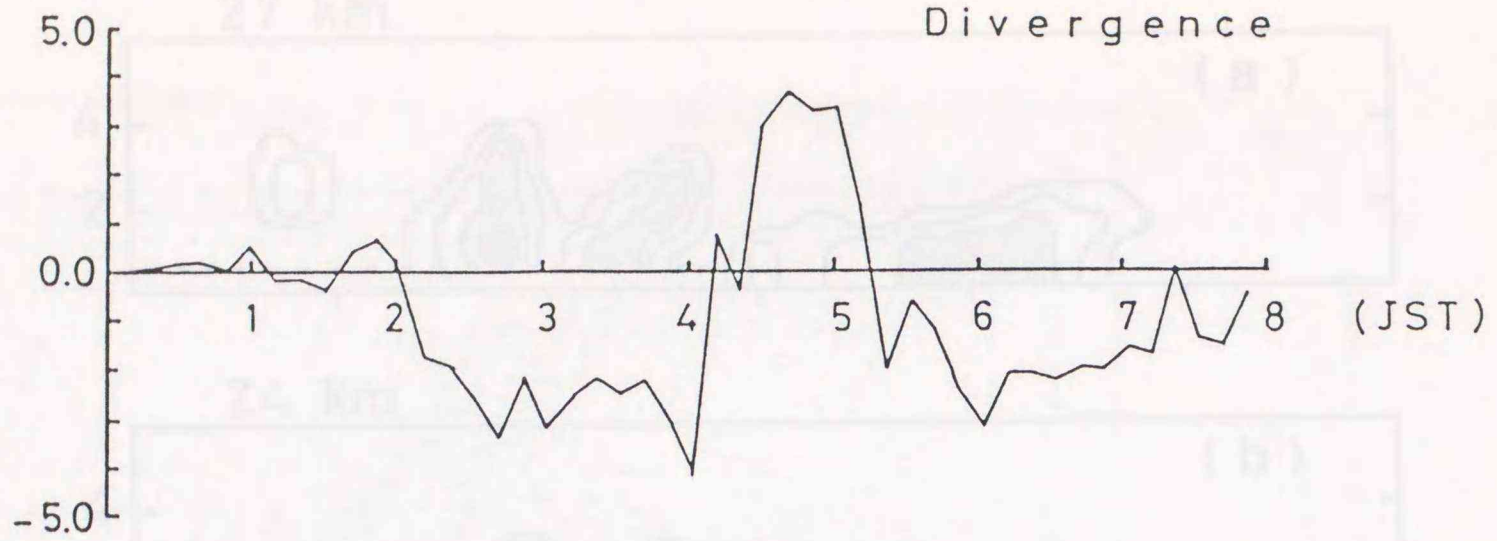

Fig. 4-8 Time changes of the divergence (top) and vorticity (bottom) calculated by 10 minute average wind data of Haboro, Yagishiri and Onishika stations.

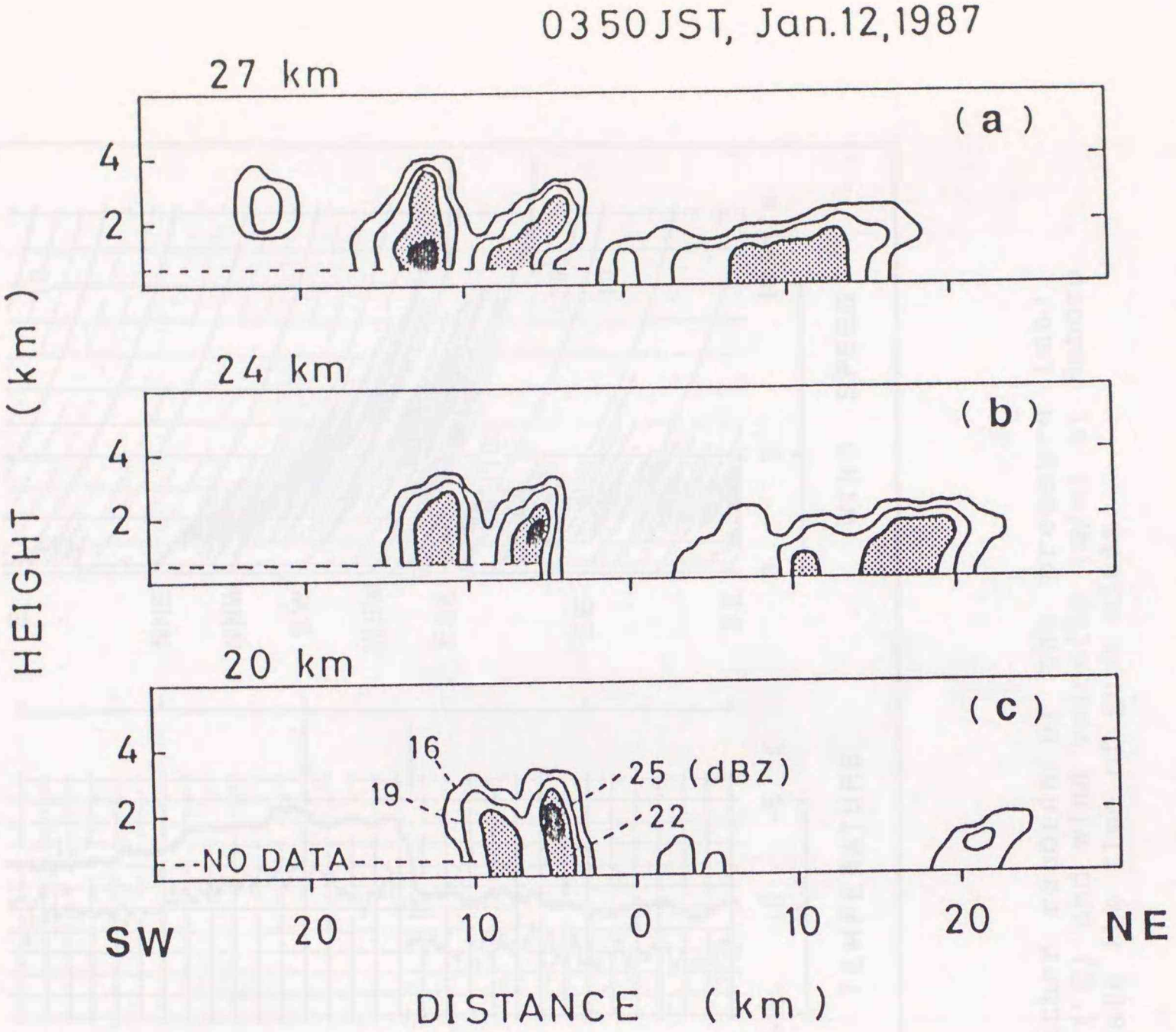

Fig. 4-9 RHI radar displays at 0350 JST perpendicular to the 315° direction as shown A-A' line in Fig. 4-5. Three cross sections of 27 km (a), 24 km (b) and 20 km (c) correspond to the rear of the mesocyclone center, the center of the mesocyclone and the front of the mesocyclone center, respectively.

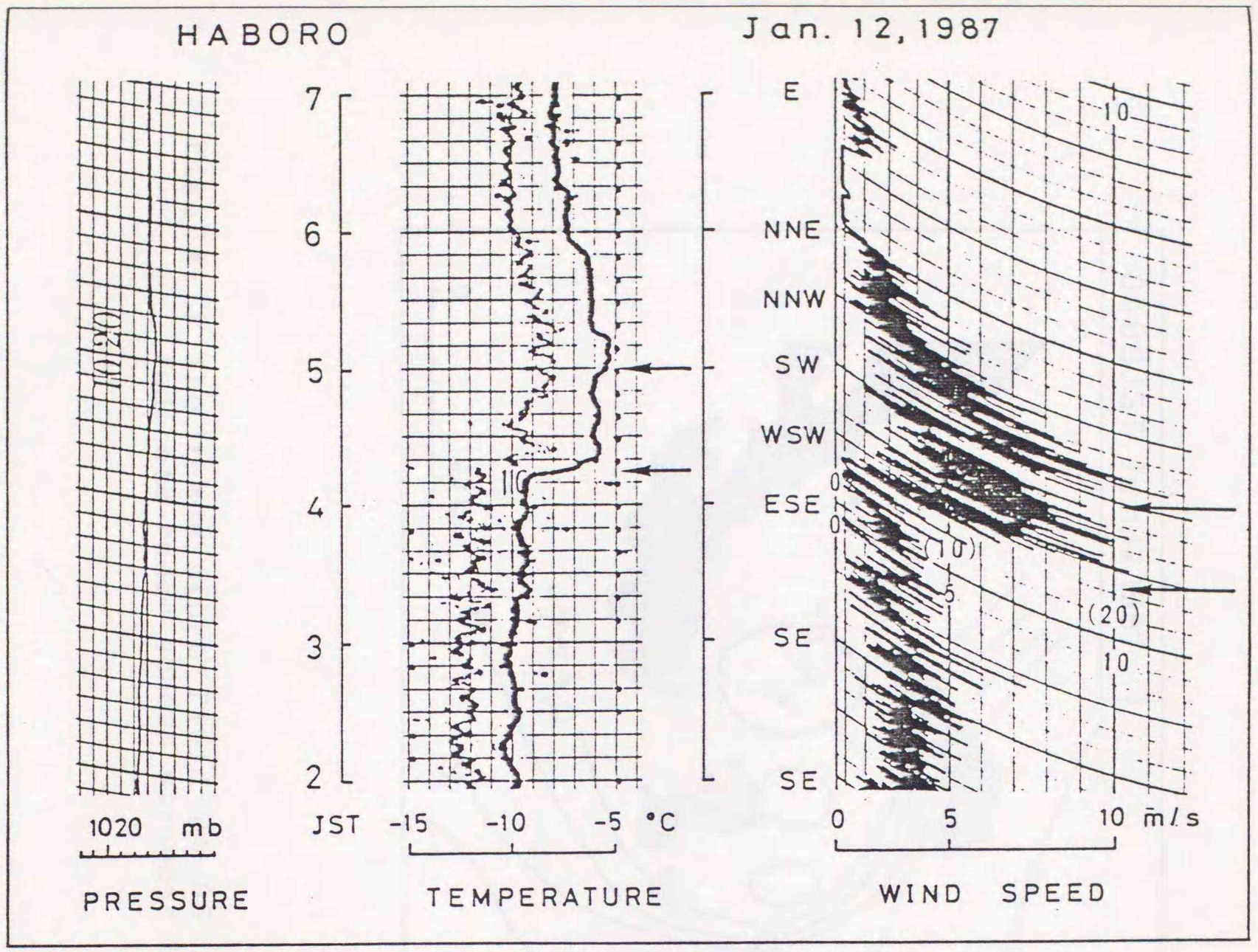

Fig. 4-10 Surface weather records of the pressure (mb), temperature (°C) and wind velocity (m/s) at Haboro. Arrows indicate the time of gust winds.

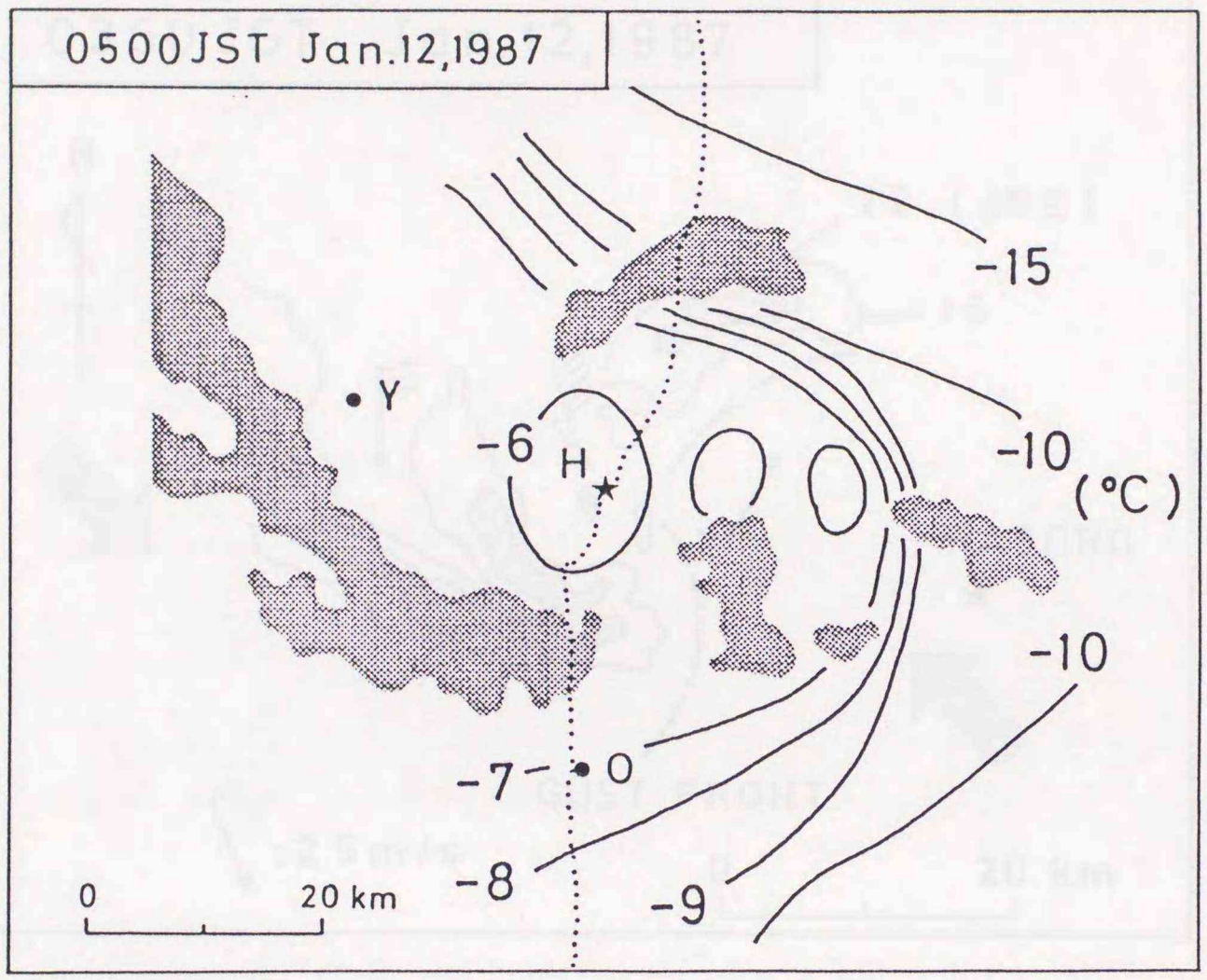

Fig. 4-11 The temperature field at 05 JST. Shaded areas indicate radar echoes stronger than 16 dBZ.

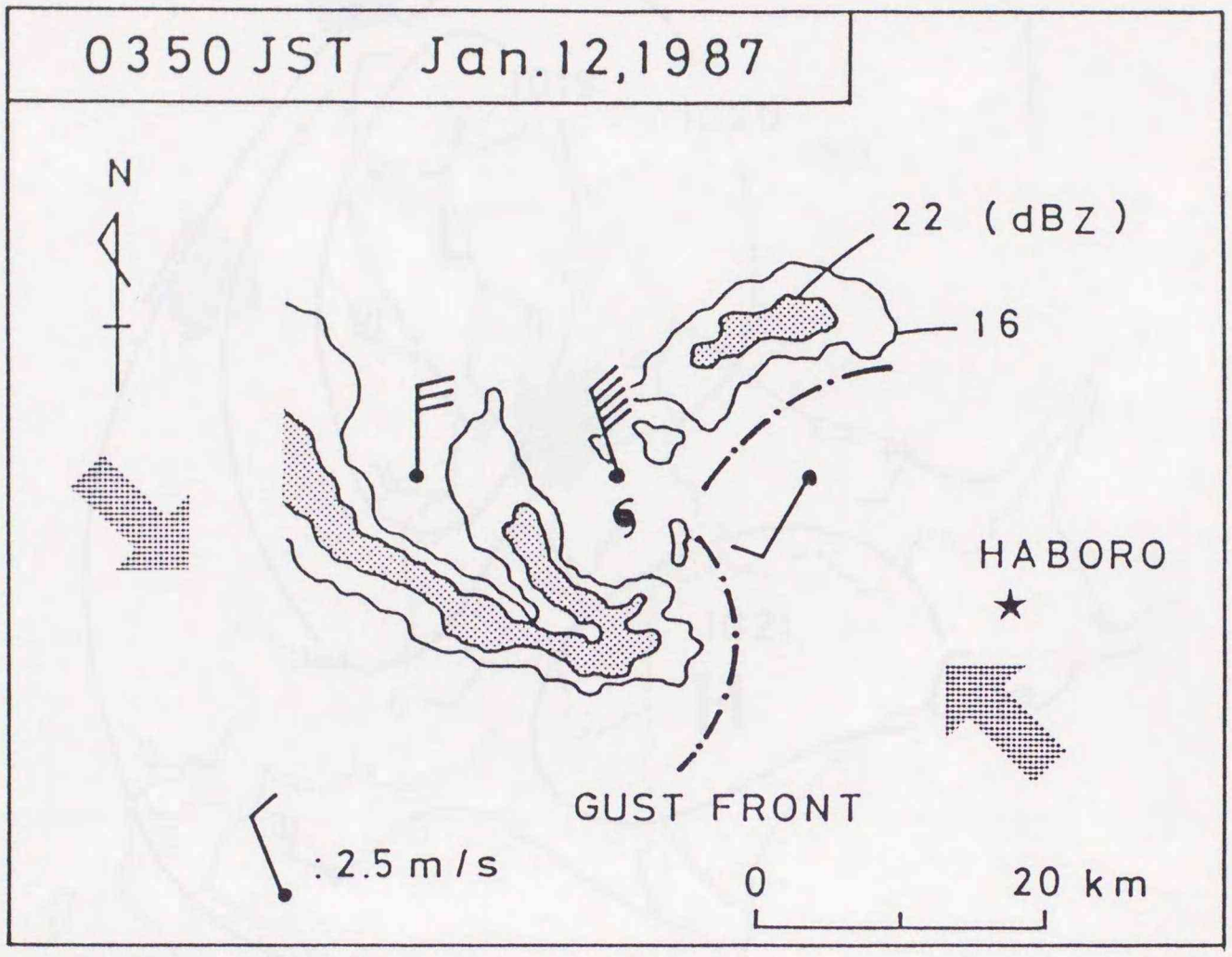

Fig. 4-12 The schematic figure of gust fronts in the mesocyclone.

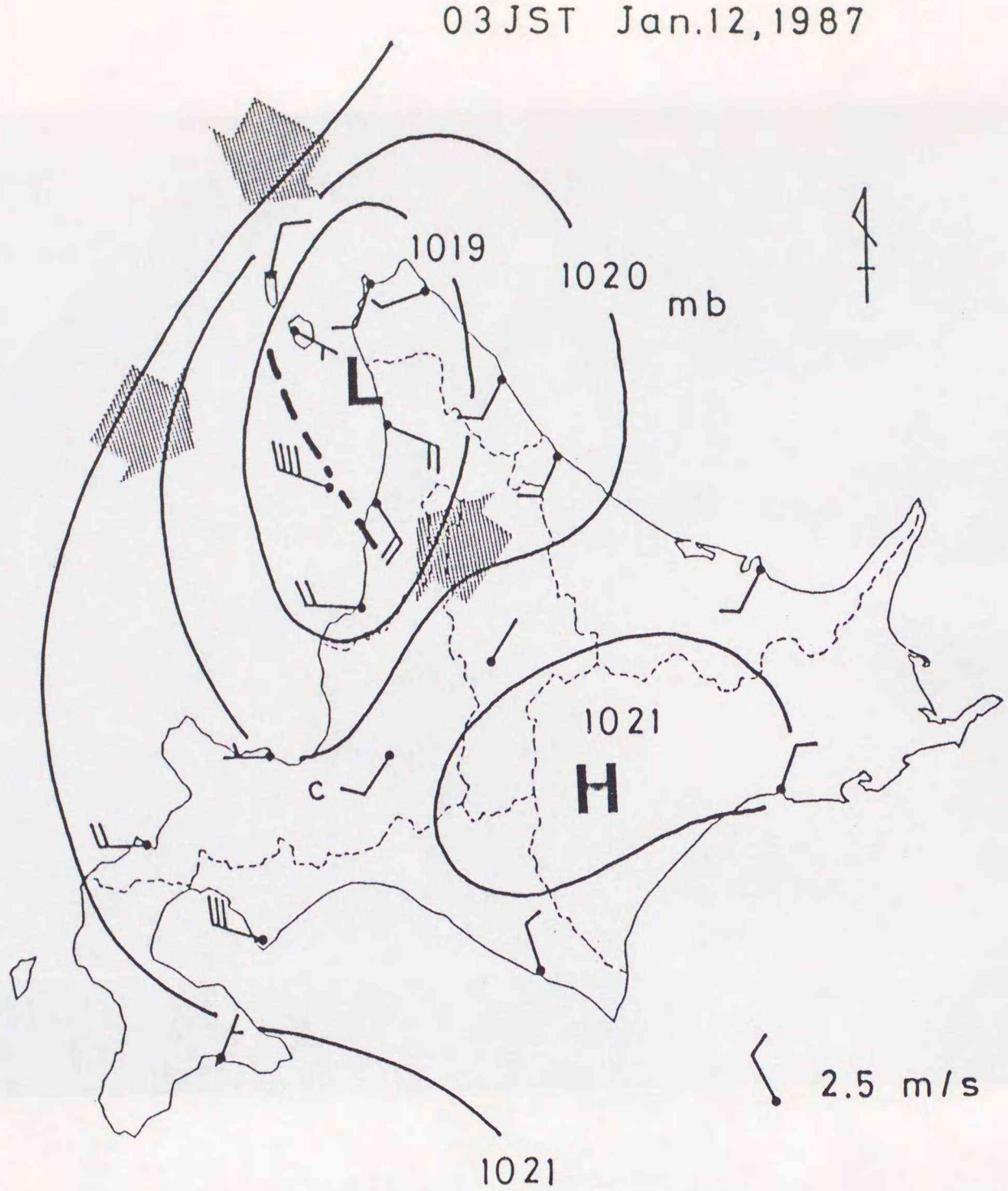

Fig. 4-13 Mesoscale surface weather chart. The dashed line indicates a surface wind shear line formed by the differential winds (wide arrows).

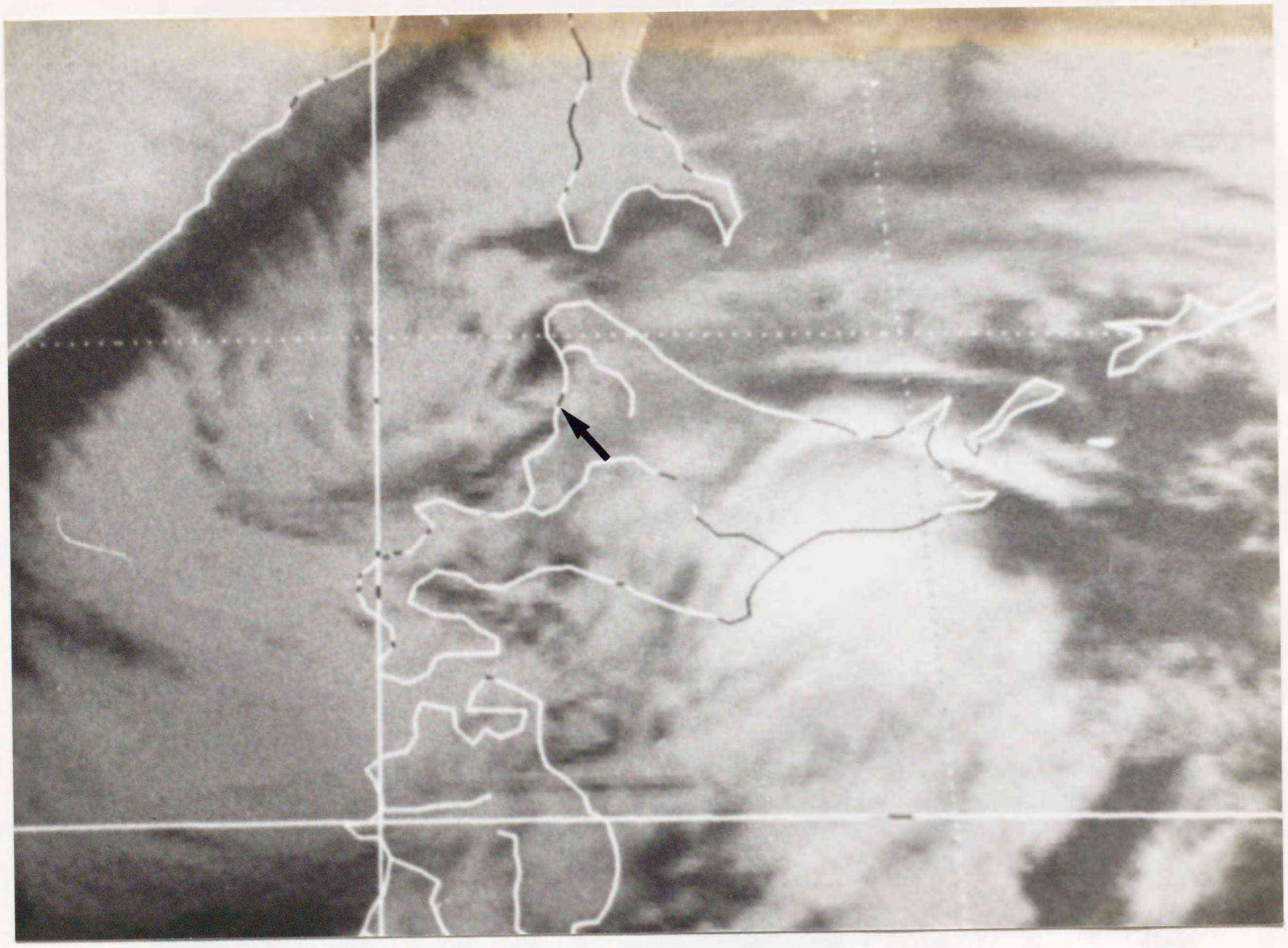

Fig. 4-14 GMS infrared picture at 01 JST January 15,1987.

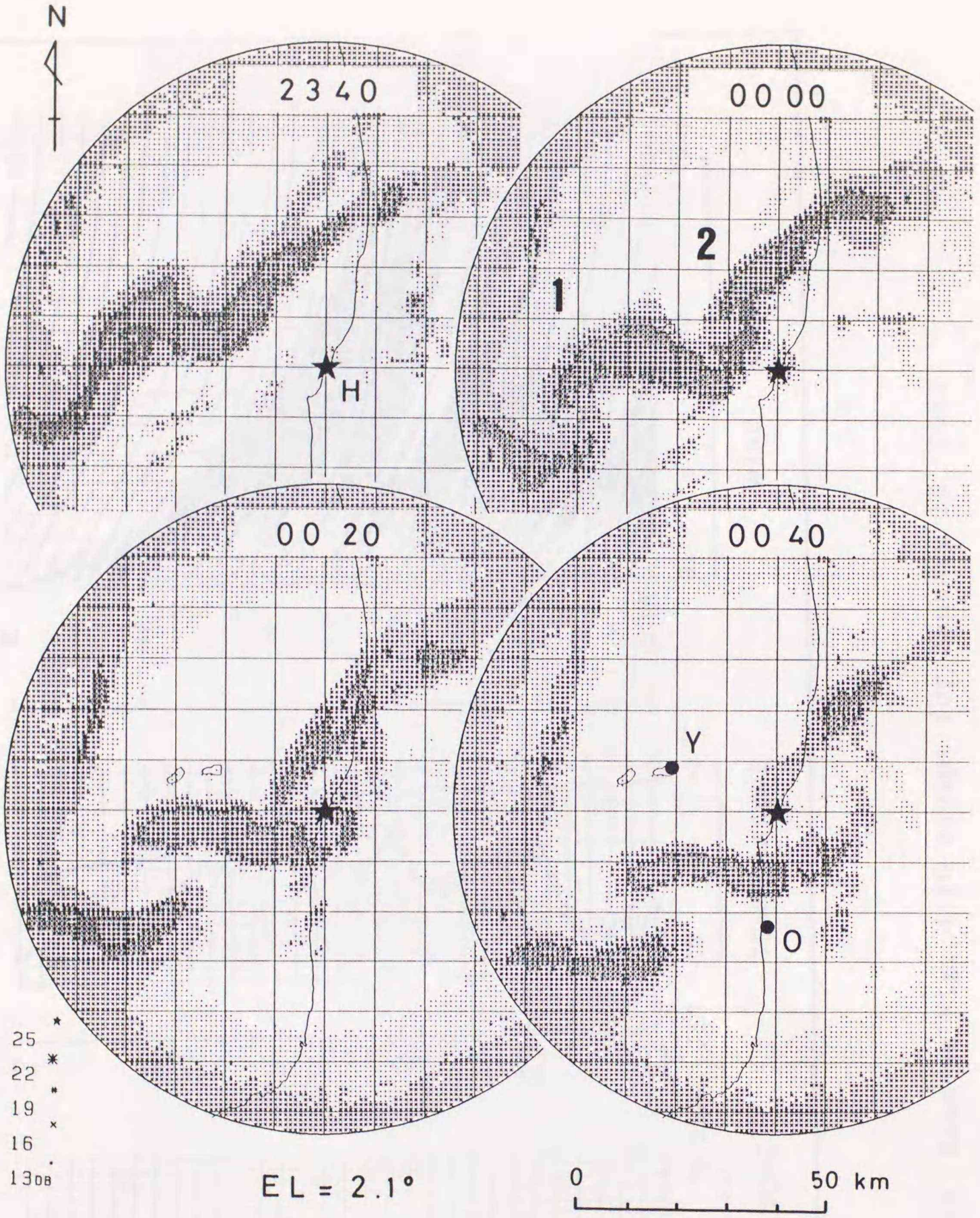

Fig. 4-15 Time sequence of PPI radar echo patterns.

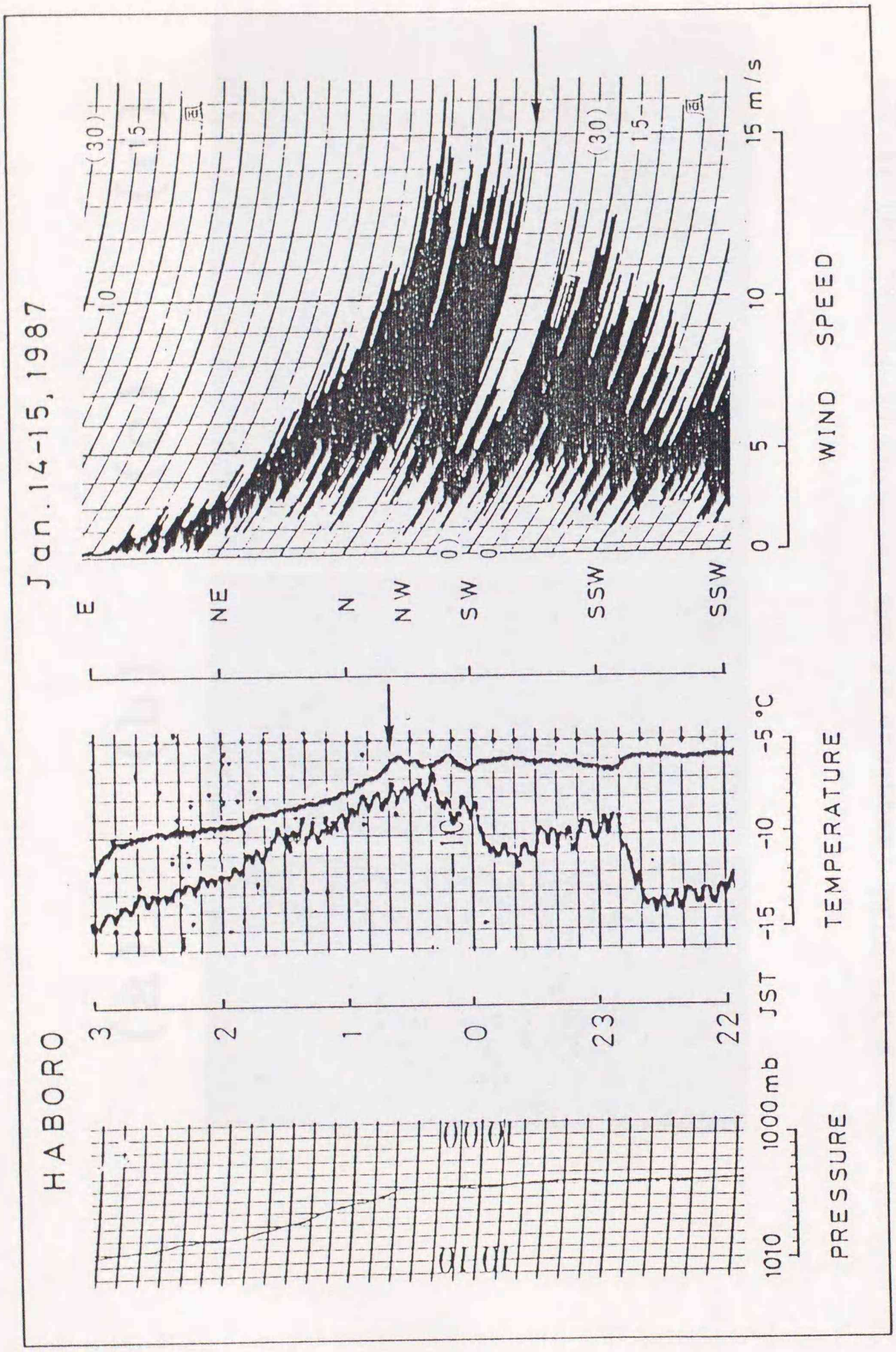

Fig. 4-16 Same as Fig. 4-10 except for January 15, 1987.

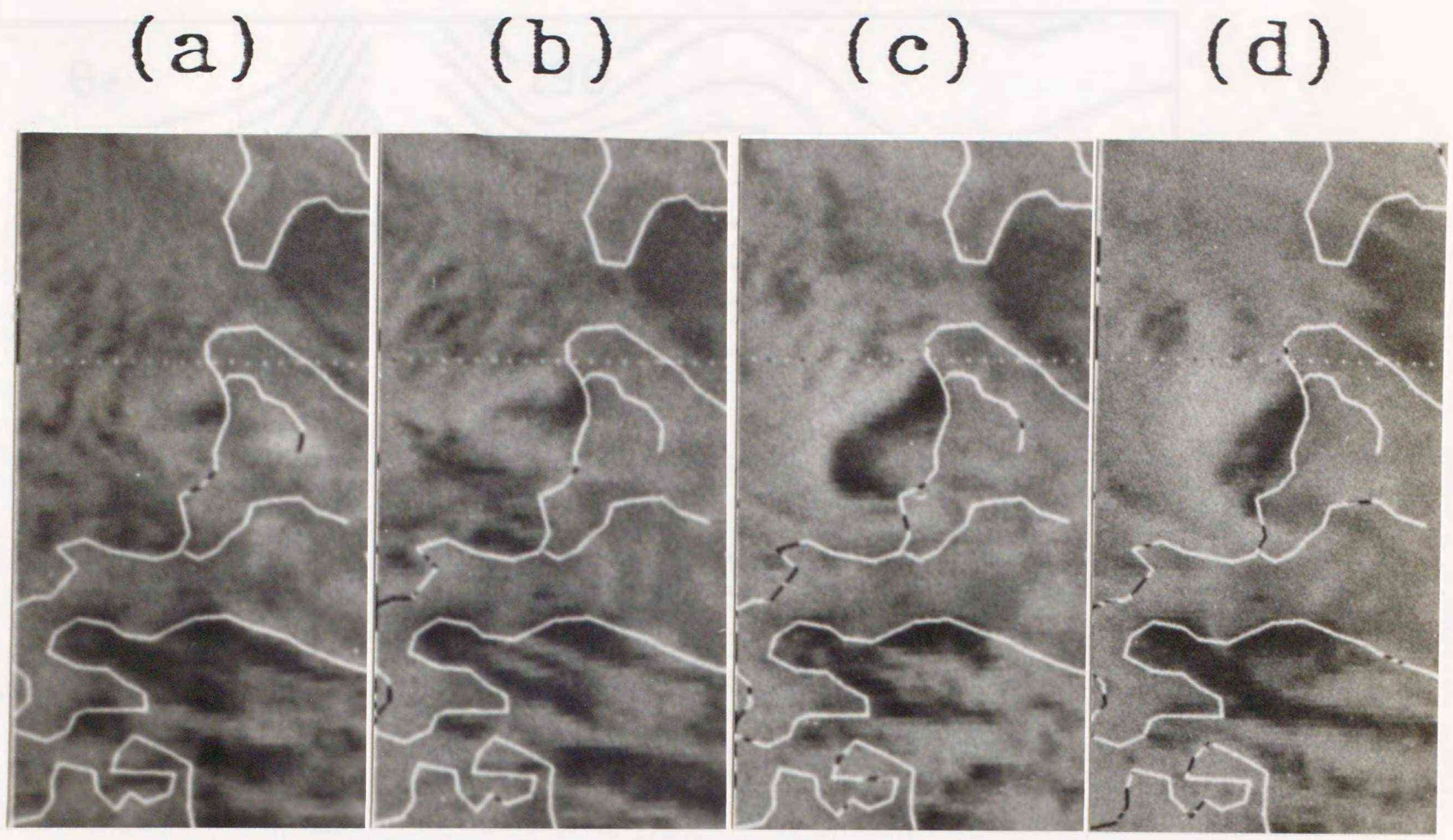

Fig. 4-17 Time sequence of GMS infrared pictures. (a) 18 JST Jan. 31, 1987. (b) 21 JST. (c) 01 JST Feb. 1. (d) 03 JST.

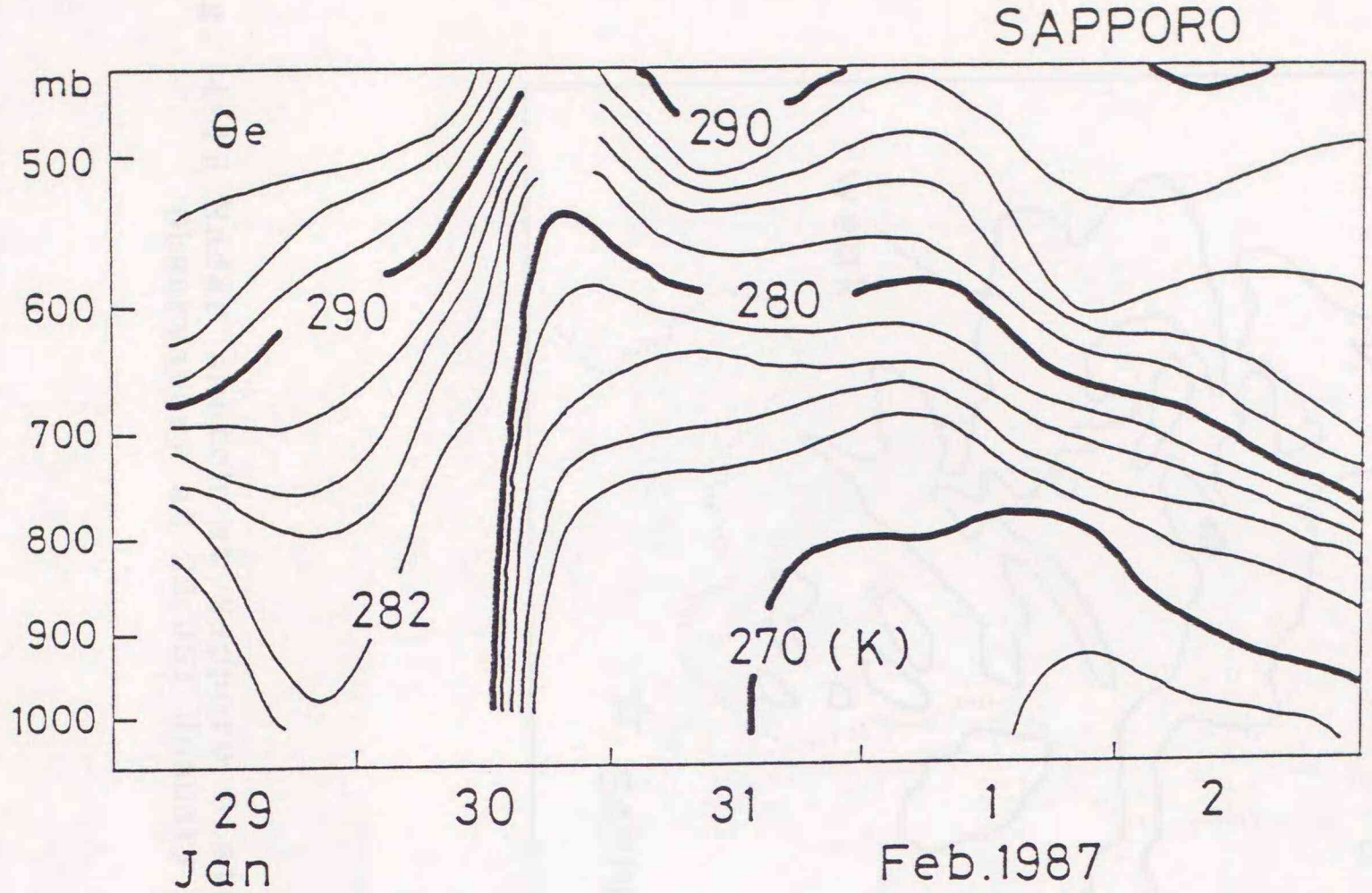

Fig. 4-18 Time height cross section of equivalent potential temperature at Sapporo.

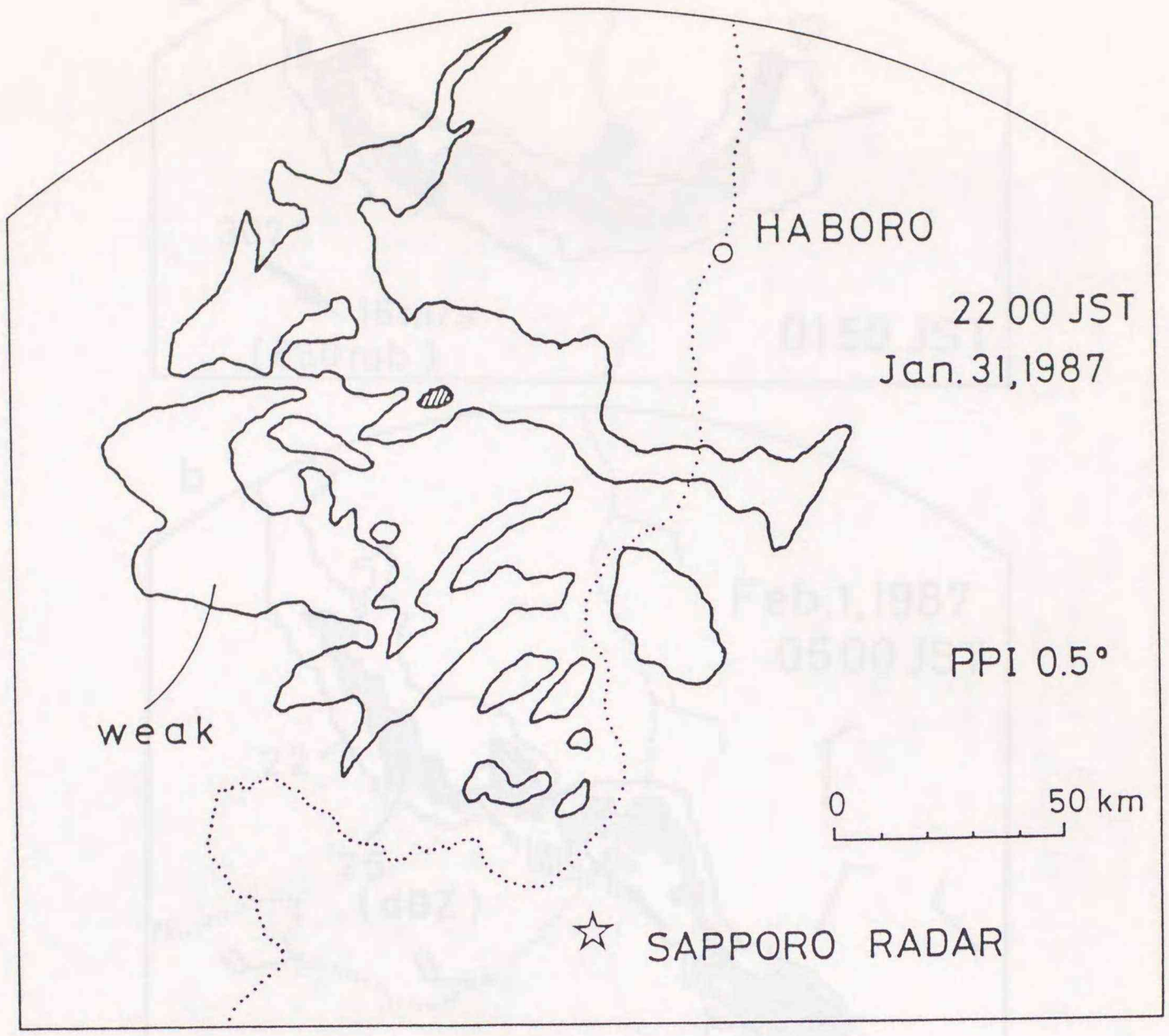

Fig. 4-19 Radar sketch at Sapporo District Meteorological Observatory at 22 JST January 31, 1987.

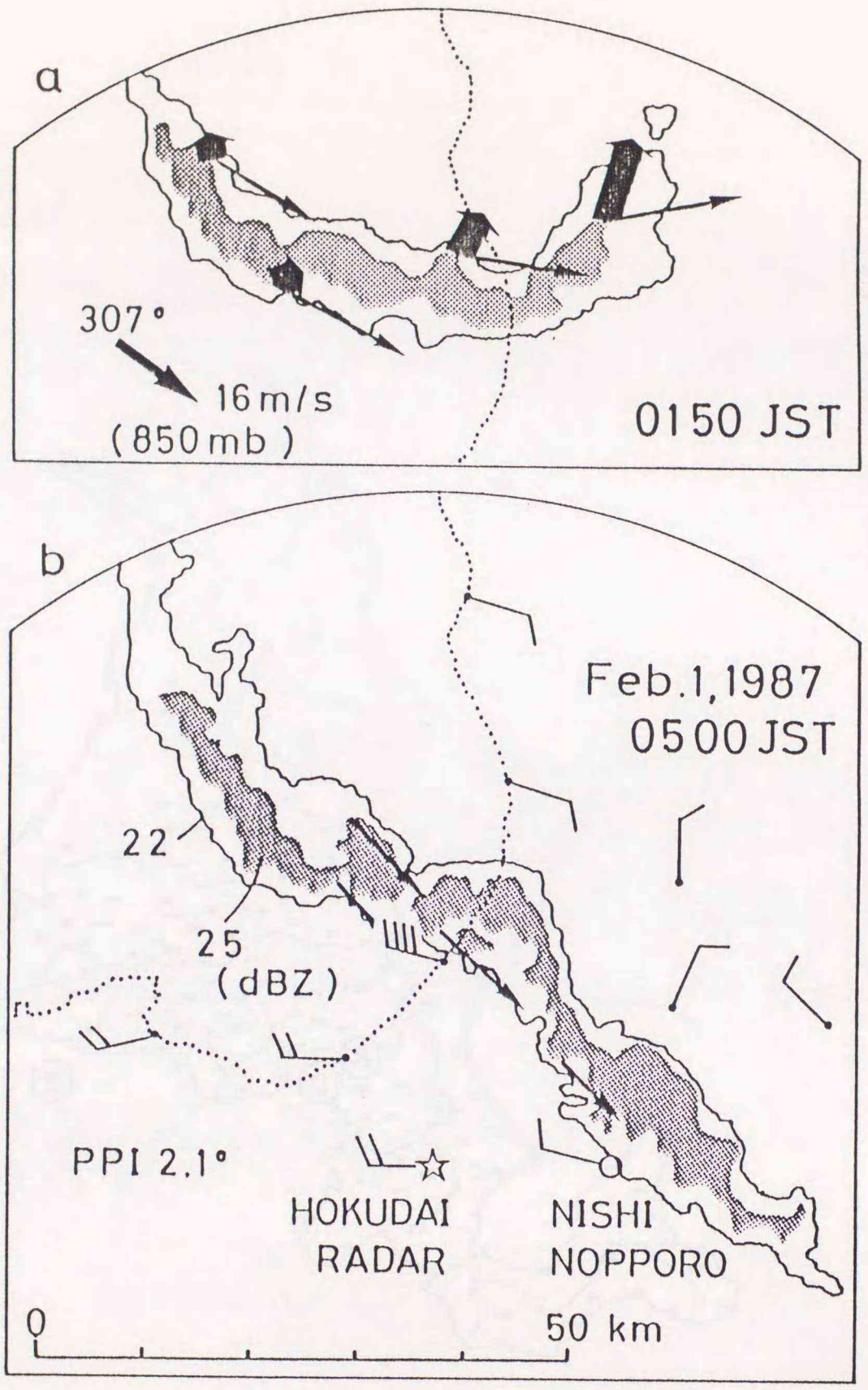

Fig. 4-20 PPI radar echo patterns at Hokkaido University, at the mature stage of the cyclone (a) and after the dissipation of the cyclone (b). Thin arrows and thick arrows indicate 10 minute displacement vector and storm relative vector, respectively.

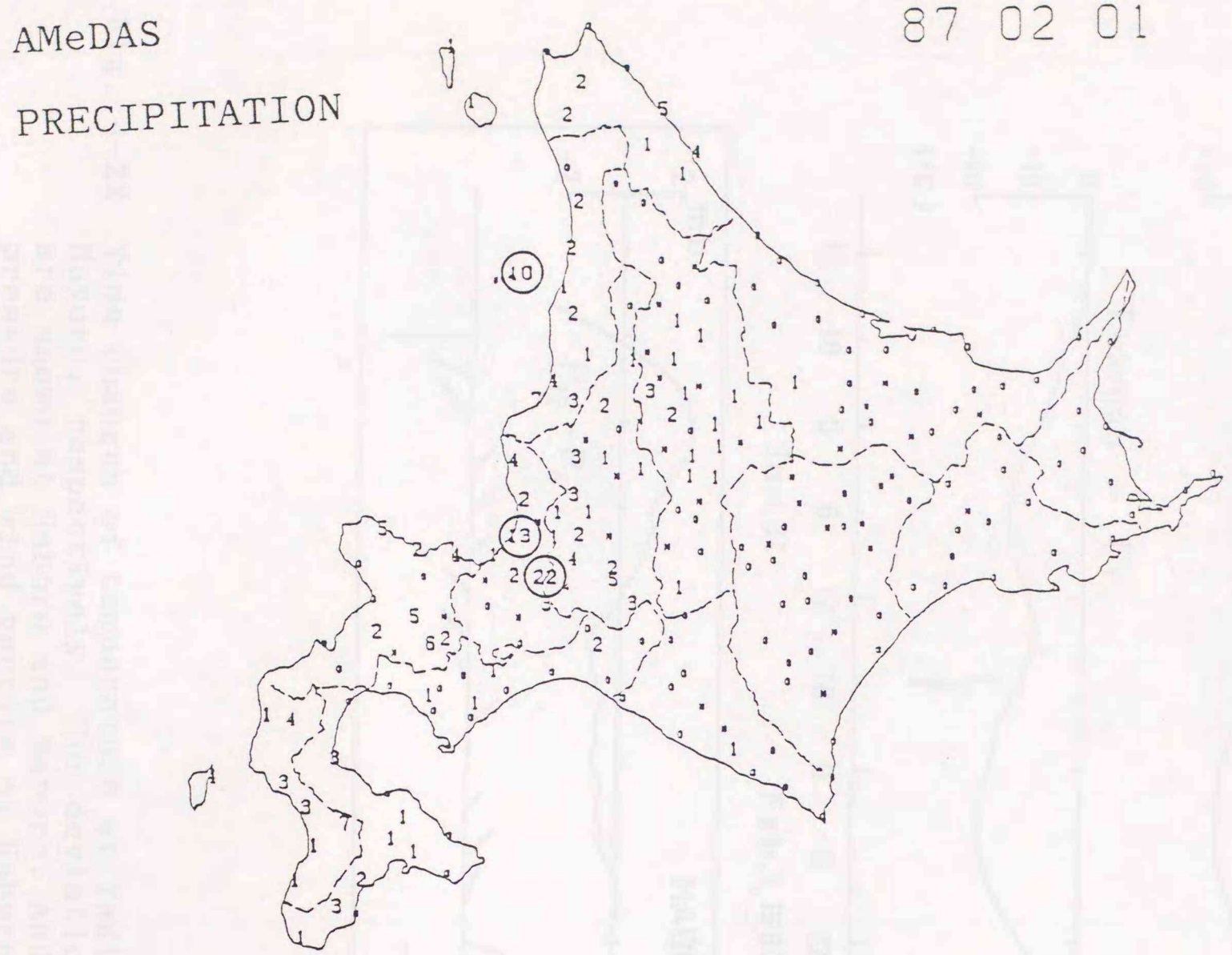

Fig. 4-21 AMeDAS precipitation data (mm in water) for 12 hours in the morning on February 1, 1987. Circles and N denote stations > 10 mm and no data, respectively.

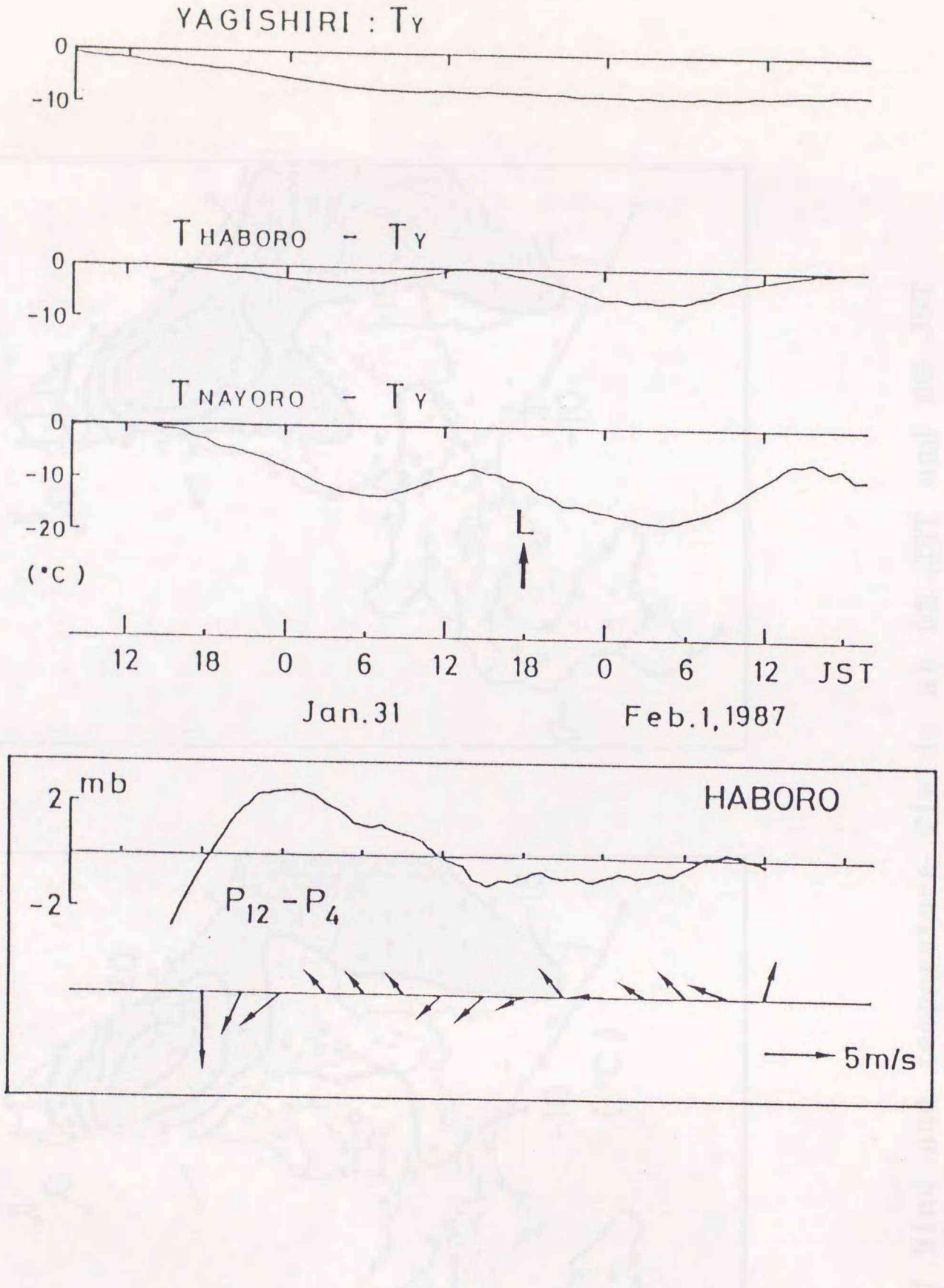

Fig. 4-22 Time changes of temperature at Yagishiri, Haboro and Nayoro, respectively. The deviations from Yagishiri are shown at Haboro and Nayoro. And the running mean pressure and wind vectors at Haboro are also shown.

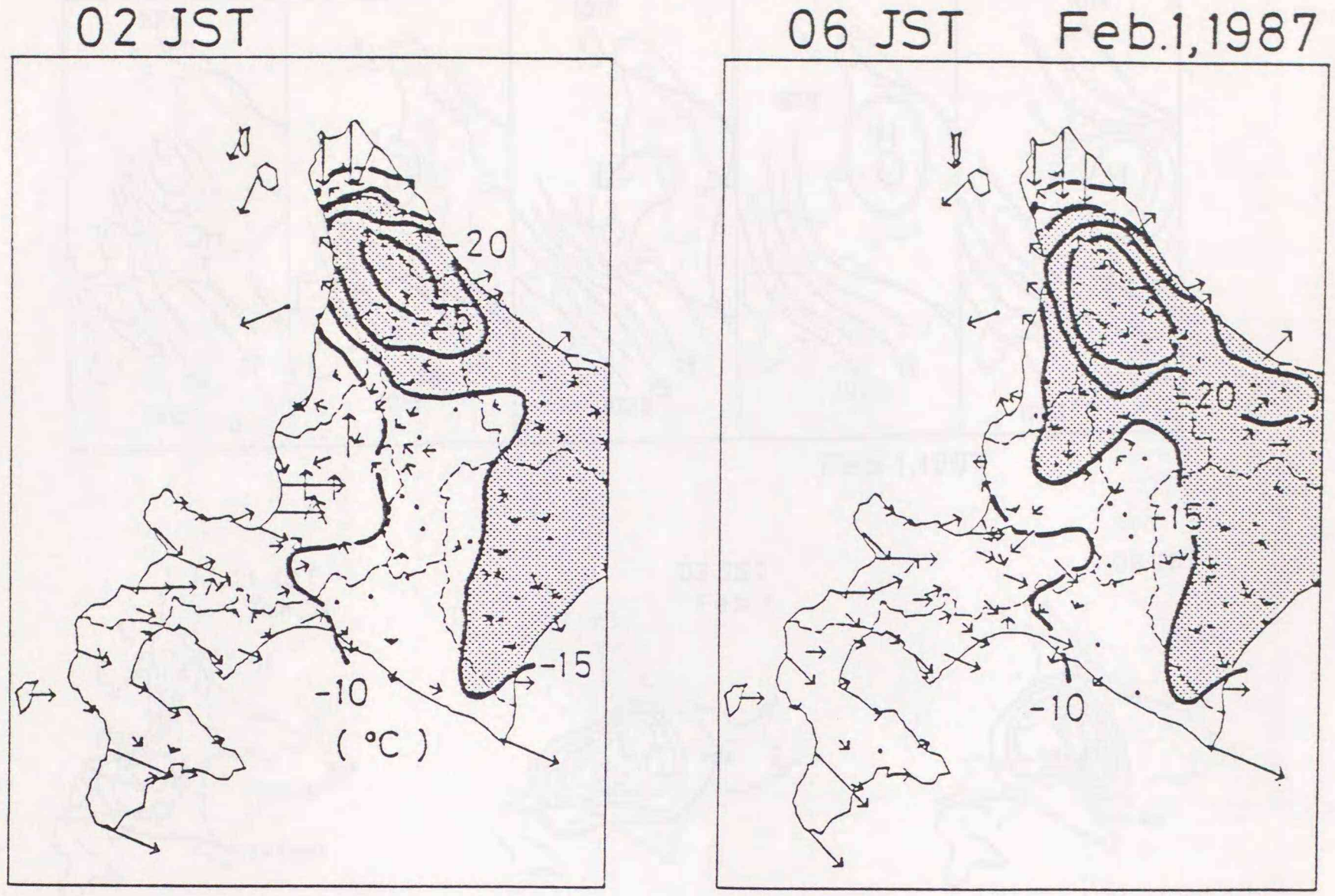

Fig. 4-23 Wind and temperature fields at 02 JST and 06 JST February 1, 1987.

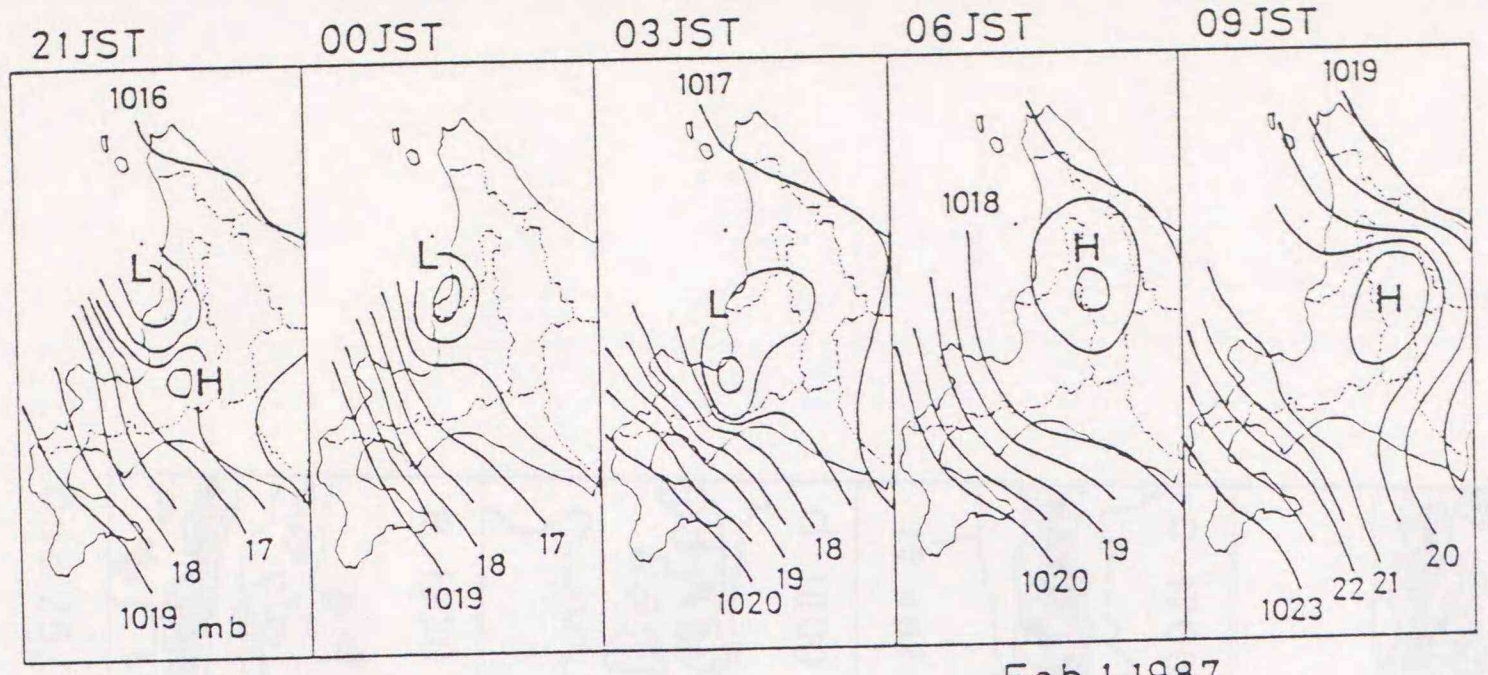

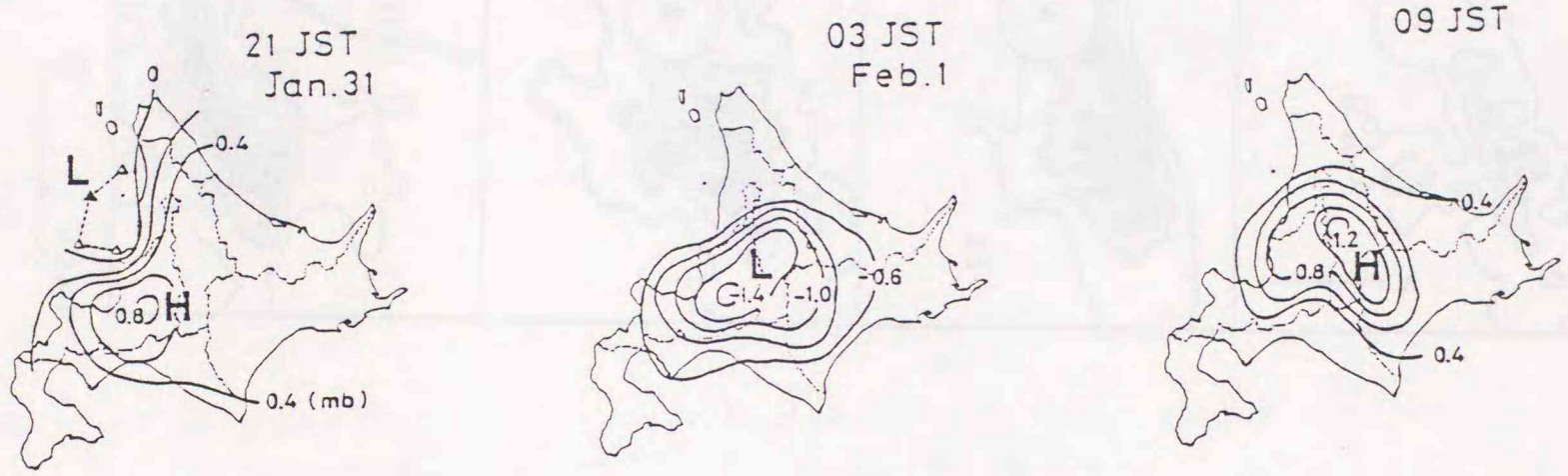

Fig. 4-24 Three hourly pressure fields around Hokkaido (top) and the pressure deviations from the running mean for 12 hours (bottom).

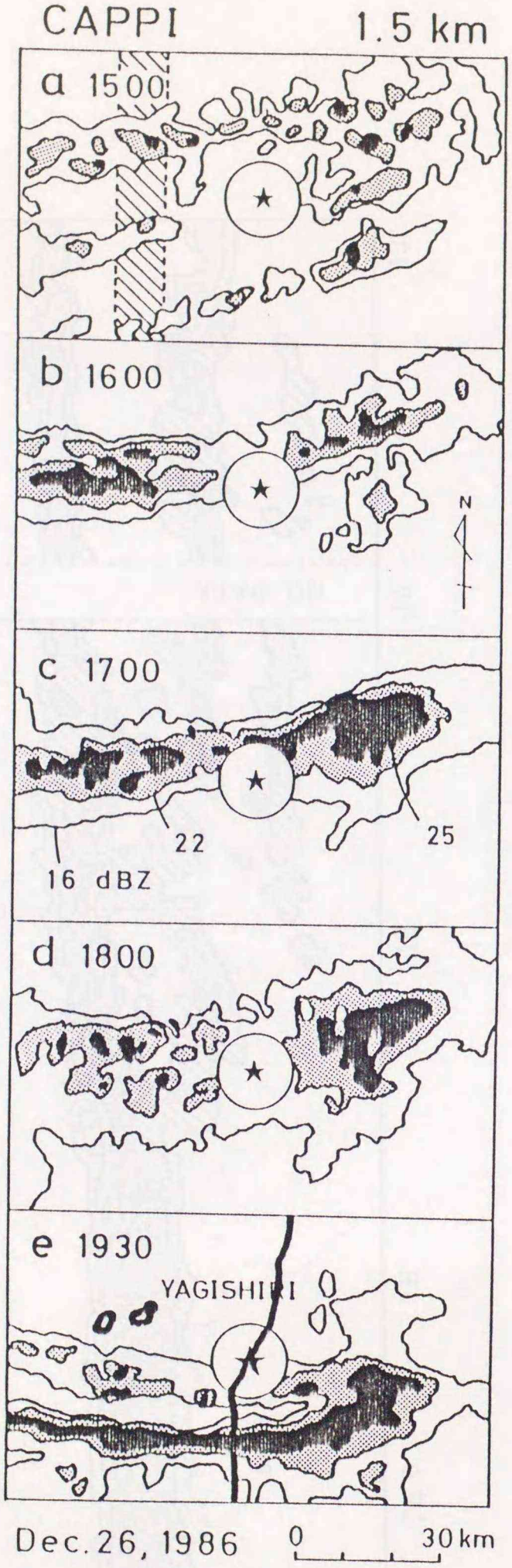

Fig. 4-25 Time sequence of the CAPPI radar displays on December 26, 1986.

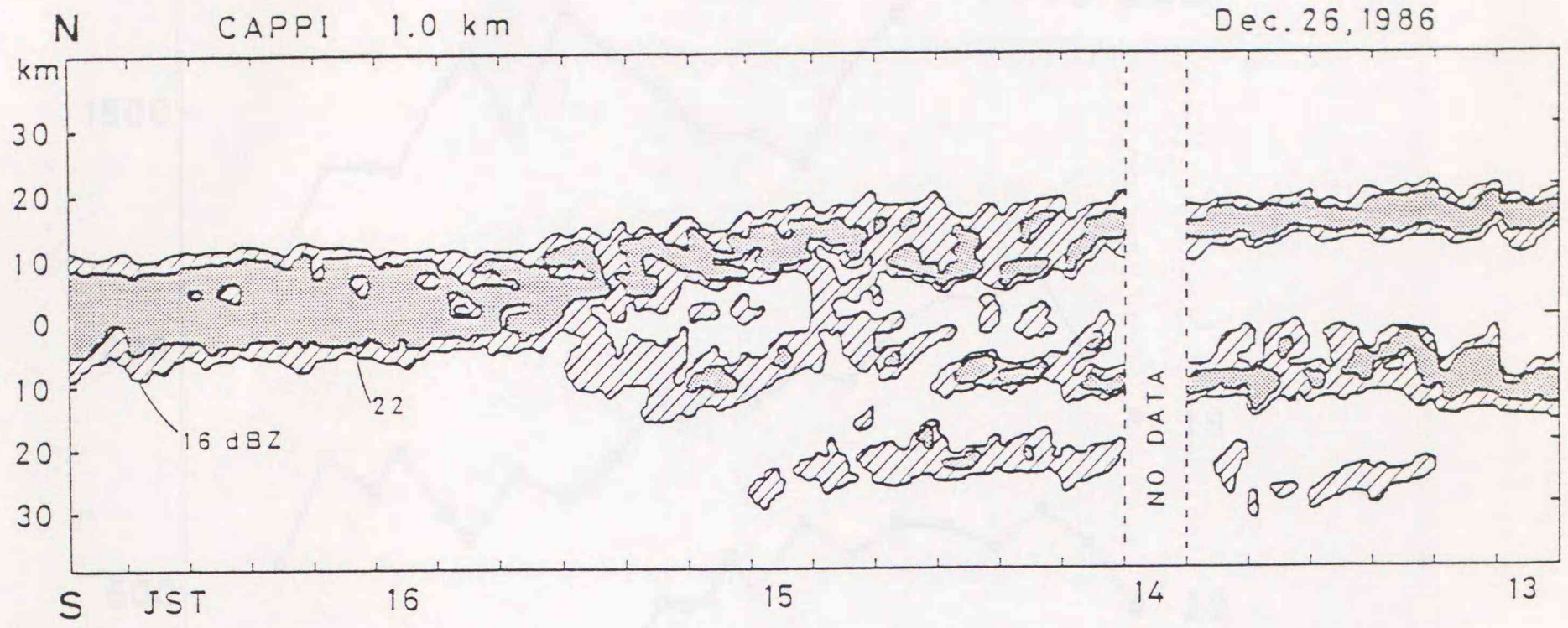

Fig. 4-26 South-north time section of the echo in the rectangular region in Fig. 4-25 (a).

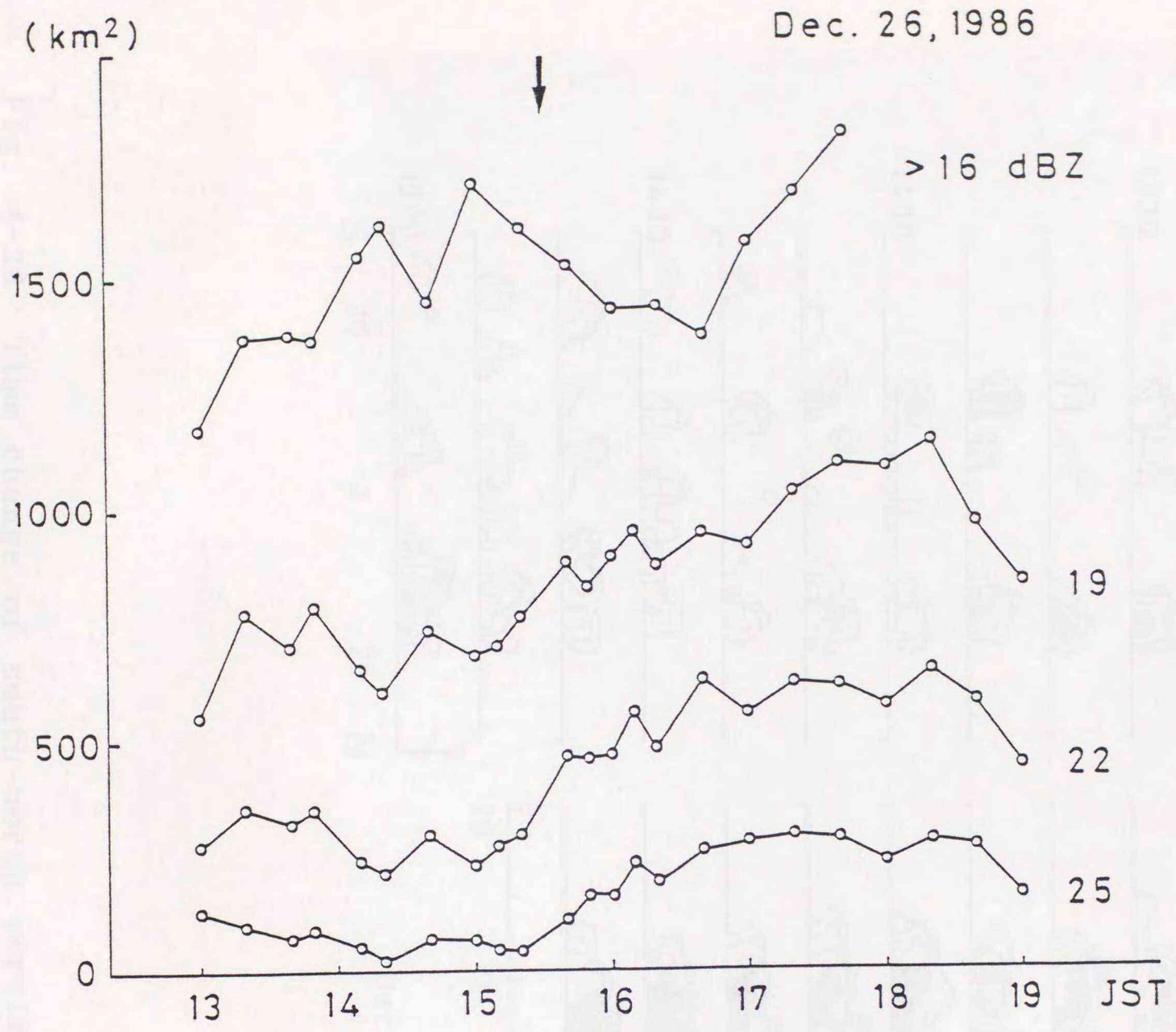

Fig. 4-27 Time changes of each echo area (>16, >19, >22 and >25 dBZ). An arrow denotes the time of the merging.

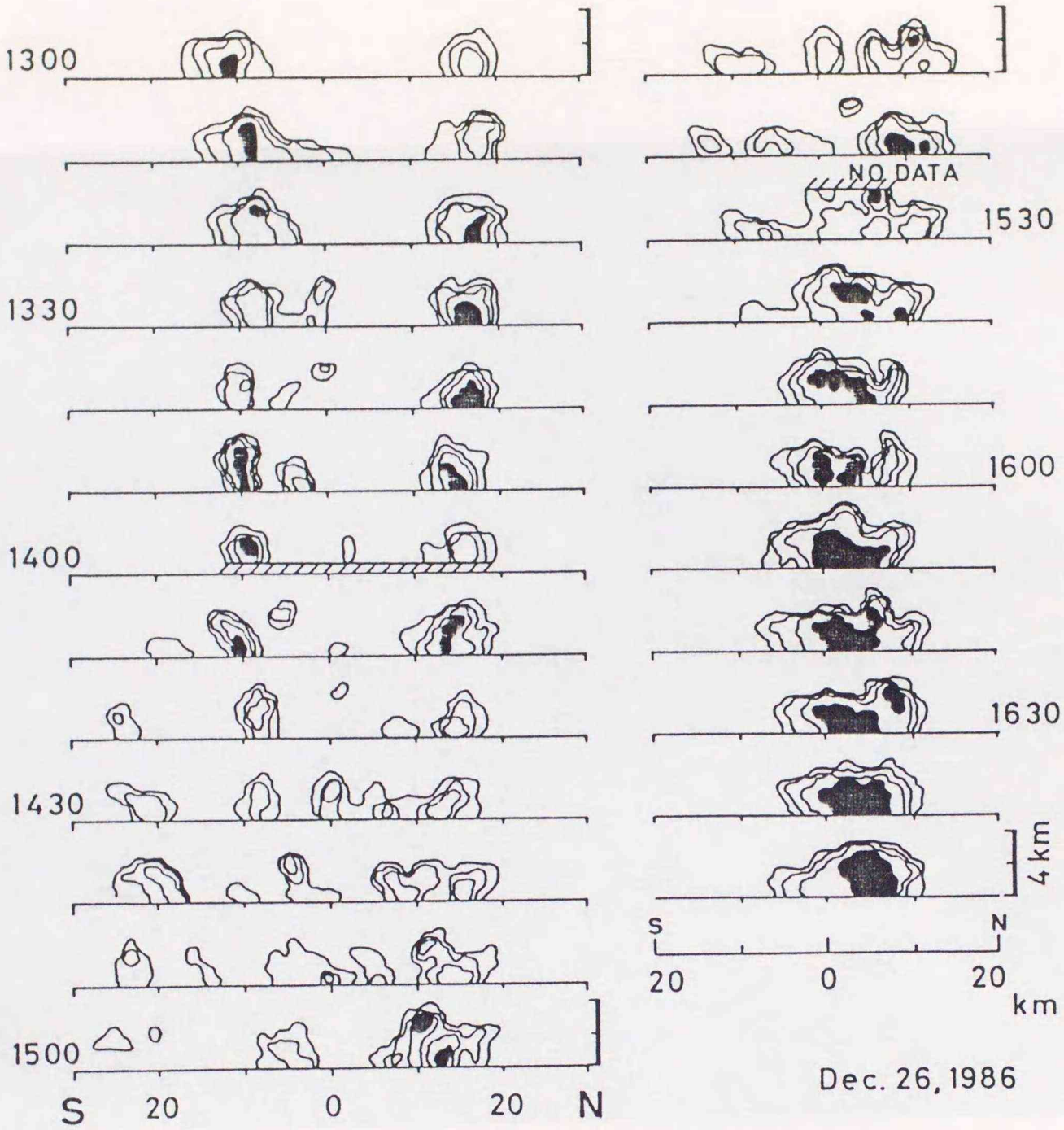

Fig. 4-28 Time change of south-north vertical cross sections of the band echoes observed at 20 km offshore.

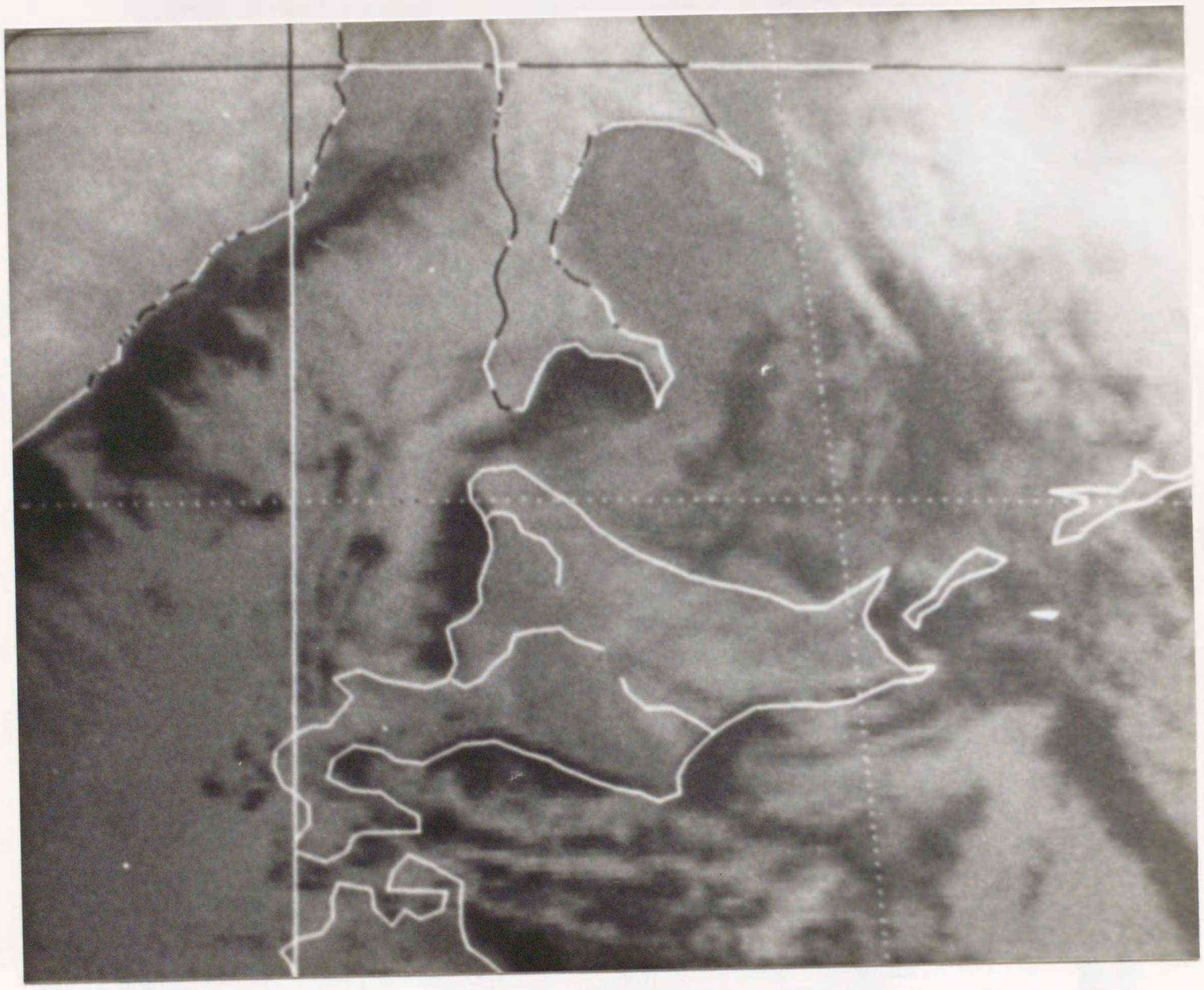

Fig. 4-29 GMS infrared picture of CBC at 03 JST Jan. 14, 1987.

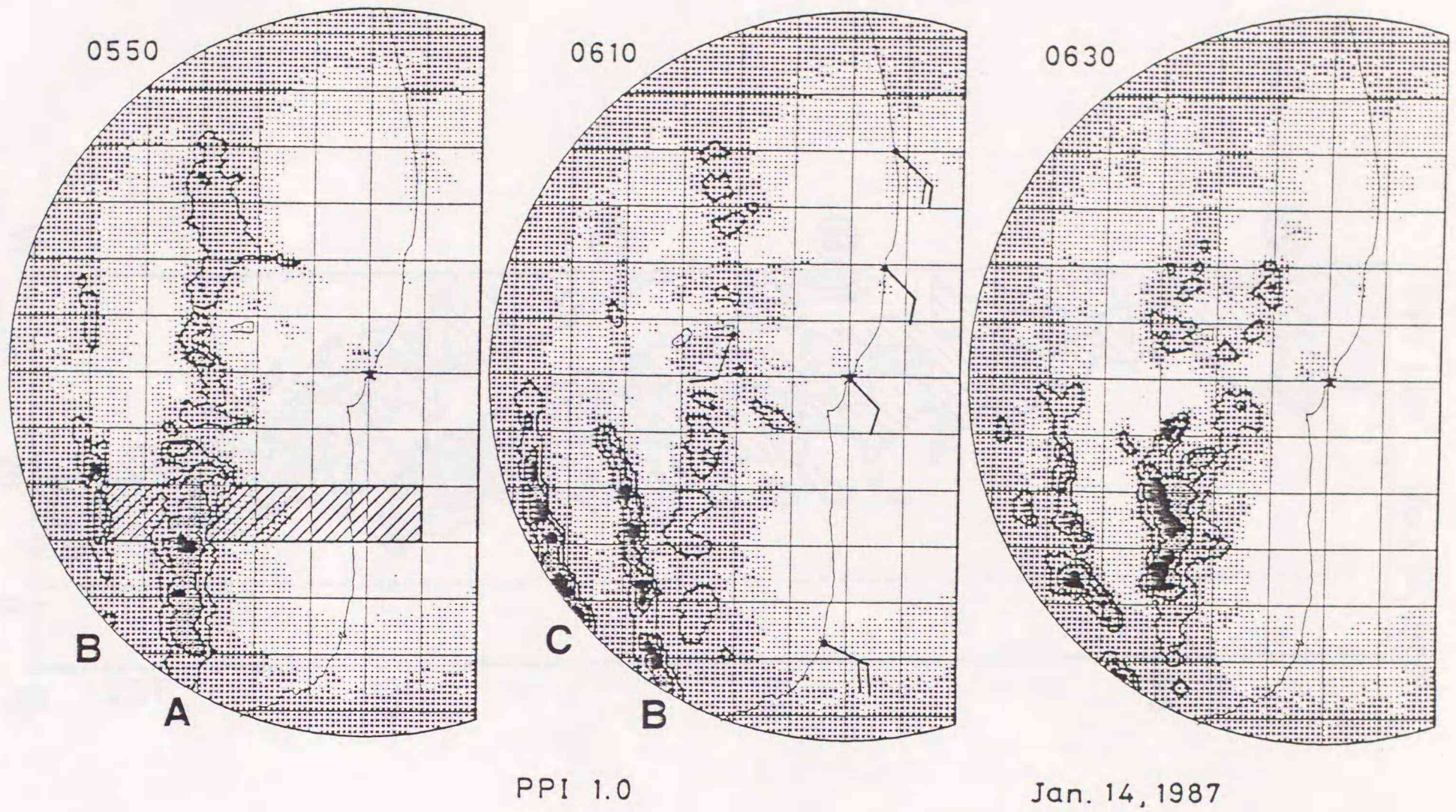

Fig. 4-30 Time sequence of the PPI radar patterns. Surface winds are shown in the center.

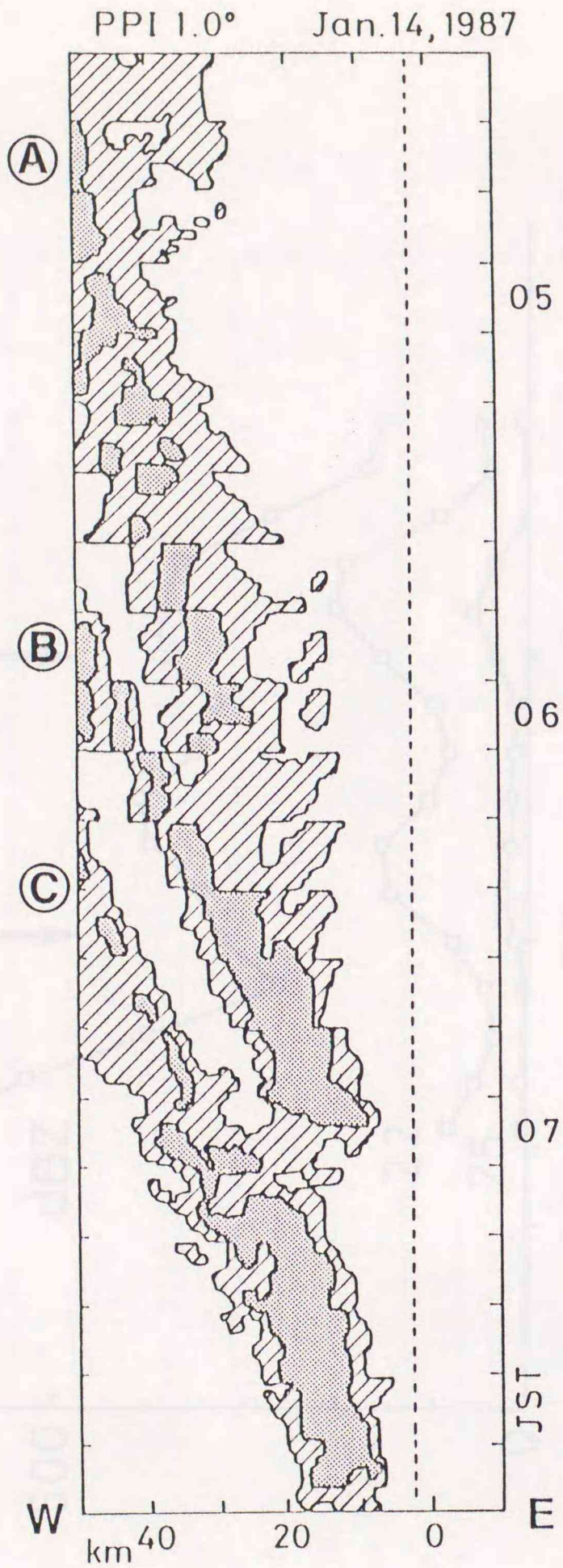

Fig. 4-31 East-west time section of the echo in the rectangular region in Fig. 4-30.

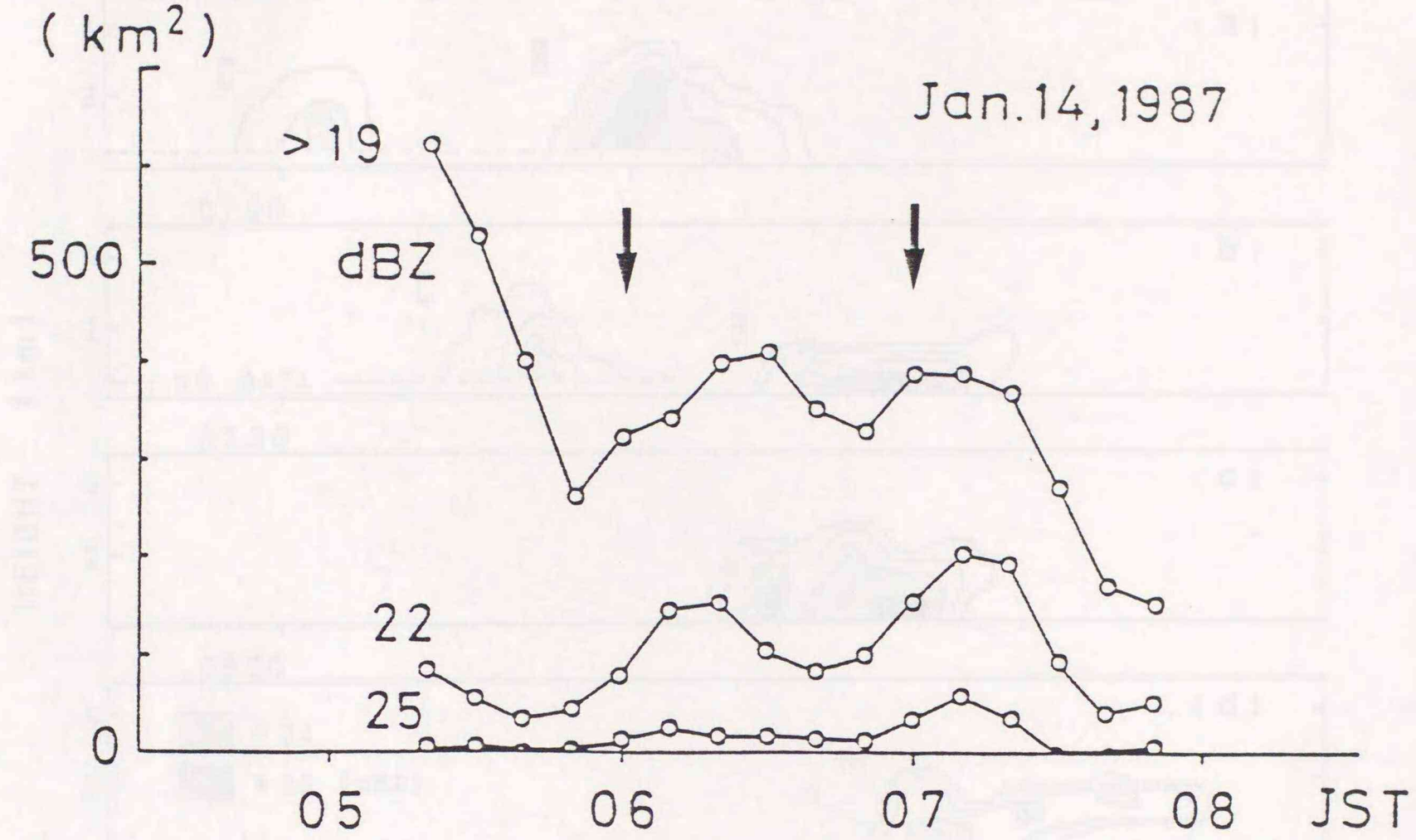

Fig. 4-32 Same as Fig. 4-27 except for January 14, 1987.

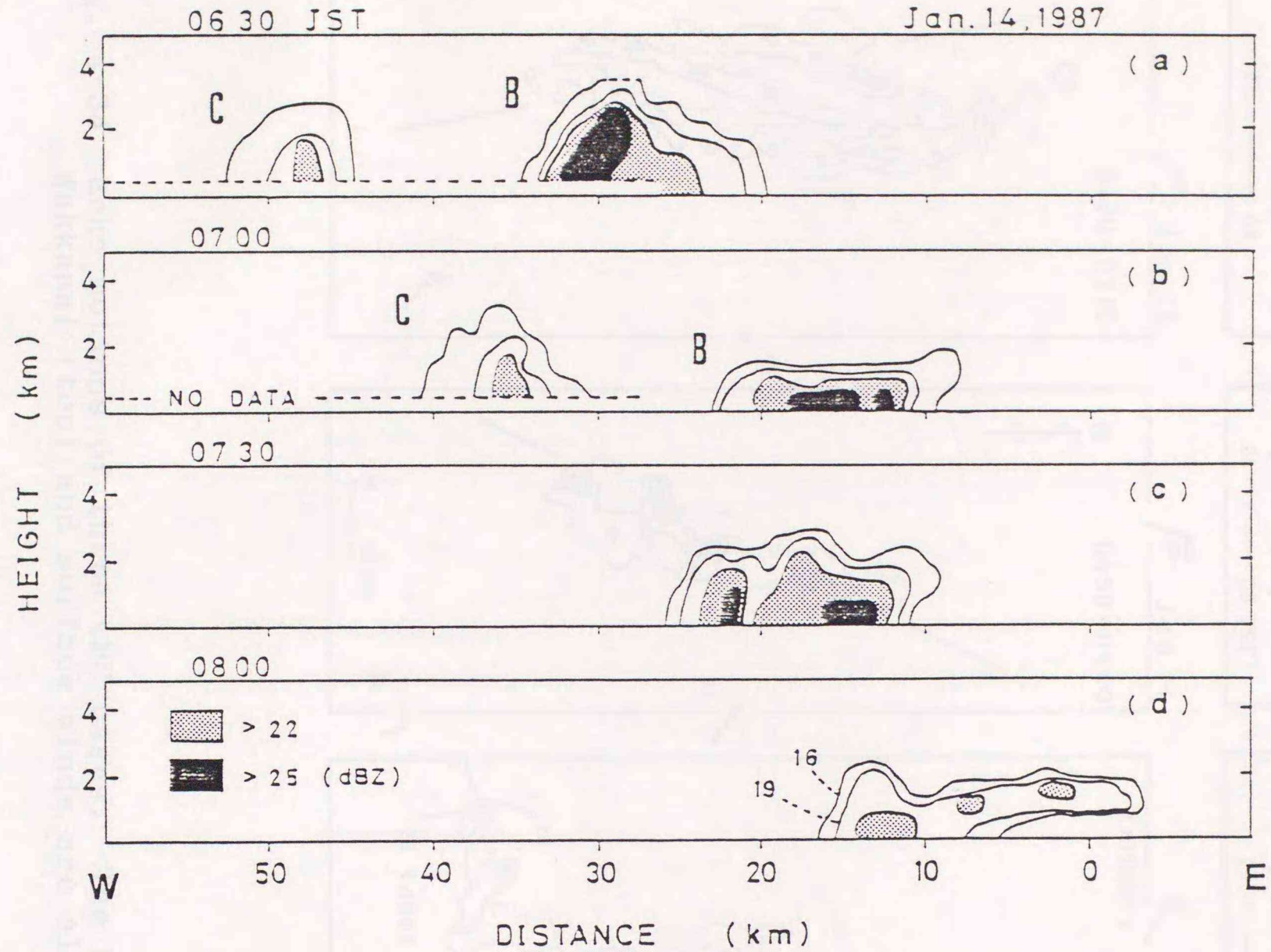

Fig. 4-33 Time change of west-east vertical cross sections of the band B and the band C at 20 km southward from the radar site.

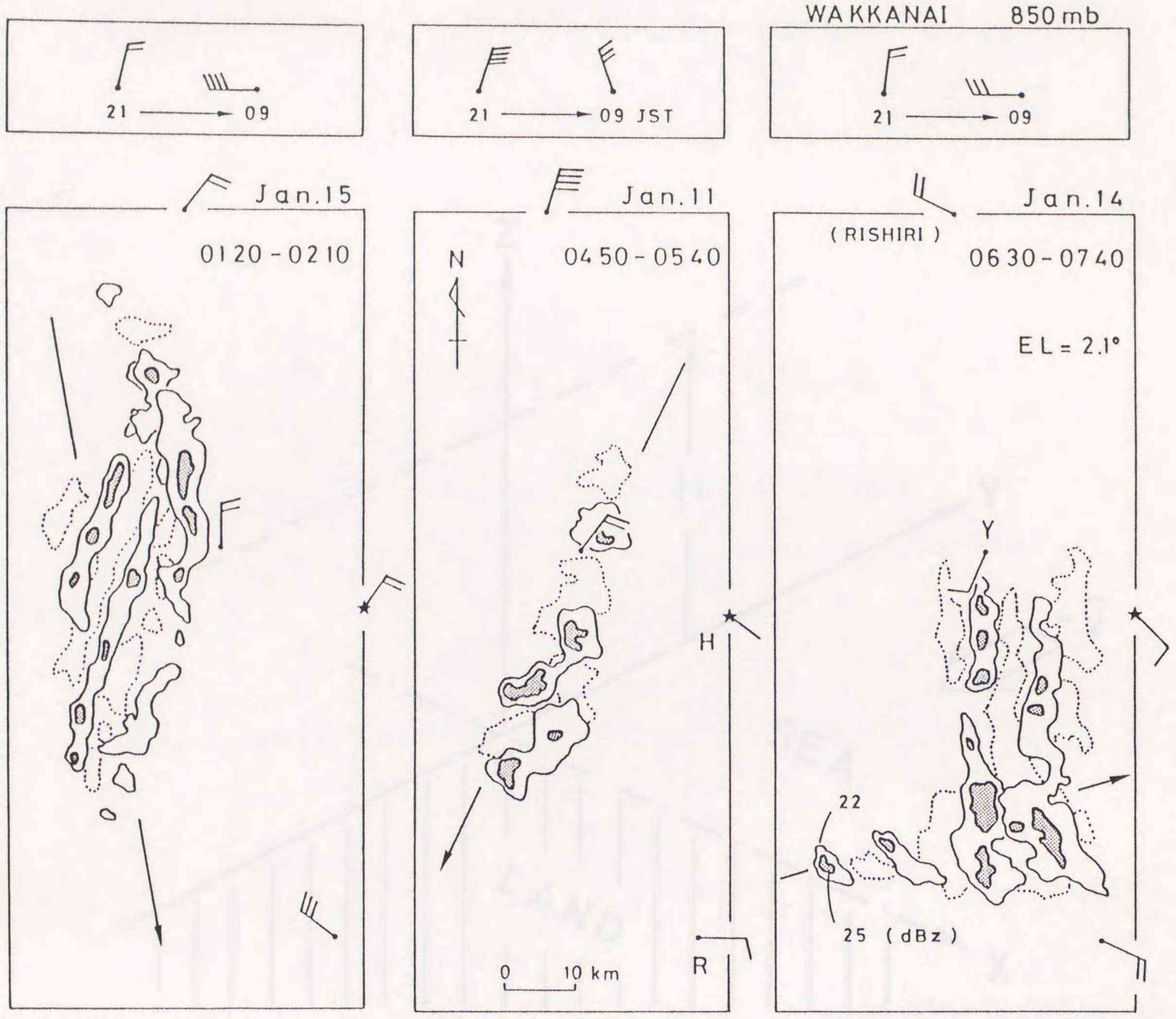

Fig. 4-34 Echo motions of three CBC cases. The 850 mb wind at Wakkanai (top) and surface winds are also shown.

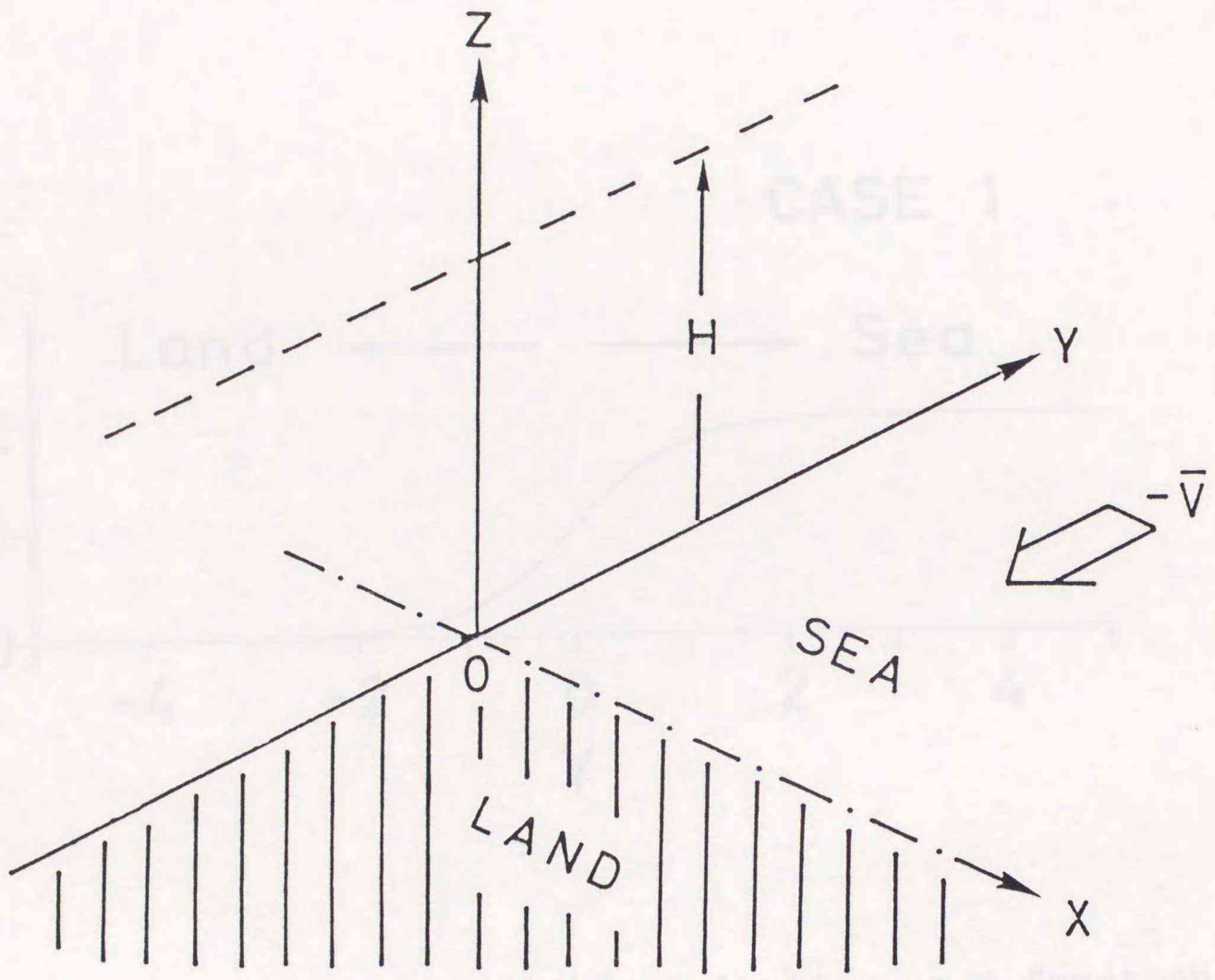

Fig. 5-1 The physical structure of the model. -V indicates the geostrophic wind in the initial condition.

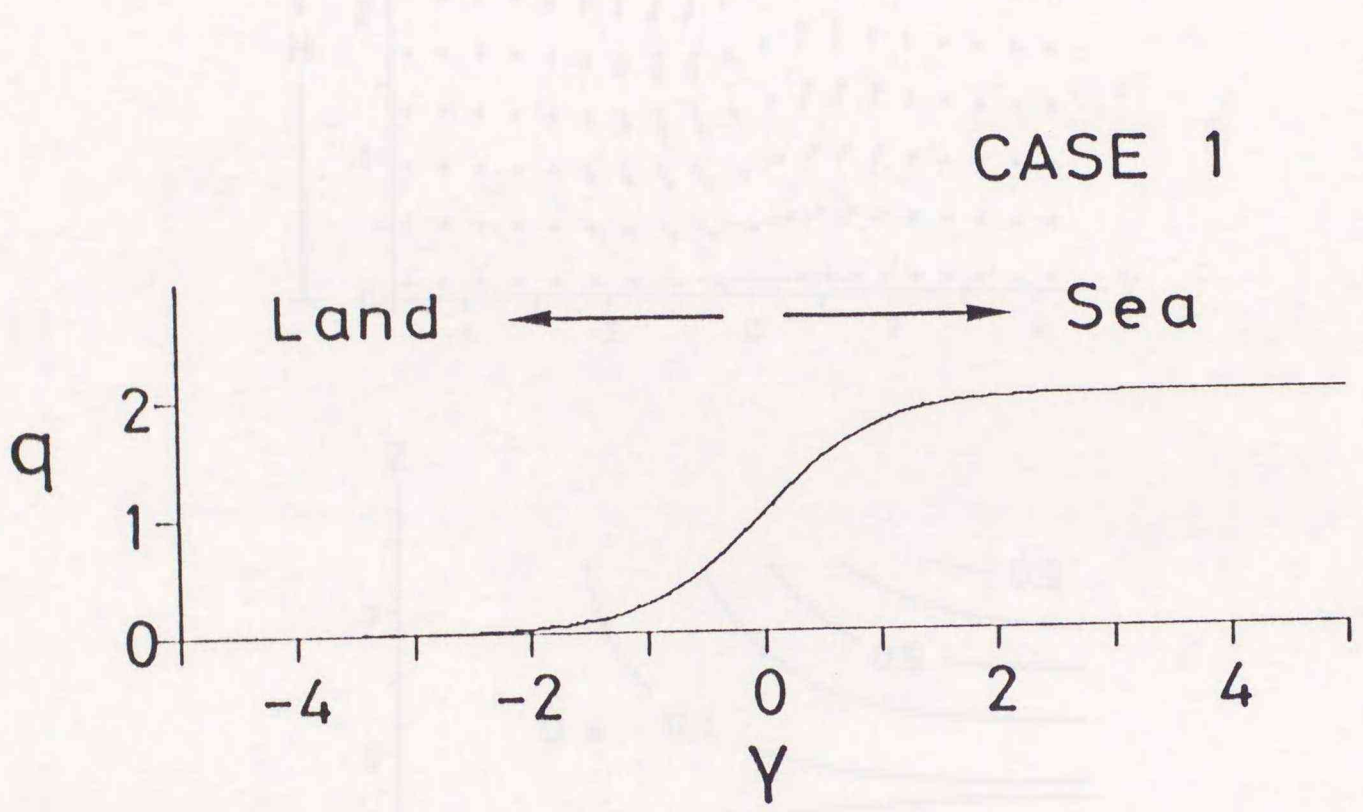

Fig. 5-2 The surface heating distribution as a function of y (Case 1).

CASE 1

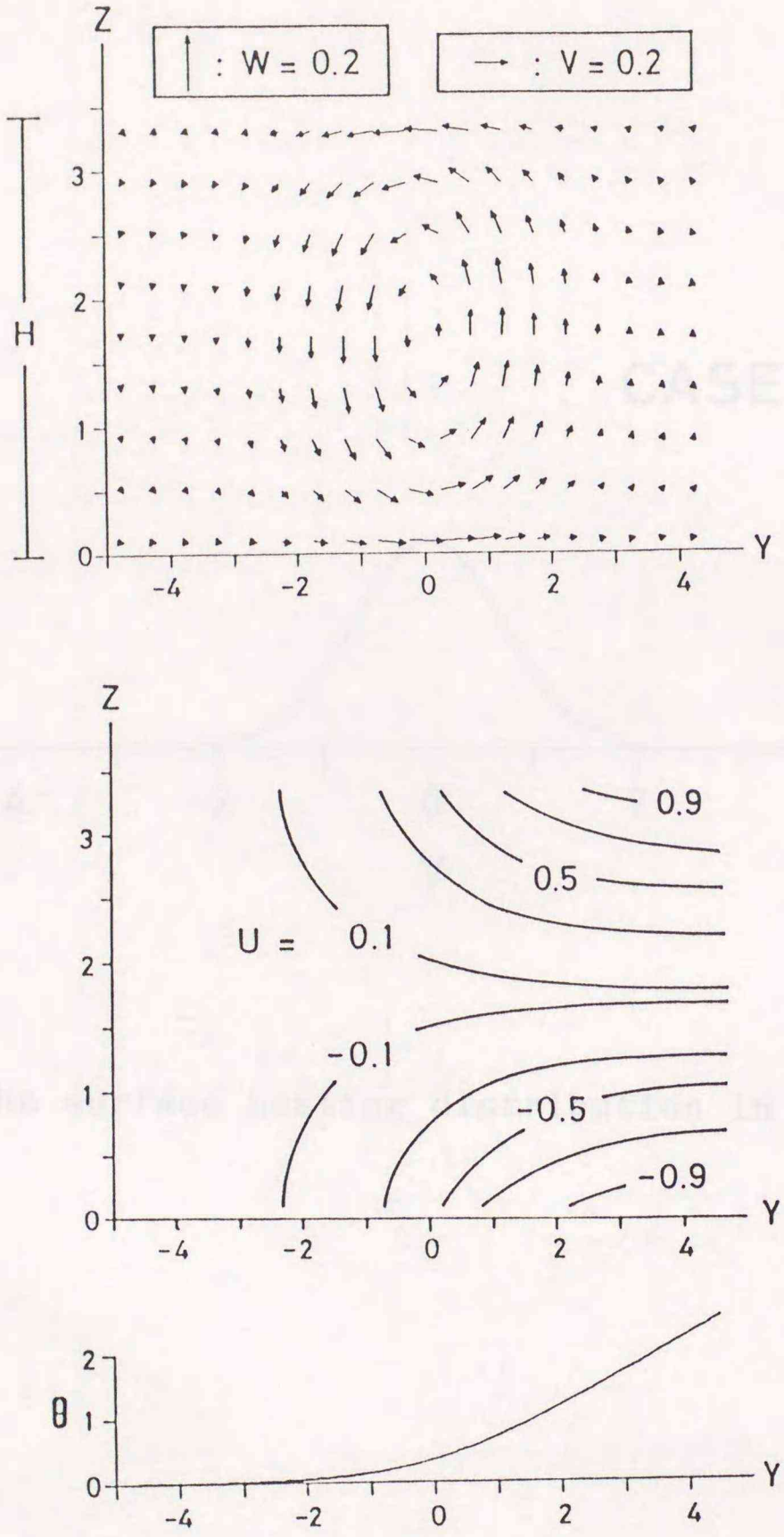

Fig. 5-3 The perturbation solutions of the v and w wind components (top), u component (center) and the potential temperature (bottom) under the condition of the heating in the Fig. 5-2.

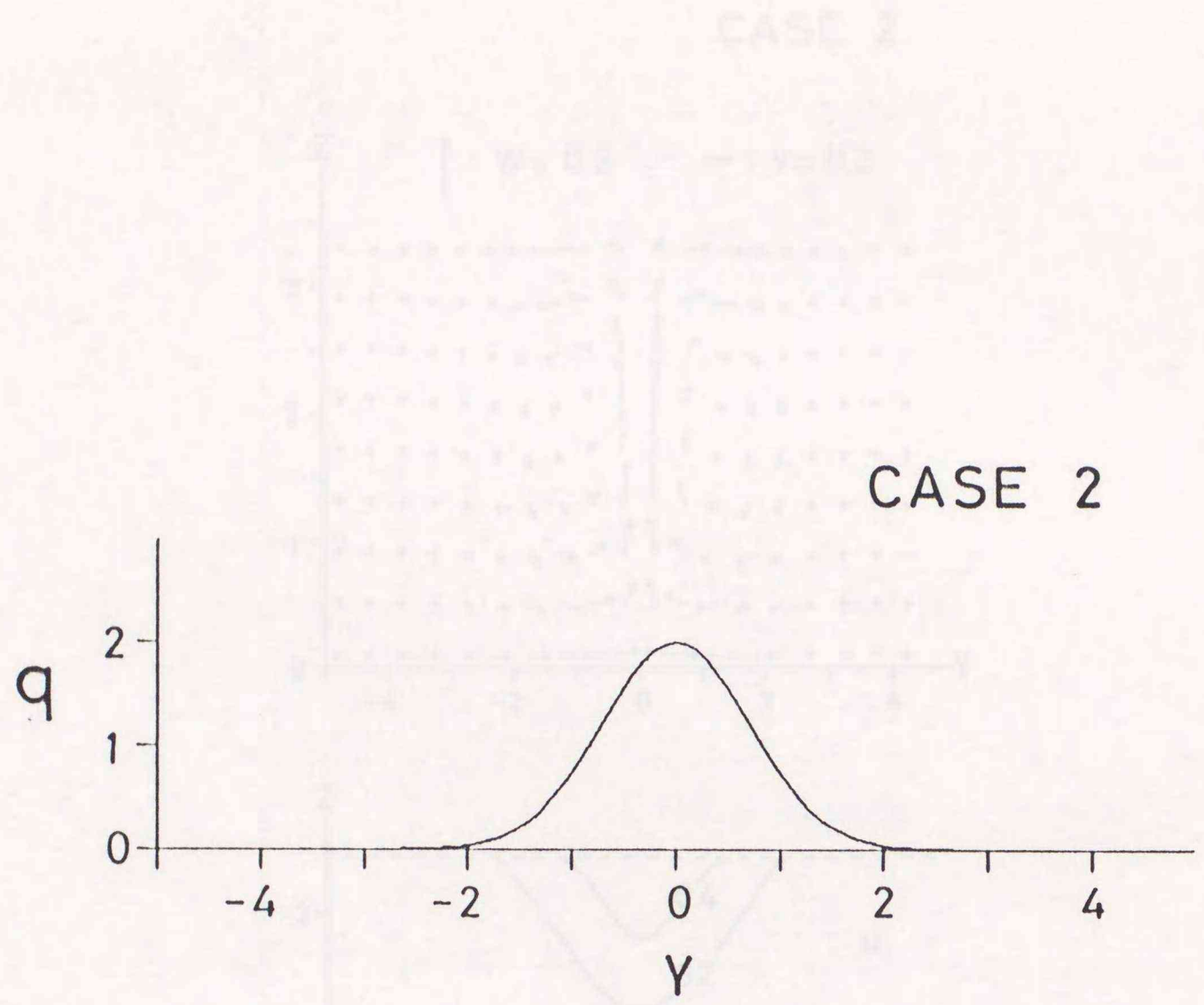

Fig. 5-4 The surface heating distribution in the second case.

CASE 2

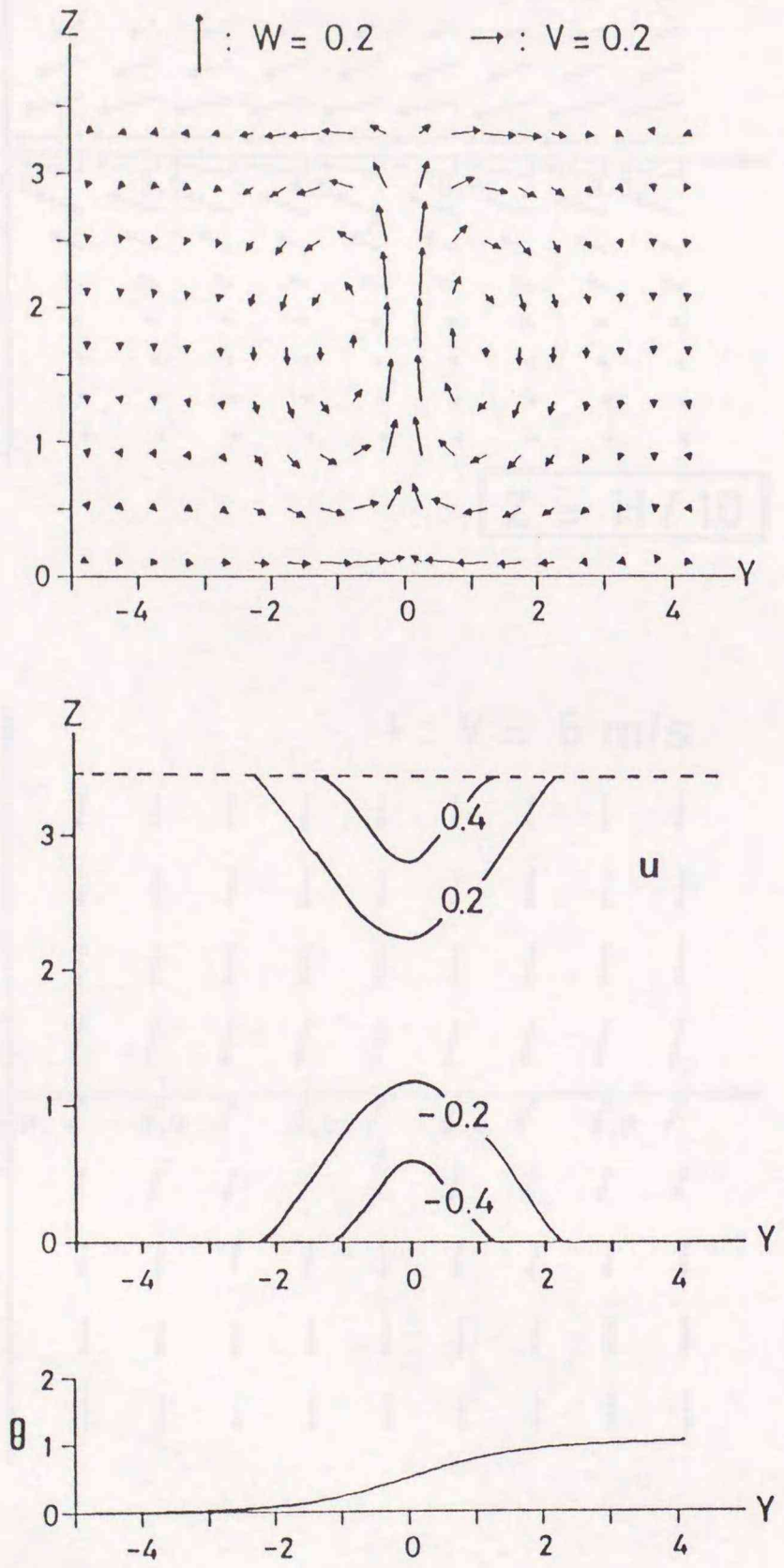

Fig. 5-5 Same as Fig. 5-3 except for the condition of the heating in the Fig. 5-4.

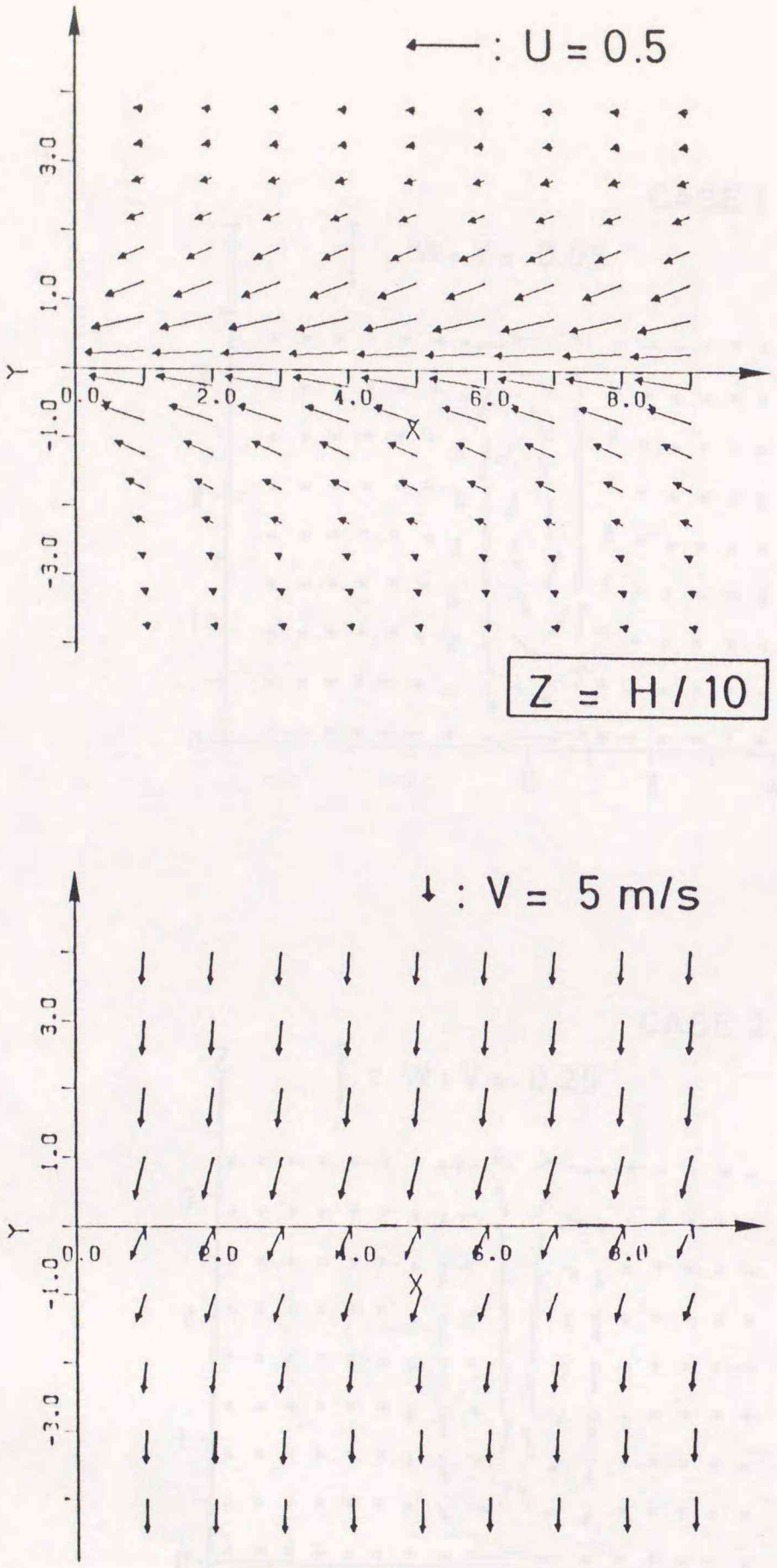

Fig. 5-6 The surface wind field of the x-y plane (top). The wind field multiplied by the geostrophic wind of 5 m/s is also shown (bottom).

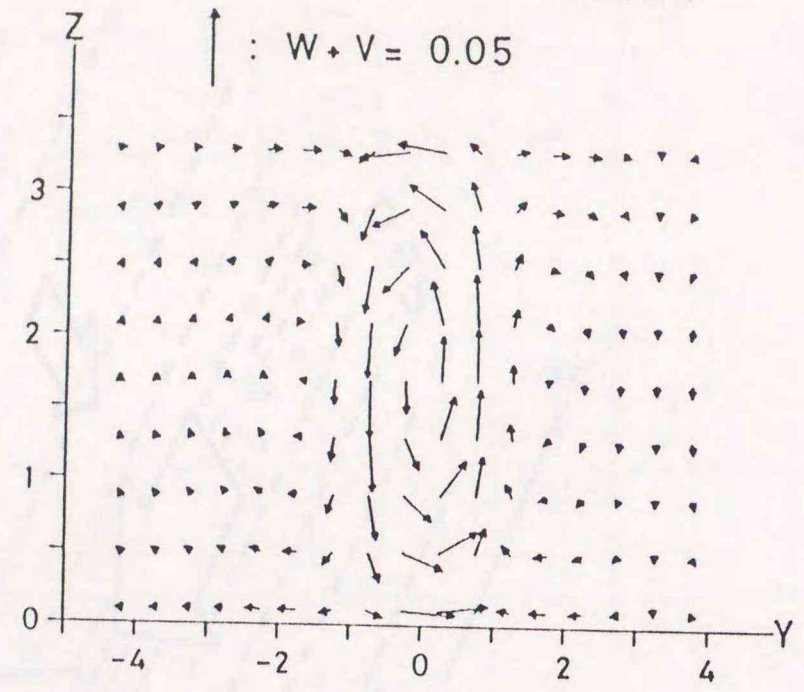

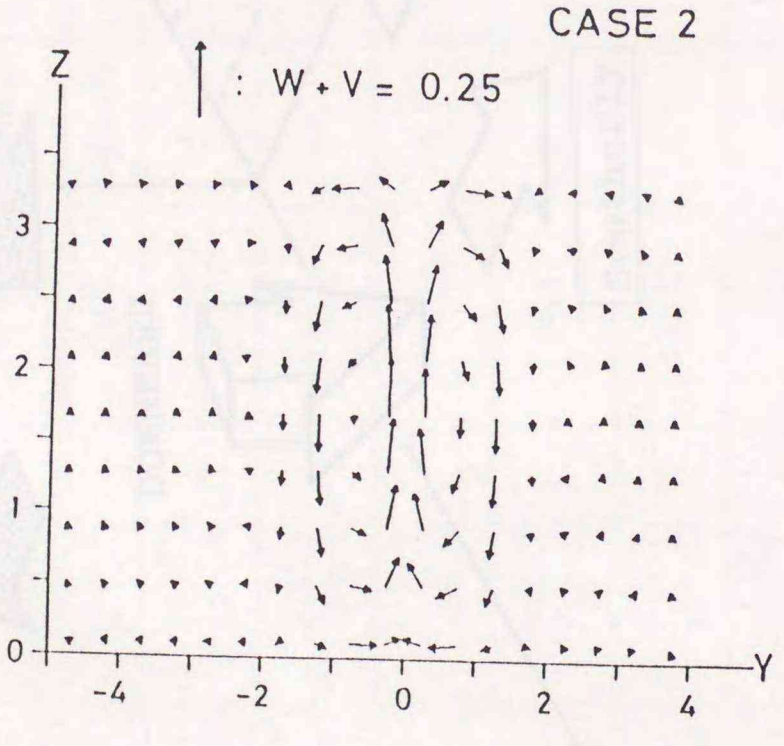

Fig. 5-7 The first order solutions of the v and w wind components, in case 1 (top) and case 2 (bottom), respectively.

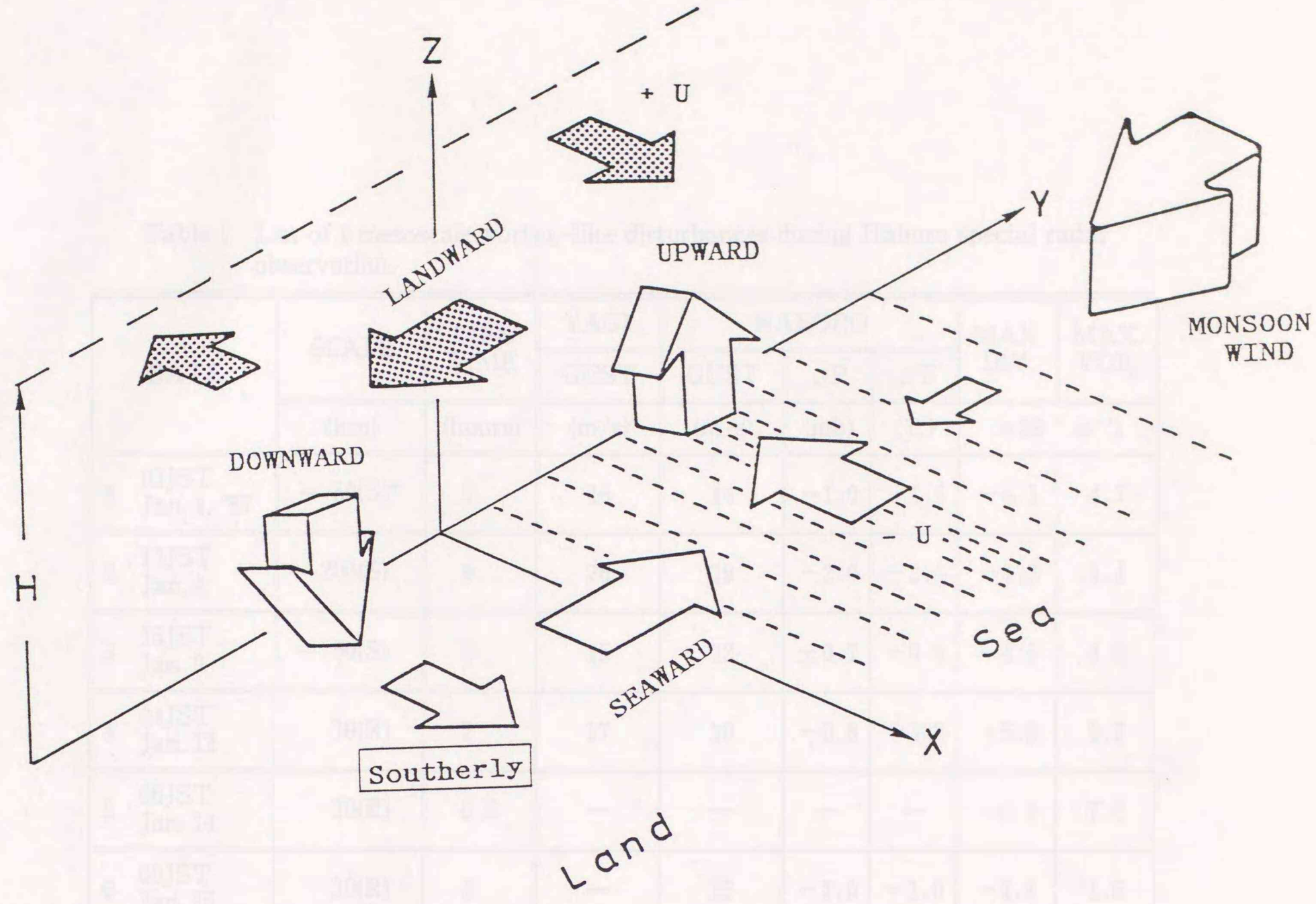

Fig. 5-8 The schematic figure of non-geostrophic winds shown by wide arrows. Dashed lines indicate sea surface isotherms.

Table 1 List of 6 mesoscale vortex-like disturbances during Haboro special radar observation.

	DATE	SCALE	LIFE TIME	YAGI.	HABORO			MAX. DIV.	MAX. VOR.
				GUST	GUST	⊿P	⊿T		
		(km)	(hours)	(m/s)	(m/s)	(mb)	(℃)	$\times 10^{-4}$ (s^{-1})	
1	03JST Jan. 4, '87	~ 50(S)*	2	16	14	−1.0	+1.8	−6.1	4.7
2	13JST Jan. 4	~200(S)	9	26	19	−2.0	−2.0	−1.3	1.4
3	15JST Jan. 9	~ 50(S)	3	15	12	±0.7	+0.9	−4.6	4.0
4	04JST Jan. 12	30(R)	2	17	10	−0.8	+3.2	−5.9	1.7
5	06JST Jan. 14	20(R)	0.5	—	—	—	—	−4.4	7.0
6	00JST Jan. 15	30(R)	2	—	15	−2.0	−1.0	−1.8	1.5

* (S) : Satellite, (R) : Radar

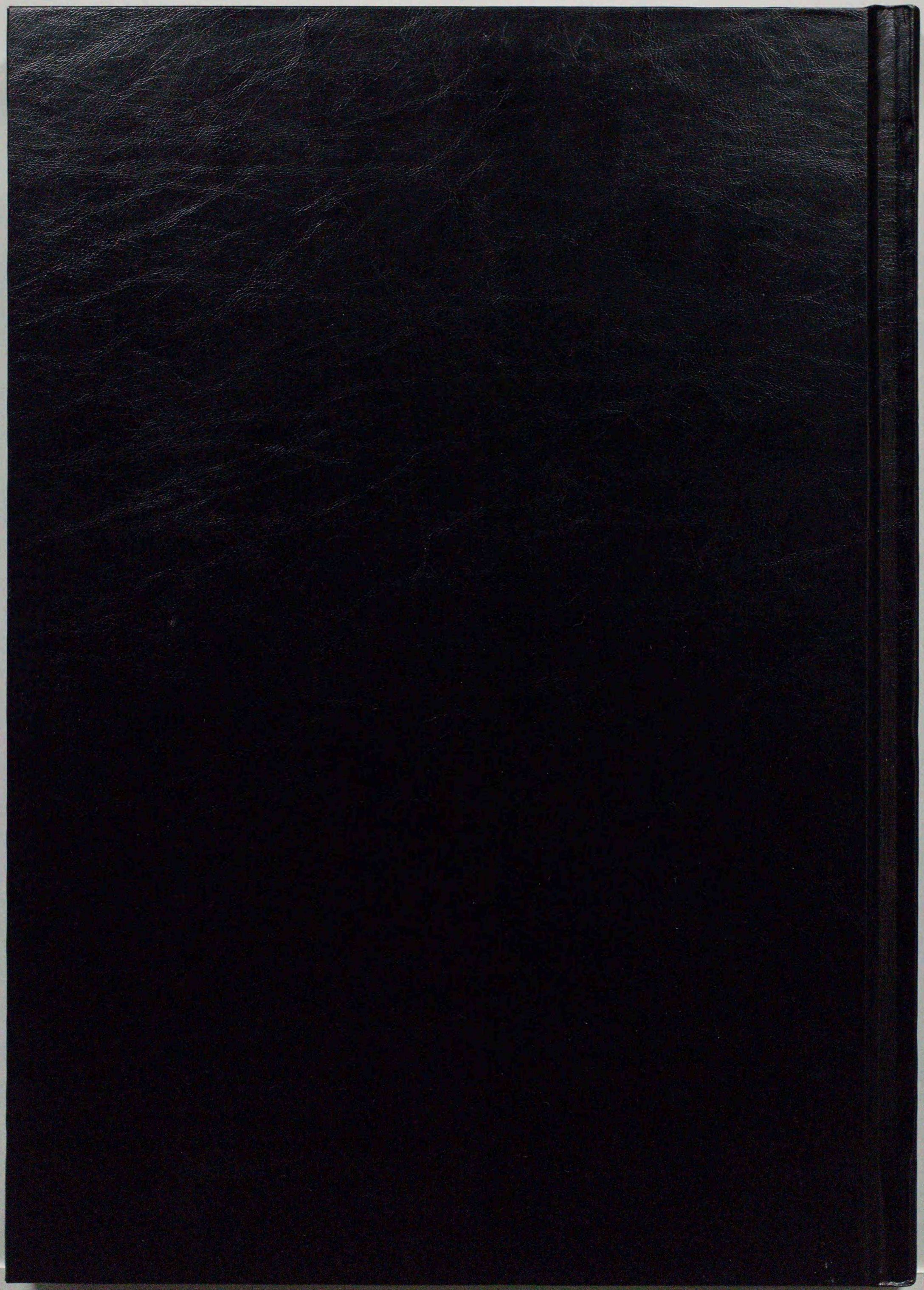

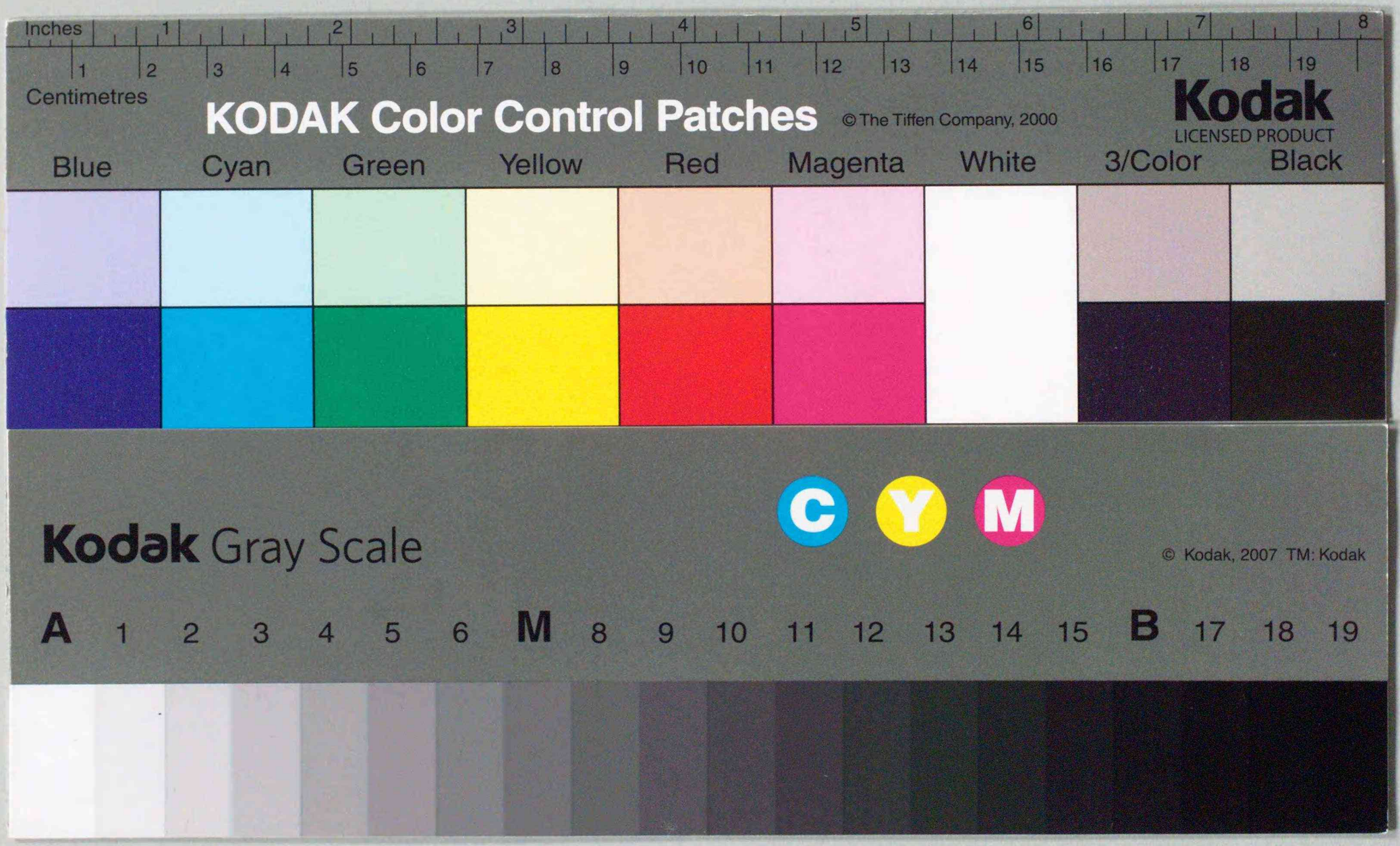
Inches
Centimetres
KODAK Color Control Patches
© The Tiffen Company, 2000
Kodak
LICENSED PRODUCT
Blue
Cyan
Green
Yellow
Red
Magenta
White
3/Color
Black
Kodak Gray Scale
C
Y
M
© Kodak, 2007 TM: Kodak
A 1 2 3 4 5 6 M 8 9 10 11 12 13 14 15 B 17 18 19